

IMPLEMENTING AUTONOMOUS UNMANNED AERIAL VEHICLE  
TACTICS ON QUADROTOR AIRCRAFT USING LINEAR MODEL  
PREDICTIVE CONTROL

IMPLÉMENTATION DE TACTIQUES DE DRÔNES AUTONOMES SUR  
DES QUADRIROTOR EN UTILISANT UNE APPROCHE PAR  
COMMANDE PRÉDICTIVE LINÉAIRE

A Thesis Submitted

to the Division of Graduate Studies of the Royal Military College of Canada

by

Mohamad Iskandarani, B.Eng., RMC  
2 Lt.

In Partial Fulfillment of the Requirements for the Degree of  
Master of Applied Science

April, 2014

© This thesis may be used within the Department of National  
Defence but copyright for open publication remains the property of the author.

*I would like to dedicate this thesis to all those who made this opportunity possible. To Capt. Schamuhn for believing in me and supporting me during my last year of undergraduate studies at RMC. To all my RMC professors who wrote letters of reference, educated me and turned a blind eye when I fell asleep in their class. To my family who will patiently listen to my rants and sooth all frustrations the best they could. To Ahmed Hafez for his endless patience and for encouraging me through out. Thank you all, I am deeply blessed.*

## Acknowledgements

I would first and foremost like to thank Dr. Sidney Givigi for all his help. Sidney, you are a great supervisor and I appreciate all the freedom and flexibility you gave me during these two years of hard work. Thank you for rewarding me with amazing opportunities: from conferences around the world to your unwavering support in the lab. You not only made me a good researcher, but a globe trekker and a dancing king too. It would be my honor to work along side you in the future.

I would also like to thank all RMC staff and personnel, from teachers to technical staff, who were patient with me and gave me the tools necessary for success. What has been done is impossible without you.

Finally, I would like to thank Defense Research and Development Canada, Directorate of Technical Airworthiness and Engineering Support, the Canadian Forces, and the Royal Military College of Canada for providing such a great opportunity.

## Abstract

Iskandarani, Mohamad. M.A.Sc. Royal Military College of Canada, April, 2014.  
*Implementing Autonomous Unmanned Aerial Vehicle Tactics on Quadrotor Aircraft  
Using Linear Model Predictive Control.* Supervised by Dr. S. Givigi.

UAVs are gaining great interest due to their wide area of applications in the military and civilian fields. Applying these UAVs autonomously and in a decentralized manner to the accomplishment of various tasks is a growing trend in the field of cooperative robotics. Among these challenging group tasks we find certain UAV tactics, such as dynamic encirclement and formation flights, operating under the umbrella of safe and robust tactic switching. Dynamic encirclement is defined as the situation in which a target is isolated and surrounded by a UAV team in order to maintain awareness and containment of it. Formation flights allow for line abreast, triangle or cross formations while in flight, during which the team members match distance and speed with the others. In this thesis, the problem of switching from formation flights to dynamic encirclement is considered, and a decentralized Linear Model Predictive Control (LMPC) strategy is formulated. Other control techniques such Taylor series linearization (TSL) and Feedback Linearization (FL) are used to linearize the complex tactics models. It is shown, through simulation results and experimental validation, that the designed control policy is effective for a team of  $N$  UAVs in formation flights switching to dynamic encirclement of a stationary and moving target. With real-world flight tests, the Qball-X4 quadrotor aircraft is used as a validation platform.

**Keywords:** Linear Model Predictive Control, Unmanned Aerial Vehicles, Autonomous Vehicles, Cooperative Robotics

## Résumé

Iskandarani, Mohamad. M.Sc.A. Collège militaire royal du Canada, avril, 2014.  
*Implémentation de tactiques de drones autonomes sur des quadrirotors en utilisant une approche par commande prédictive linéaire.* Thèse dirigée par S. Givigi, Ph.D.

Les drones, appliqués aux domaines civils et militaires, ont suscités un intérêt croissant à cause de leur potentiel. L'utilisation des drones, d'une façon autonome et décentralisée, pour l'accomplissement de tâches variées est une tendance croissante dans la communauté de la robotique coopérative. Parmi ces tâches complexes, on trouve des tactiques de drones, tels que l'encerclement dynamique et les vols en formations, où les véhicules accomplissent un transfert stable et robuste d'une tactique à l'autre. Limiter le mouvement et avoir conscience d'une cible est considéré comme partie intégrante de l'encerclement dynamique. Les vols en formations, tels que ligne de front, triangle et croix, permettent aux membres de l'équipe de maintenir les distances et les vitesses requises par rapport aux autres. Dans ce mémoire, le problème de transfert stable des vols en formation à l'encerclement dynamique est considéré et une stratégie de commande prédictive linéaire est formulée. Autres techniques de contrôles, telles que la linéarisation par séries de Taylor et la linéarisation par rétroaction, sont employées pour simplifier les modèles non-linéaires représentant les tactiques. Il est démontré, à travers des résultats en simulation et des validations expérimentales, que la politique de contrôle proposée est efficace pour une équipe de  $N$  drones qui changent de vols en formation à encerclement dynamique. Par rapport aux vols expérimentaux, le quadrirotor Qball-X4 est utilisé.

**Mots clés :** Asservissement prédictive linéaire, Drones, Véhicules autonomes, Robotique Coopérative

## Co-Authorship Statement

- M. Iskandarani, S. Givigi, A. Beaulieu and A. Rabbath, Linear Model Predictive Control for the Encirclement of a Target Using a Quadrotor Aircraft, in *21st Mediterranean Conference on Control and Automation (MED 2013)*, pages 1550-1556. IEEE, 2013.
- M. Iskandrani, A. Hafez, S. Givigi, A. Beaulieu, and A. Rabbath, Using multiple quadrotor aircraft and linear model predictive control for the encirclement of a target, in *IEEE International Conference SYSCON 2013*, pages 1-7. IEEE, 2013,
- A. Hafez, M. Iskandrani, S. Givigi, S. Yousefi, A. Beaulieu, Using Linear Model Predictive Control Via Feedback Linearization for Dynamic Encirclement in *American Control Conference (ACC 2014)*. IEEE, 2014
- A. Hafez, M. Iskandarani, S. Givigi, S. Yousefi, A. Beaulieu, Applying Quadrotor Aircraft to Dynamic Encirclement, in *IEEE International Conference SYSCON 2014*. IEEE, 2014
- M. Iskandarani, S. Givigi, G. Fusina, A. Beaulieu, Unmanned Aerial Vehicle Formation Flying using Linear Model Predictive Control, in *IEEE International Conference SYSCON 2014*. IEEE, 2014
- A. Hafez, M. Iskandarani, S. Givigi, S. Yousefi, A. Beaulieu, UAVs in Formation and Dynamic Encirclement via Model Predictive Control, in IFAC 2014

# Table of Contents

<b>Abstract</b> . . . . .	iv
<b>Résumé</b> . . . . .	v
<b>Co-Authorship Statement</b> . . . . .	vi
<b>List of Figures</b> . . . . .	ix
<b>List of Algorithms</b> . . . . .	xiv
<b>List of Symbols</b> . . . . .	xv
<b>List of Acronyms</b> . . . . .	xvi
<b>Chapter 1. Introduction</b> . . . . .	1
1.1. UAV applications . . . . .	1
1.2. UAV tactics . . . . .	2
1.3. Control techniques . . . . .	3
1.3.1. Model Predictive Control . . . . .	3
1.3.2. Feedback Linearization . . . . .	4
1.4. Motivation . . . . .	5
1.5. Thesis Statement . . . . .	6
1.6. Contributions . . . . .	6
1.7. Organisation . . . . .	7
<b>Chapter 2. Background</b> . . . . .	9
2.1. UAV Tactics . . . . .	9
2.1.1. Swarming . . . . .	9
2.1.2. Assignment . . . . .	10
2.1.3. Formation Reconfiguration . . . . .	10
2.1.4. Encirclement . . . . .	11
2.2. Research focus . . . . .	12
2.3. Control Techniques and Tools . . . . .	14
2.3.1. Model Predictive Control . . . . .	14
2.3.2. Taylor series Linearization . . . . .	16
2.3.3. Feedback Linearization . . . . .	17
2.4. The Qball-X4 quadrotor . . . . .	18
2.5. Experimental area . . . . .	19
<b>Chapter 3. Problem Formulation</b> . . . . .	21
3.1. LMPC Policy . . . . .	21
3.2. System Dynamics . . . . .	22

3.2.1.	System Identification . . . . .	23
3.2.2.	Encirclement Tactic . . . . .	25
3.2.3.	Formation Flight dynamics . . . . .	32
3.3.	Tactics Switching Logic . . . . .	34
3.4.	Conclusion . . . . .	35
<b>Chapter 4.</b>	<b>Simulation Results . . . . .</b>	<b>36</b>
4.1.	Encirclement using TSL . . . . .	36
4.1.1.	One UAV encircling a stationary target using TSL . . . . .	36
4.1.2.	Two UAVs encircling a stationary target using TSL . . . . .	37
4.1.3.	Three UAVs encircling a stationary target using TSL . . . . .	37
4.2.	Encirclement using FL . . . . .	37
4.2.1.	One UAV encircling a stationary target using FL . . . . .	38
4.2.2.	Three UAVs encircling a stationary target using FL . . . . .	38
4.2.3.	Three UAVs encircling a moving target using FL . . . . .	39
4.3.	Formation . . . . .	40
4.3.1.	Three UAVs in formation flights . . . . .	40
4.4.	Tactics Switching . . . . .	41
4.4.1.	Case #1: One UAV encircling a stationary target . . . . .	41
4.4.2.	Case #2: Three UAVs encircle a stationary target . . . . .	42
4.5.	Conclusion . . . . .	42
<b>Chapter 5.</b>	<b>Experimental Results . . . . .</b>	<b>77</b>
5.1.	Encirclement using TSL . . . . .	77
5.1.1.	One UAV encircling a stationary target . . . . .	77
5.1.2.	One UAV encircling a stationary target using TSL . . . . .	78
5.1.3.	Two UAVs encircling a stationary target using TSL . . . . .	79
5.2.	Encirclement using FL . . . . .	79
5.2.1.	One UAV encircling a stationary target using FL . . . . .	79
5.2.2.	Two UAVs encircling a stationary target using FL . . . . .	80
5.2.3.	Three UAVs encircling a stationary target using FL . . . . .	80
5.3.	Formation . . . . .	81
5.3.1.	Three UAVs in a line abreast formation . . . . .	81
5.4.	Tactics switching . . . . .	81
5.5.	Conclusion . . . . .	82
<b>Chapter 6.</b>	<b>Conclusion . . . . .</b>	<b>101</b>
6.1.	Contributions . . . . .	102
6.2.	Future work . . . . .	102
6.3.	Conclusion . . . . .	103
<b>References</b>	<b>. . . . .</b>	<b>104</b>
<b>Curriculum Vitae</b>	<b>. . . . .</b>	<b>110</b>

## List of Figures

Figure 2.1. Formation reconfiguration example: switching from triangle to line abreast formation . . . . .	11
Figure 2.2. Multi-UAV team encircling a stationary target. . . . .	12
Figure 2.3. Generalized form of MPC, where the prediction is being done at time $t_0$ ; each time step is $t_{0+n\delta}$ , $u_{max}$ and $u_{min}$ are the upper and lower bound constraints on the inputs respectively and $y_{max}$ and $y_{min}$ are the upper and lower bound constraints on the outputs respectively. [35] . . .	15
Figure 2.4. Schematic of the feedback linearization concept. Notice that the addition of the input transformation linearizes the system. . . . .	18
Figure 2.5. Qball-X4 quadrotor aircraft. The frame around the motors and CPU assembly is strictly for equipment safety. . . . .	19
Figure 2.6. UAV motor rotation along side Cartesian coordinate system. The orange strip shows the tail of the aircraft. . . . .	20
Figure 3.1. Qball-X4 response to a step input in a Cartesian plane and its equivalent linear second order system. . . . .	25
Figure 3.2. Linearization points around a circular path. The radius is 1 m. .	28
Figure 3.3. Summary of system identification, state transformation and FL. .	30
Figure 3.4. The triangular, cross and line abreast UAV formations. Notice that the red UAV represents the team leader. . . . .	33
Figure 4.1. Single UAV encircling a stationary target in anti-clockwise direction. The green diamond represents the UAV's starting position of $(1, 0)$ while the dashed blue line shows a reference circle. The orange diamond represents the stationary target at the origin. . . . .	44
Figure 4.2. Radius and angle of encirclement for a single UAV around a stationary target. Notice that the radius steady-state error is less than 10%. . . . .	45
Figure 4.3. Radii, angle of encirclement and angle of separation for the case of 2 UAVs, starting at $(1, 0)$ and $(-1, 0)$ , encircling a stationary target. The dashed red line represents UAV 1 while the green line represents UAV 2. The blue line shows the separation angle between both UAVs. . . . .	46
Figure 4.4. Radii and angle of encirclement for the case of 3 UAVs, starting at $(1, 0)$ , $(-0.5, 0.86)$ and $(-0.5, -0.86)$ , encircling a stationary target. The dashed red line, green line and dashed blue line represent UAV 1, 2 and 3 respectively. . . . .	47
Figure 4.5. Angle of separation between the 3 UAVs. Notice that all the means are close to $\frac{2\pi}{3}$ rad. . . . .	48

Figure 4.6. Single UAV encircling a stationary target in anti-clockwise direction. The green diamond represents the UAV's starting position of $(2,0)$ while the dashed blue line shows a reference circle. The orange diamond represents the stationary target at the origin. . . . .	49
Figure 4.7. Radius and angular speed for a single UAV encircling a stationary target using FL. . . . .	50
Figure 4.8. Radii and angular speeds for one UAV with different initial positions.	51
Figure 4.9. Three UAVs, for Case #1, encircling a stationary target using FL. Each UAV is represented by a red, green or blue diamond while the target is shown as an orange diamond. . . . .	52
Figure 4.10. The radii of encirclement and angular velocities for three UAVs encircling a stationary target at the origin using FL. UAV 1 is shown in red and is initialized at $(2,0)$ , UAV 2 is shown in green and is initialized at $(-1,1.732)$ with angle $\frac{2\pi}{3}$ rad from UAV 1, while UAV 3 is shown in blue and is initialized at $(-1,-1.732)$ with angle $\frac{4\pi}{3}$ rad from UAV 1. . . . .	53
Figure 4.11. Angular separation for three UAVs encircling a stationary target using FL. . . . .	54
Figure 4.12. Three UAVs, for Case #2, encircling a stationary target. Each UAV is represented by a red, green or blue diamond while the target is shown as an orange diamond. . . . .	55
Figure 4.13. The radii of encirclement and the angular velocities for three UAVs encircling a stationary target at the origin. UAV 1 is shown in red and is initialized at $(2,0)$ , UAV 2 is shown in green and is initialized at 1.5 m from the target with angle $\frac{5\pi}{6}$ rad from UAV 1, while UAV 3 is shown in blue and is initialized at 2.5 m from the target with angle $\frac{7\pi}{6}$ rad from UAV 1. . . . .	56
Figure 4.14. Angular separation for three UAVs encircling a stationary target starting at different locations and angles. The UAVs converge to a separation of $\frac{2\pi}{3}$ . . . . .	57
Figure 4.15. Three UAVs, for Case #1, encircling a moving target. Each UAV is represented by a red, green or blue line while the moving target is shown as a black dashed line. . . . .	58
Figure 4.16. The radii of encirclement and angular velocities for three UAVs encircling a target moving in a straight line, starting at $(5,5)$ . UAV 1 is shown in red and is initialized at $(10,0)$ , UAV 2 is shown in green and is initialized at $(5,10)$ with angle $\frac{2\pi}{3}$ rad from UAV 1, while UAV 3 is shown in blue and is initialized at the origin with angle $\pi$ rad from UAV 1. . . . .	59
Figure 4.17. Angular separation for three UAVs encircling a target moving in a straight line. . . . .	60
Figure 4.18. Three UAVs, for Case #2, encircling a moving target. Each UAV is represented by a red, green or blue line while the moving target is shown as a black dashed line. . . . .	61

Figure 4.19. The radii of encirclement and the angular velocities for three UAVs encircling a sinusoidally moving target starting at (5,5). UAV 1 is shown in red and is initialized at (10,0), UAV 2 is shown in green and is initialized at (5,10) with angle $\frac{2\pi}{3}$ rad from UAV 1, while UAV 3 is shown in blue and is initialized at the origin with angle $\pi$ rad from UAV 1. . . . .	62
Figure 4.20. Angular separation for three UAVs encircling a sinusoidally moving target starting at (5,5). The UAVs converge to a desired angle of separation of $\frac{2\pi}{3}$ . . . . .	63
Figure 4.21. UAV team members in triangular formation flying towards the positive x direction. They maintain required distance and speed with each other. . . . .	64
Figure 4.22. The distance in x and y between UAV 2 and UAV L. The distance matches the required value of 3 m. . . . .	65
Figure 4.23. The distance in x and y between UAV 3 and UAV L. The distance matches the required value of 3 m. . . . .	66
Figure 4.24. The speeds of UAV members during the triangular formation. Since the team travels in the positive x direction, the speed in y converges to 0 m/s. . . . .	67
Figure 4.25. UAV team members in cross formation flying towards the positive x direction. They maintain required distance and speed with each other. . . . .	68
Figure 4.26. UAV team members in cross formation flying towards the positive x direction. They maintain required distance and speed with each other. . . . .	69
Figure 4.27. The speeds of UAV members during the cross formation. Since the team travels in the positive x direction, the speed in y converges to 0 m/s. . . . .	70
Figure 4.28. UAV team members switching from formation flight to dynamic encirclement tactic while maintaining the required separating distance during the formation phase and the desired radius and angular velocity during the encirclement phase. UAV 1, 2 and 3 are represented by the blue, red and green diamonds respectively while the target is the black diamond. . . . .	71
Figure 4.29. The speed of the UAV team in the x-direction during formation phase. . . . .	72
Figure 4.30. The radius of encirclement and angular velocity for UAV1 encircling a stationary target at (35,-2). . . . .	73
Figure 4.31. Three UAVs, switch from the formation tactic to encirclement tactic around a moving target. UAV 1, 2 and 3 are represented by the blue, red and green diamonds respectively while the target is the black diamond. . . . .	74
Figure 4.32. The radii of encirclement and angular velocities for three UAVs encircling a target moving in a straight line, starting at (35,-5). . . . .	75
Figure 4.33. Angular separation for three UAVs encircling a target moving in a straight line. All vehicles converge to an angle of separation of $\frac{2\pi}{3}$ rad. . . . .	76

Figure 5.1. Path completed by the Qball-X4 quadrotor for the encirclement of a stationary target. The vehicle takes off from a stationary position at $(0m, 0m)$ (represented by the orange 'x'). The blue line consists of the ideal circular path, while the red line is the UAV's actual path. . . . .	83
Figure 5.2. Height of Qball-X4 along side actual UAV $x$ and $y$ positions. The height during testing is maintained at $0.6m$ . The green line in the height plot shows the actual hieght of the UAV. The red lines in the position plots represent the $x$ and $y$ paths completed by the UAV. The blue lines represnt the path produced as a result of the chosen radius and angular velocity. . . . .	84
Figure 5.3. MPC cost function performance and control signal. Notice that the MPC cost becomes smaller with time. The MPC control signal represents the two manipulated variables calculated with similar weights. . . . .	85
Figure 5.4. Radius and speed of the UAV. The blue lines represent the desired radius of $1m$ and desired speed of $0.1047m/s$ . . . . .	86
Figure 5.5. Single Qball-X4 encircling a stationary target in anti-clock wise direction. The green diamond represents the UAV's starting position of $(1, 0)$ while the dashed blue line shows a reference circle. the orange diamond represents the stationary target at the origin. . . . .	87
Figure 5.6. Radius and angle of encirclement for a single Qball-X4 around a stationary target. Notice that the radius steady-state error is less than 15 %. . . . .	88
Figure 5.7. Radii, angle of encirclement and angle of separation for the case of 2 Qball-X4, starting at $(1, 0)$ and $(-1, 0)$ , encircling a stationary target. The dashed red line represents Qball 1 while the green line represents Qball 2. The blue line shows the separation angle between both UAVs. . . . .	89
Figure 5.8. Single UAV encircling a stationary target in anti-clockwise direction. The green diamond represents the UAV's starting position of $(0, 1.5)$ while the dashed blue line shows a reference circle. The orange diamond represents the stationary target at the origin. . . . .	90
Figure 5.9. Radius and angular velocity of Qball-X4 encircling a stationary target. The blue line represents the desired radius and angular velocity. . . . .	91
Figure 5.10. The radii of encirclement and the angular velocities for two UAVs encircling a stationary target at the origin. . . . .	92
Figure 5.11. Angular separation for two UAVs encircling a stationary target. The UAVs converge to a separation of almost $\pi$ . . . . .	93
Figure 5.12. The radii of encirclement and the angular velocities for three UAVs encircling a stationary target at the origin. . . . .	94
Figure 5.13. Angular separation for two UAVs encircling a stationary target. The UAVs converge to a separation of almost $2\pi/3$ . . . . .	95
Figure 5.14. Distances in $x$ between UAV 2, 3 and the leader going in the negative $y$ direction. The required distance is $1.7$ m . . . . .	96
Figure 5.15. Distances in $y$ between UAV 2, 3 and the leader going in the negative $y$ direction. The required distance is $0$ m . . . . .	97

Figure 5.16. Distances in x between UAV 2, 3 and the leader going in the negative y direction. The required distance is 1.7 m. This is part of a tactic switching flight test where UAV L decides to encircle the target . . . . .	98
Figure 5.17. Distances in y between UAV 2, 3 and the leader going in the negative y direction. The required distance is 0 m. This is part of a tactic switching flight test where UAV L decides to encircle the target . . . . .	99
Figure 5.18. The radius of encirclement and the angular velocity for one UAV encircling a stationary target found at (0,1). This is part of a tactic switching flight test where UAV L decides to encircle the target . . . . .	100

## List of Algorithms

1. Tactics Switching Logic . . . . .	34
--------------------------------------	----

## List of Symbols

$X$	Current $x$ position of UAV
$Y$	Current $y$ position of UAV
$X_d$	Desired $x$ position of UAV
$Y_d$	Desired $y$ position of UAV
$r$	Radius of UAV w.r.t. target
$R_D$	Desired radius w.r.t. target
$\theta$	Angle of UAV w.r.t. target
$\omega$	Angular velocity of UAV
$T$	Cartesian to polar transformation matrix
$\bar{X}$	State-vector
$\bar{Y}$	Output vector
$u_1, u_2$	New inputs found through feedback linearization
$\theta_{lead}$	Angle difference between the UAV being considered and the one in front of it
$\theta_{lag}$	Angle difference between the UAV being considered and the one behind it
$\Delta\theta_D$	Desired angular separation between two UAVs
$N$	Number of UAVs in the team
$E_x$	Error in $x$ between two UAVs
$E_y$	Error in $y$ between two UAVs
$J$	LMPC cost function
$k$	Number of time steps
$\bar{Z}(k+i+1 k)$	State-vector, used in cost function, predicted for time $k+i+1$ at time $k$
$\Delta u(k+i+1 k)$	Variation in input, used in cost function, predicted for time $k+i$ at time $k$
$\bar{D}(k+i+1 k)$	References, used in cost function, sampled for time $k+i+1$ at time $k$
$L$	Least-squares cost function
$n$	Number of parameters to be estimated
$e(t)$	White gaussian noise attributed to estimation
$\sigma^2$	Covariance
$\Theta$	Vector of parameters related to the system being estimated
$\hat{\Theta}$	Vector of estimated parameters
$\Phi$	Vector of measured outputs and known inputs related to the system being estimated

## List of Acronyms

MPC	Model Predictive Control
MP	Model Predictive
LMP	Linear Model Predictive
DMPC	Decentralized Model Predictive Control
NMPC	Nonlinear Model Predictive Control
LMPC	Linear Model Predictive Control
LBMPC	Learning Based Model Predictive Control
TSL	Taylor Series Linearization
FL	Feedback Linearization
3DOF	Three Degrees Of Freedom
6DOF	Six Degrees Of Freedom
PWM	Pulse Width Modulation

## Chapter 1

# Introduction

Due to their great importance especially in the last two decades, Unmanned Vehicles have attracted great attention and concern in both military and civilian communities. Therefore, the efforts in research and development have gained great prominence throughout the world. These platforms such as Unmanned Aerial Vehicles (UAV), underwater exploiters, satellites and robots are widely investigated as they have potential applications [12, 3].

### 1.1 UAV applications

The use of UAVs for various military and civilian missions has received growing attention in the last decade and this provides an opportunity for new operational paradigms. These vehicles are developed to be capable of working in different circumstances and weather with the assistance of human control and have the ability to handle different complicated or uncertain situations. They may have different shapes, sizes, configurations and characteristics. They are either described as a single air vehicle (with associated surveillance sensors), or a UAV system, which usually consists of three to six air vehicles, a ground control station, and support equipment [9].

Although many single UAV applications can be carried out successfully through manual operation, only autonomous systems can provide solutions to some applications, such as extensive continuous reconnaissance operations lasting weeks or months [41]. Victim search and rescue along-side reconnaissance operations are some applications where autonomous UAVs are utilized [12], thus minimizing human resources, risk of injury, and manned aerial vehicle costs. This autonomous operation is integral to cooperative tactics utilizing teams of UAVs to accomplish a task. Some of these tasks include formation flying, such as encirclement and swarming. Accordingly, for-

mation algorithms have been developed over many years for autonomous UAV use. For instance, [48] explores a swarming algorithm on a group of unmanned vehicles responsible for infrastructure protection. Similarly, [50] implemented a target capturing algorithm in order to follow a sinusoidally moving target. Also, [56] implemented a feedback control law in a cooperative hunting behaviour on a mobile robot troop enclosing a target. Moreover, several recent independent results in target search [10], target observation [42], cooperative transportation [39], and path coordination [52], have made it clear that more complex applications, that were beyond the reach of single units, became achievable using multiple systems working cooperatively and autonomously.

## 1.2 UAV tactics

UAV Tactics are defined as the general strategies used by individuals in a UAV team to achieve a desired outcome, or, in other words, it is the way the UAVs act to perform a certain required mission [35]. These strategies can be either centralized, as in the case where a group of UAVs receives coordinated instructions from one centralized decision maker, or decentralized, in which the UAVs are responsible for making individual decisions. Research and experiments in the last decade have dealt with the different tactics that can be carried out by a team of UAVs, and a wide variety of approaches to effectively implement these tactics have been proposed.

In UAVs, dynamic encirclement is considered to be a strategy in which a team of UAVs assumes positions around a target to restrict its movements. In real life, dynamic encirclement tactic has been used in defending a secure airspace against an invading aircraft, maintaining surveillance over a ground target and in protecting the borders against invading targets. The target-capturing problem has received much attention in multi-agent research because of its ability to provide safety. Target-capturing has two main problems. The first one is to understand the behavior of dynamic encirclement where the target is brought to a desired position and orientation depending upon the UAVs' motions, this algorithm ensures that the target

will never escape from the UAV team. The second problem is the enclosing behavior where multiple UAVs are controlled in a distributed manner to converge to an assigned formation in the tracking of a moving target focusing on avoiding collision with each other and with the target [50, 53].

In [20, 29], an encirclement tactic for a group of vehicles was created by using a cyclic pursuit strategy. A hybrid control system consisting of a feedback control law and a reactive control framework is used to control a team of mobile robots to capture and enclose a target. Moreover, to solve the problem of steering a group of uni-cycle type mobile robots to reach desired positions and orientations around a target and then encircle it may be found in [56, 30].

## 1.3 Control techniques

### 1.3.1 Model Predictive Control

In the past 20 years, Model Predictive Control (MPC) has evolved considerably and it remains an attractive solution to control problems for its intuitive concept and ability to handle complex dynamics and multivariable cases. MPC is one of the most advanced control methodologies which has made a significant impact on industrial control engineering. MPC can handle multi-variable control problems, which takes into account actuator limitations allowing operation within given constraints [13]. Several works have already considered the use of MPC for control of autonomous vehicles. In [1], Alexis et al. use MPC to control the position of a quadrotor. In [47], Richards and How use a Decentralized MPC (DMPC) control scheme in a group of UAVs to achieve collision avoidance. In [27], a Nonlinear MPC (NMPC) control scheme is used to stabilize vehicle dynamics and generate trajectories in multiple flying robots in dynamic environments. In [54], Sutton and Bitmead consider NMPC for the control of an autonomous submarine. Finally, in [51] and [17], MPC strategies are considered for multi-vehicle formation control. The use of the MPC method makes it possible to add hard constraints to the state, controls and outputs of the linear state

space model and with the help of the orthonormal functions, computation effort is decreased [44], however this is not explicit in real life where systems are represented by nonlinear state space models.

Dynamic encirclement of a stationary target with multiple UAVs using a decentralized NMPC was successfully presented, also, the effect of communications between the vehicles was discussed, and a stabilizing control policy was derived and demonstrated by simulation results [36, 37]. A combination between Taylor Series Linearization (TSL) and decentralized LMPC is used on a team of UAVs for dynamic encirclement of a stationary target [23]. This control policy allowed real-time implementation on the Qball-X4 quadrotor aircraft. Also, a decentralized NMPC was applied to UAV teams to encircle two stationary and movable targets [19].

### 1.3.2 Feedback Linearization

Feedback Linearization (FL) technique is a common approach used in the control of nonlinear systems. Different combinations of FL and various types of controllers are used to overcome the nonlinear dynamics of UAVs during their flights in [33, 40, 18]. For instance, in [6], a combination of an FL controller and a high order sliding mode observer is applied to a quadrotor aircraft. The high order sliding mode observer is used to observe and estimate the effects of external disturbances such as wind and noise. In [55], Holger Voos uses FL to linearize the flight dynamics of a micro-quadrotor, while a combination of two control loops are used to control the altitude and velocity of the UAV. In [38], a dynamic feedback controller is used to convert the inner loop of the quadrotor into a linear, controllable, and non-interactive loop. This positively affects the stability and robustness of the model against wind, turbulence, and parametric uncertainties.

## 1.4 Motivation

Let's consider the following scenario: A team of UAVs is on a surveillance mission in contested territory. They assume a line abreast formation (form a line) or a triangle formation in order to map the environment or take aerial photographs. The team realizes that it is getting close to a possible threat, in this case a stationary vehicle containing smuggled weapons. Dynamic encirclement around the target commences in order to maintain awareness of it. This containment is necessary since the team members may take pictures of the target to be fed back to the proper intelligence agencies. This scenario demonstrates the importance of using both encirclement tactic and formation flight during military operations.

In previous works, autonomous tactics have been applied to teams of UAVs in a centralized manner. Centralized control is computationally intensive specially when dealing with large teams of UAVs. Moreover, if the ground station or UAV responsible for delegating tasks is damaged or unable to function, the mission/task becomes infeasible. Also, considering large teams of UAVs, bandwidth might be limited, specially when communicating over long distances. An encumbered communication channel might also cause mission failure in a centralized scenario as each UAV requires constant communication with the ground station. In our research, all control algorithms will be executed by each team member, increasing the chances of mission success. This decentralized application of control is important for scaling the control designs to larger teams of UAVs.

Another difference between our research and other works in the field is linear process models. Encirclement and other tactics have been accomplished on teams of UAVs using nonlinear plants. When using MPC, the use of nonlinear plants results in non-convex optimization problems that cannot run in real-time and must be validated through hours of simulation. For instance, [35] successfully accomplishes the task of encirclement using  $N$  UAVs in simulation. The author uses nonlinear MPC for his work which can not run in real-time on Qball-X4 quadrotors. We propose linearizations for such process models using FL and TSL, and apply them to real-life

vehicles. This research provides the first steps towards understanding the challenges when operating LMPC and UAV tactics on the Qball-X4 platform. Moreover, when using linearized systems, we must remember that there are assumptions taken when disregarding the nonlinearities. The final linearized system will not exactly replace the nonlinear one. The assumptions taken when linearizing the system will be respected in the elaboration of the theory and algorithms presented in this research.

## 1.5 Thesis Statement

The thesis statement of this work is that LMPC, working in concert with TSL and FL, creates a suitable control policy for stable tactic switching implemented in real-time on a multi-UAV system. The validation of our thesis along with its elaborated theory and algorithms using LMPC policy is done by experimentally demonstrating that:

- During the encirclement tactic the team of UAVs maintains a required radius, angular velocity and angle of separation between its members;
- During the formation flight the team of UAVs keeps the required distances between members at given formation speed; and
- The team remains stable during the switching between tactics.

The validation is done both in a simulated environment and later verified using physical platforms. The results are demonstrated within a given margin of error which takes into consideration parameter weights, system constraints as well as wind disturbance caused by UAV propellers flying in a confined space.

## 1.6 Contributions

The contributions of this work are as follows:

- System identification for the Qball-X4 low-level control
- Creation of a nonlinear dynamic encirclement model for multi-UAV teams

- Creation of a linear formation flight model suitable for line abreast, triangle and cross formations for multi-UAV teams
- Linearization of dynamic encirclement model using Taylor Series Linearization and Feedback Linearization
- Development and validation of Linear Model Predictive Control as a suitable control policy
- Real-time operation of proposed control policy

Our result contributions show a multi-UAV team:

- Encircling both stationary and moving targets;
- Engaging in formation flights using line abreast, triangle and cross formations; and
- Switching from one UAV tactic to another in a stable manner.

Verification of algorithms described above in a real-time physical environment using a multi-Qball X4 team wraps up this work.

## 1.7 Organisation

This thesis is organized as follows. In Chapter 2, a literature review and background covering works related to our research is presented. We review UAV tactics in general paying special attention to the tactics that are closely related to our work. The control techniques associated with this thesis are described in the same chapter. Among these techniques, we name MPC, TSL and FL. In Chapter 3, we outline the system identification done on the low-level control of the Qball and all subsequent transformations used to derive dynamic encirclement and formation flight models. Accordingly, the linearization approaches and the corresponding cost function are also discussed. In Chapter 4, we show the successful use of the LMPC policy applied on a multi-UAV team accomplishing the tactics described in Chapter 2. We then validate the same

controller on a multi-Qball X4 team as shown in the real-world results of Chapter 5. Finally, in Chapter 6, we conclude this thesis with closing remarks and discuss some future research.

## Chapter 2

# Background

In this chapter, we briefly describe UAV tactics and give examples from research in this field. We then provide our research focus as it applies to this thesis, followed by a quick description of certain control techniques used. Among these, we name Model Predictive Control, Taylor Series Linearization and Feedback Linearization.

### 2.1 UAV Tactics

UAV tactics are the general strategies used by individuals in a team of autonomous UAVs to achieve a desired outcome [35]. Cooperative tactics operate under centralized control, where a group of UAVs receives coordinated instructions from one centralized decision maker, or decentralized control, in which the UAVs are responsible for making individual decisions. We will be concentrating on decentralized control in this research. The main reason for this choice is that decentralized control is more robust than centralized control to communication failure with other UAVs or the ground station. Also, decentralized control proves to be scalable to a larger number of vehicles [35]. The tactics discussed here are swarming, assignment, formation reconfiguration and encirclement.

#### 2.1.1 Swarming

Integral to cooperative robotics, swarming is similar to other tactics such as flocking and formation. Flocking, for instance, refers to a group of assembled individuals and encompasses both swarming and formation [35]. According to [35], a formation is an assembled group of individuals in which an individual's location within the group conforms to some predetermined spatial pattern. Swarms are formations except that they do not use a pre-determined spatial pattern within the group. The UAVs in the team are usually required to respect the Reynolds rules of flocking [46]:

- i Avoid collisions with nearby flockmates;
- ii Attempt to match velocity of other team members; and
- iii Attempt to stay close to other flockmates.

Applications of swarming are numerous and deal with surveillance [7], search and destroy tasks [22] [26] and mapping [11] among other strategies highlighted in the introduction.

### 2.1.2 Assignment

Concerning the assignment tactic, the objective for the UAV team is to maximize the chances of success in the desired mission by assigning targets according to the capabilities of the vehicles. Since the computation required for optimizing the cost function for large teams of UAVs is computationally demanding, a methodology of Team Dynamics and Tactics (TDT) is proposed in [15]. The main purpose of TDT is to offer an effective target selection algorithm and an optimal weapon selection algorithm to destroy or reduce the opposing force's combat capabilities. The author of [4] proposes a game theoretical approach with the UAVs being self-interested decision-makers in order to assign targets optimally. In [2], a stochastic formulation for the UAV target assignment problem, where improving the effectiveness of the assignment based on future implications for the UAVs, is considered. The author of [2] describes a UAV whose mission is to destroy Surface-To-Air (SAM) missile batteries while avoiding risky paths. Proper assignment of the targets then becomes necessary.

### 2.1.3 Formation Reconfiguration

Formation reconfiguration is defined as the change of UAV formation in response to an external factor. The change encompasses positions of individual team members, breaking into smaller groups or forming larger ones. We see in [8] that a team of UAVs changes its position in order to evade an enemy team of UAVs using a differential game theoretic approach. In [32], a team of unmanned combat vehicles is controlled within

multiple formations of varying dimensions. The objective is for the team to reach a target location despite uncertain stochastic dynamics, limitation in computational capability and conflicting objectives. This tactic may also encompass others as it describes the switching from one tactic to another, such as encirclement to swarming. Fig. 2.1 shows a quick example of formation reconfiguration.

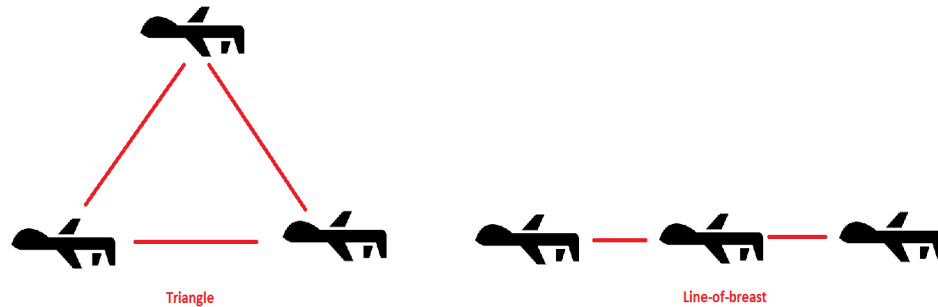


Figure 2.1: Formation reconfiguration example: switching from triangle to line abreast formation

#### 2.1.4 Encirclement

Encirclement is a task accomplished by a UAV in order to maintain awareness and containment of a given target. The aim of the UAV team encircling this target is to maintain close proximity at all times. This may be done when the team members choose positions around the target as seen in [50]. The authors use Lyapunov and graph theories, with an emphasis on cooperation and consensus between multi-agent systems, to encircle a maneuvering target. In this work, a nonlinear model of the UAV is used with constraints on the Lyapunov control policy. A cyclic pursuit strategy along side a design methodology of a distributed cooperative controller for target-enclosing operations by multiple dynamic agents is seen in [28] and [20]. In these works, differently from [50], a linear model is derived for the vehicle and an unconstrained feedback control law is implemented to ensure encirclement. Furthermore, linearization of the vehicle dynamics is done using virtual structures and feedback control as seen in [24] and [25].

The encirclement tactic may be described as one or more vehicles maintaining a required radius, angular velocity and angle of separation with respect to the target and other team members. This approach, shown in a general schematic in Fig. 2.2, is used extensively in this thesis.

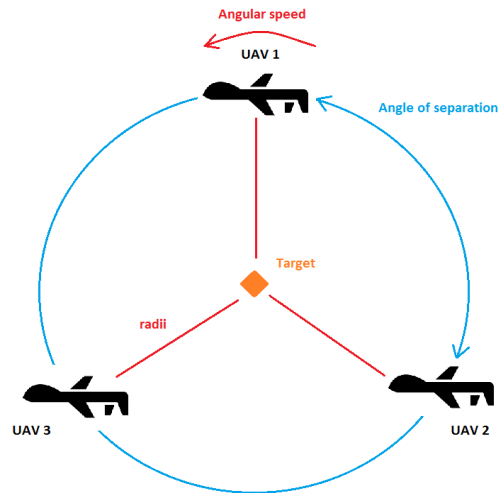


Figure 2.2: Multi-UAV team encircling a stationary target.

## 2.2 Research focus

The field of UAV tactics and control is vast, covering many facets such as centralized versus decentralized control as well as real-time operation versus offline simulation. In this thesis we focus our attention on the formation and encirclement tactics and the process of switching from one to the other while maintaining stability.

The control of autonomous quadrotor aircraft using MPC has been explored by several authors over the years. In [1], the authors maintain a UPATcopter prototype unmanned quadrotor at desired height using MPC. In [36], a nonlinear Decentralized MPC (DMPC) policy is put in place for the encirclement of a stationary and moving target by a group of UAVs. The authors of [34] use MPC to control a helicopter with three Degrees Of Freedom (3DOF) set on a table using a support arm.

This thesis uses a different approach than the ones stated above to accomplish the task of encirclement of a stationary target using multiple Quadrotor aircraft. For

instance, according to [1] a UAV is maintained at a desired height, which means that the controller's main objective is to stabilize the vehicle at a given  $x$  and  $y$  coordinate. In this thesis, the Model Predictive (MP) controllers will generate the desired paths for the UAV team and not just maintain stable hover. The desired path produced is then passed to low-level controllers composed of Proportional-Integral-Derivative (PID) that are responsible for stable flight. In [34] MPC is used to control a 3DOF aircraft. We use the Qball-X4, a six Degrees Of Freedom (6DOF) quadrotor [43] which adds to the complexity of the control scheme. NMPC cannot be implemented in real-time due to its computational complexity and lengthy cost function optimizations. To remedy this situation, this thesis considers an LMPC policy to control the UAV team in their encirclement task. Furthermore, similar LMPC policies are applied to the formation tactic.

The field of formation control holds multiple structure approaches. For instance, the leader-follower strategy has one of the UAVs as leader while the rest are considered followers. This may be seen in [16] and [49]. The disadvantage of using this approach is clear because the failure of the leader means the failure of the mission. Another formation control approach is a virtual structure, where the UAVs follow a certain moving point thus forming a rigid body. The formation is considered a single object which makes it difficult for collision avoidance and disturbance rejection [45]. In the behaviour approach, the goal of the mission and its corresponding constraints, are laid out for the team who decides the manner with which to accomplish the task in a decentralized way. As seen in [31] this strategy is suitable for uncertain environments but lacks theoretical guarantees of stability. In this thesis, we will adopt a control strategy within the leader-follower umbrella with respect to the formation tactic. In order to implement this approach, LMPC will be used for high-level decentralized control.

Finally, we will combine both encirclement and formation tactics and switch from one to the other on the fly based on a simple decision algorithm. Some parameters used in the decision making process are target proximity and threat level. The stability of switching will be discussed in Chapter 3. In the following sections, we will

discuss the control techniques implemented in order to accomplish these tactics.

## 2.3 Control Techniques and Tools

This thesis utilizes LMPC for the control of the vehicles and the implementation of the tactics described in section 2.1. However, since the dynamics of the vehicles are nonlinear, some sort of linearization technique is necessary. The section is arranged as follows: in subsection 2.3.1 we describe the basic ideas behind MPC and also provide some references on the use of the technique for UAV control. Section 2.3.2 discusses briefly how a nonlinear system can be linearized by using Taylor Series. Finally, section 2.3.3 presents Feedback Linearization.

### 2.3.1 Model Predictive Control

MPC was first developed to deal with complex chemical processes but rapidly made its way into the UAV control due to its ability to predict optimal inputs and deal with multi-variable cases. The main characteristics of MPC according to [13] are:

- Explicit use of a model to predict the process output at future time instants (over the prediction horizon);
- Calculation of a control sequence minimizing an objective function; and
- Receding strategy, so that at each instant the horizon is displaced toward the future, which involves the application of the best control signal of the sequence calculated at each step.

A scheme of MPC operation may be seen in Fig. 2.3. The MPC algorithm works as follows:

- i At every time step  $t_0$ , we predict inputs and states of the system based on the model derived;
- ii Derive control signals based on the predicted states after minimization of the cost function that takes into consideration weights and constraints;

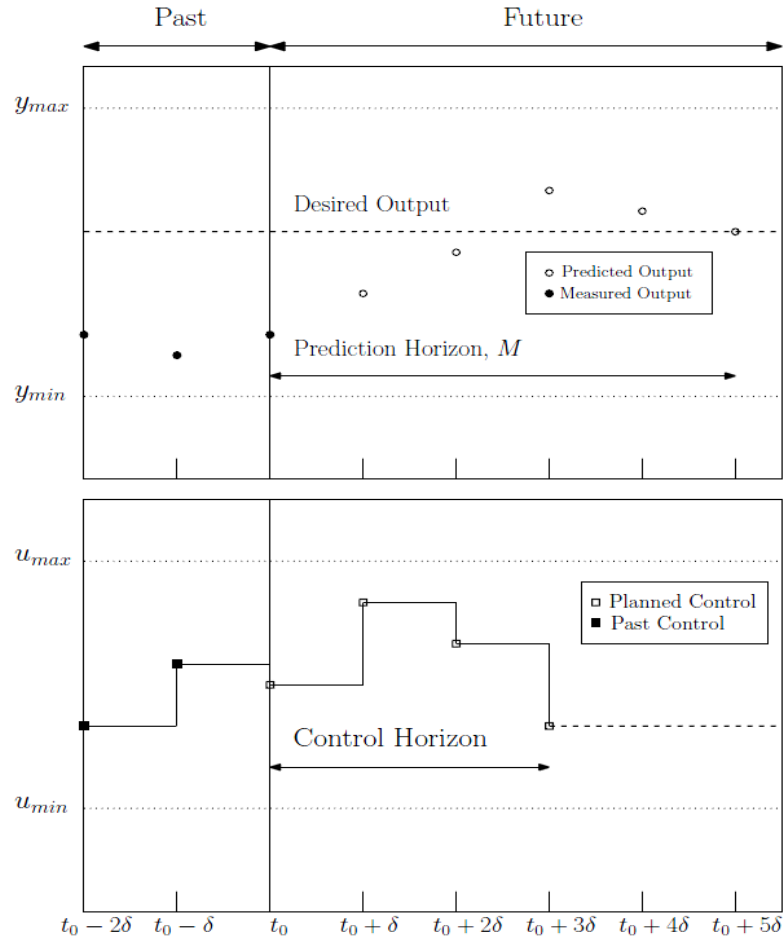


Figure 2.3: Generalized form of MPC, where the prediction is being done at time  $t_0$ ; each time step is  $t_0+n\delta$ ,  $u_{max}$  and  $u_{min}$  are the upper and lower bound constraints on the inputs respectively and  $y_{max}$  and  $y_{min}$  are the upper and lower bound constraints on the outputs respectively. [35]

- iii Apply the first control signal in the sequence found to the vehicle and move the horizon one step in the future; and
- iv Restart the whole process for the new time  $t_{0+\delta}$

Using MPC in UAV control has been explored by multiple authors. For instance, the authors of [47] use a Decentralized MPC (DMPC) control scheme in a group of UAVs to achieve collision avoidance. In [27] we see a Nonlinear MPC (NMPC) control scheme used to stabilize vehicle dynamics and generate trajectories for multiple flying robots in dynamic environments. In [34], controlling the movement of a helicopter on

a support arm is done with MPC. Furthermore, [51] along side [17] show the formation of multiple UAVs being maintained by MPC strategies. Finally, a hierarchical MPC approach is used for stabilization and autonomous navigation of a formation of UAVs, under constraints on motor thrusts, angles and positions, and under collision avoidance constraints [5].

In this work we will focus on the use of linear versions of MPC. Therefore, we need to linearize the nonlinear processes involved in UAV tactics and dynamics. In the next two subsections we will discuss the two techniques used in our simulations and experiments to linearize the derived models.

### 2.3.2 Taylor series Linearization

TSL is a method of linearizing nonlinear systems by using first-order approximations. The more linearizations you have, the closer the linear system will be to the nonlinear one. As a general example, we consider the following continuous-time state-space model [21]:

$$\begin{aligned}\dot{x} &= f(x) + g(x)u \\ y &= h(x)\end{aligned}\tag{2.1}$$

where  $x$  is the state-vector;  $y$  is the output vector;  $f, g$  and  $h$  are nonlinear functions and  $u$  is a vector of manipulated input variables. Consider TSL of equation (2.1) about an equilibrium point  $(u_0, x_0, y_0)$ :

$$\begin{aligned}\dot{x} &= \left[ \frac{\partial f(x_0)}{\partial x} + \frac{\partial g(x_0)}{\partial x} \right] (x - x_0) + g(x_0)(u - u_0) \\ y - y_0 &= \frac{\partial h(x_0)}{\partial x} (x - x_0)\end{aligned}\tag{2.2}$$

The resultant linear state-space model may be written in the form:

$$\begin{aligned}\dot{x} &= Ax + Bu \\ y &= Cx\end{aligned}\tag{2.3}$$

The model shown above is an exact representation of the nonlinear one found in (2.1) only at the point  $(x_0, u_0)$ . Without loss of generality, we disregard higher order

derivatives because we assume that they have little influence on the overall system. According to [21], a control strategy based on a linearized model may yield unsatisfactory performance and robustness at other operating points. This is why we choose multiple operating points when linearizing more complex systems such as the encirclement model; this is shown in section 3.2.2.2.

### 2.3.3 Feedback Linearization

FL linearizes the system by introducing suitable control inputs through a change of variables. The advantage here compared to TSL is that the resultant linear model is an exact representation of the original nonlinear model over a large set of operating conditions. Most FL techniques are based on two main approaches: input-output linearization and state-space linearization [21]. In this thesis, we concentrate on the first approach where the objective is to create a linear map between a set of new inputs  $l$  and the existing outputs  $y$ . For instance, consider the two-dimensional nonlinear system:

$$\begin{aligned}\dot{x}_1 &= f_1(x_1, x_2) + g_1(x_1, x_2)u \\ \dot{x}_2 &= f_2(x_1, x_2) \\ y &= x_1\end{aligned}\tag{2.4}$$

where  $x_1, x_2$  are states;  $u$  is a single input;  $f_1, f_2, g_1$  are nonlinear functions and  $y$  is the output. If the nonlinear function  $g_1$  is non-zero in the operating region of interest, the static state feedback control law

$$u = \frac{l - f_1(x_1, x_2)}{g_1(x_1, x_2)}\tag{2.5}$$

changes the first equation in (2.4) to  $\dot{x}_1 = l$  [21]. Thus, the linearized control law exactly linearizes the map between the transformed input  $l$  and the output  $y$ . We can now design a linear controller to satisfy control objectives such as maintaining radius and angular velocity. The input-output linearization method of FL is summarized in Fig. 2.4.

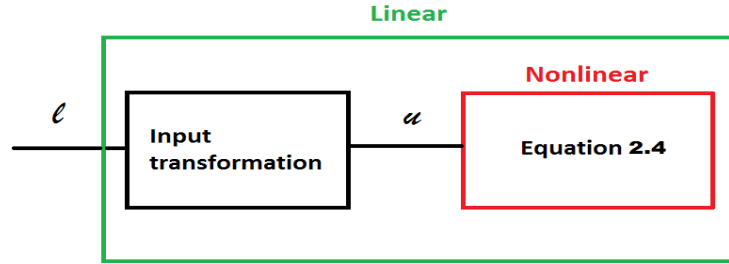


Figure 2.4: Schematic of the feedback linearization concept. Notice that the addition of the input transformation linearizes the system.

## 2.4 The Qball-X4 quadrotor

The Qball-X4 Aircraft is a quadrotor designed by Quanser (Fig. 2.5). Similarly to [1], we assume that the structure of the UAV is rigid and symmetrical. The center of gravity is found in the middle of the design, positioned at equal distance away from the four motors. Since each motor rotates in the opposite direction from its axis counterpart, a motion neutral frame is created [14]. Fig. 2.6 represents the coordinate system used throughout this work. Notice that the pitch angle  $\alpha$  is in the same direction as the  $y$  axis while the roll angle  $\phi$  is in the same direction as the  $x$  axis. The height is perpendicular to both axes but is not part of the LMPC strategy. The authors of [14] highlight an accurate description of the quadrotor's movement and present the Qball-X4 dynamical equations. The position of the UAV is varied by slightly changing the roll and pitch angles in the  $x$  and  $y$  direction respectively. It is important here to highlight that the UAV dynamics are based on small angle approximation, a method used to linearize the quadrotor system of equations. After linearization through small angle approximation, these equations are put into state-space form for PID design. The PID controllers are responsible for the low-level control of the nonlinear UAV dynamics. A system identification method, based the least-squares algorithm, is used to approximate the low-level dynamics and their PID control into a second order transfer function as explained in Chapter 3.



Figure 2.5: Qball-X4 quadrotor aircraft. The frame around the motors and CPU assembly is strictly for equipment safety.

## 2.5 Experimental area

Multiple systems work in concert in order to operate the Qball-X4 aircraft. The experimental setup is comprised of a processing unit running MATLAB *Simulink* and QuaRC software, Optitrack camera feedback and the Qball-X4 itself [14]. Low-level PID controllers are responsible for the height, yaw and positional movements of the UAV. The PID and the MPC are designed in MATLAB *Simulink* and compiled to C code on the processing unit by the QuaRC software. All controllers are then ported wirelessly to the UAV and operate in real-time on the UAV's GUMSTIX microcontroller without any dependence on the ground station other than the position feedback measurements, which is done through a set of sixteen OptiTrack V100:R2 cameras that pick up a unique pattern, called trackable, made of reflective balls glued to the UAV frame. This trackable can be seen in Fig. 2.5. The Optitrack system acts as a pseudo-GPS (or Local Positioning System (LPS)) that localizes the vehicle

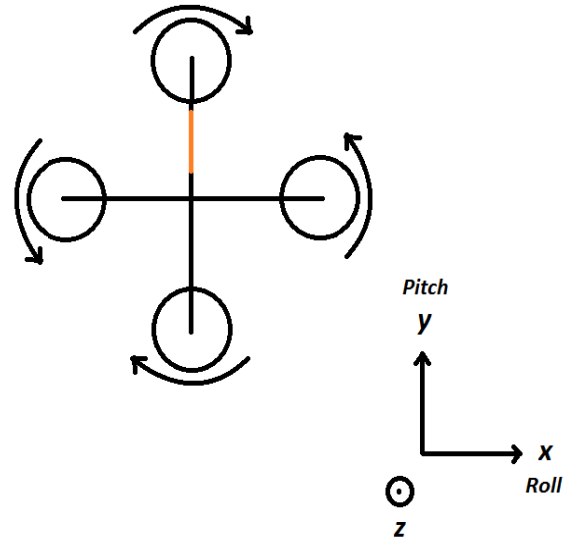


Figure 2.6: UAV motor rotation along side Cartesian coordinate system. The orange strip shows the tail of the aircraft.

at all times and sends this info to the processing unit. The testing arena is a 4x4m square which depends on the camera orientation and the corresponding calibration. Safety systems have been put in place to protect personnel and equipment [14].

## Problem Formulation

In this Chapter, we outline the system dynamics, including identification based on actual data, polar transformation and linearization of the models. We start with a few notes on the cost function used in the LMPC control policy. Then, we describe the system identification done on the low-level control of the Qball-X4. We also divide our arguments into two branches: the encirclement tactic and the formation tactic. The linearizations done are specific to the encirclement dynamics since those are nonlinear. The final product is a linear plant describing both the encirclement and formation tactic applied to each member of a multi-UAV team.

### 3.1 LMPC Policy

For each UAV in the team, the cost function of the MPC controller is minimized according to the weights of the outputs, and is given as follows:

$$J(\bar{Z}, \Delta u) = \sum_{i=0}^{p-1} \Gamma^T Q \Gamma + \Delta u(k+i|k)^T R_{\Delta u} \Delta u(k+i|k) \quad (3.1)$$

The components of the cost function are:

$$\Gamma = \bar{Z}(k+i+1|k) - \bar{D}(k+i+1|k) \quad (3.2)$$

where  $p$  is the prediction horizon and  $\bar{Z}(k+i+1|k)$  is the state vector. The encirclement state vector holds radius, angle of the UAV with respect to the target, radius rate of change, angular velocity and angle of separation for the leading UAV  $i$  and the lagging UAV  $j$ :

$$\bar{Z} = [r \quad \theta \quad \dot{r} \quad \dot{\theta} \quad \Delta\theta_{i,j}]^T \quad (3.3)$$

The formation state vector holds distance error in  $x$ , its time derivative, distance

error in  $y$  and its time derivative:

$$\bar{Z} = [E_x \quad \dot{E}_x \quad E_y \quad \dot{E}_y]^T \quad (3.4)$$

These states are predicted for time  $k+i+1$  at time  $k$ . Furthermore,  $\bar{D}(k+i+1|k)$  is the reference sampled for time  $(k+i+1)$  at time  $k$ ;  $\Delta u(k+i|k)$  is the manipulated variables rate calculated for time  $k+i$  at time  $k$ ;  $Q$  and  $R_{\Delta u}$  are positive semi-definite matrices that hold the weights for the output variables and the manipulated variables rate respectively. The references  $\bar{D}$  are not absolute and change depending on the other vehicle poses. The cost function in (3.1) represents a quadratic system that uses the states from equations (3.28) linearized through TSL, (3.31) linearized through FL or (3.44)-(3.47) for its prediction and optimization problem. We define real-time here as the LMPC updating its cost function and issuing control signals every 0.5 seconds. In this way, the control policy proposed may be implemented on actual quadrotor vehicles. The prediction horizon and control horizon used are eight and two respectively. The implementation of the cost function in (3.1) is done using the MATLAB *Model Predictive Control Toolbox*.

## 3.2 System Dynamics

The low-level control of the Qball-X4 is nonlinear, this is due to the nonlinear nature of the system and saturation of control signals used to guarantee the operational boundaries of the quadrotor. For example, the signals to drive the rotors (Pulse Width Modulation (PWM)) are allowed to operate in a limited range to guarantee that the system does not go out of bounds. The system also takes into consideration some assumptions such as small angle approximation. In order to abstract all these complexities away and find a linear system suitable for LMPC, we use system identification. This method will help us find a second-order system on which to build the required UAV tactics, such as encirclement and formation. The following subsections detail the process of deriving the second-order system and formulating the necessary models for encirclement and formation.

### 3.2.1 System Identification

Flight data from a Qball-X4 quadrotor is collected in order to find the process model describing the Cartesian movement of the UAV. System identification, based on a least-squares algorithm, constructs linear process models from dynamic systems, not easily found through first principles, based on input-output data. The estimated second-order discrete system may be defined first as:

$$y(k) + a_1y(k-1) + a_2y(k-2) = b_1u(k-1) + b_2u(k-2) \quad (3.5)$$

where  $u(k)$  are some known inputs,  $y(k)$  some measured outputs and  $a_1, a_2, b_1, b_2$  the parameters of the system. Equation (3.5) may be written as:

$$y(k) = \Phi^T(k)\Theta \quad (3.6)$$

where  $\Phi^T(k) = [y(k-1) \ y(k-2) \ u(k-1) \ u(k-2)]$  and  $\Theta = [-a_1 \ -a_2 \ b_1 \ b_2]^T$ .

In order to find estimated parameters of  $\Theta$ , represented by  $\hat{\Theta}$ , we minimize the following general cost function with  $n$  parameters:

$$L = \frac{1}{2} \frac{1}{n} \sum_{k=1}^n [y(k) - \Phi^T(k)\hat{\Theta}]^2 \quad (3.7)$$

We then derive the above cost function in order to find the least-squares solution

$$\frac{\partial L}{\partial \hat{\theta}} = \frac{1}{n} \sum_{k=1}^n [y(k) - \Phi^T(k)\hat{\Theta}] \Phi = 0 \quad (3.8)$$

Notice the orthogonality between the prediction errors and the data found in  $\Phi$ . We then develop the above system to get the least-squares solution found in equation (3.11)

$$\frac{\partial L}{\partial \hat{\theta}} = \frac{1}{n} \sum_{k=1}^n \Phi(k)y(k) - \frac{1}{n} \sum_{k=1}^n \Phi(k)\Phi^T(k)\hat{\Theta} = 0 \quad (3.9)$$

$$\frac{1}{n} \sum_{k=1}^n \Phi(k)y(k) = \frac{1}{n} \sum_{k=1}^n \Phi(k)\Phi^T(k)\hat{\Theta} \quad (3.10)$$

$$\hat{\Theta} = \left[ \sum_{k=1}^n \Phi(k)\Phi^T(k) \right]^{-1} \left[ \sum_{k=1}^n \Phi(k)y(k) \right] \quad (3.11)$$

where  $\left[ \sum_{k=1}^n \Phi(k)\Phi^T(k) \right]^{-1}$  is the covariance matrix. When persistently exciting  $\sum_{k=1}^n \Phi(k)\Phi^T(k)$  through the span of the  $n$ -dimensional space with  $\Phi \in \mathbb{R}^n$  we get:

$$y(k) = \Phi(k)\Theta + e(t) \quad (3.12)$$

where  $e(t)$  is a white gaussian noise, meaning that the expected value  $E(e(t)e(t - \tau)) = 0$  and the covariance  $E(e^2(t)) = \sigma^2$ . In order to implement this least-squares solution we use the MATLAB *System Identification Toolbox*.

As a result of minimizing the cost function  $L$  and finding the estimates in  $\hat{\Theta}$ , a second order system is found for both  $x$  and  $y$  coordinates. This system is dependent on the speed and acceleration of the vehicle and needs to be represented with a second order system. Fig. 3.1 shows the Qball-X4 response to a step input in both  $x$  and  $y$  coordinates, along side a linear second order plant found through system identification [23]. We can see that both responses are similar during the fifteen second period. The identification is done in discrete time but we will present the continuous time system here for ease of use. The following shows transfer functions for the  $x$  and  $y$  movements respectively:

$$X = \frac{1.7455}{s^2 + 2.616s + 1.7116} X_d \quad (3.13)$$

$$Y = \frac{0.4973}{s^2 + 1.1384s + 0.4973} Y_d \quad (3.14)$$

where  $X_d$  and  $Y_d$  are the desired positions of the Qball-X4 while  $X$  and  $Y$  are the current positions of the Qball-X4 during flight.  $X_d$  and  $Y_d$  are the inputs to the low-level control of the UAV while  $X$  and  $Y$  are the outputs of this system. These outputs are used to calculate the radius for encircling the stationary target and the angular velocity for each UAV in the team. As a result of transforming the above transfer functions, each UAV in the team will be characterized by the following state-space representation:

$$\begin{bmatrix} \dot{x} \\ \ddot{x} \end{bmatrix} = \begin{bmatrix} 0 & 1 \\ -1.7116 & -2.6116 \end{bmatrix} \begin{bmatrix} x \\ \dot{x} \end{bmatrix} + \begin{bmatrix} 0 \\ 1 \end{bmatrix} X_d \quad (3.15)$$

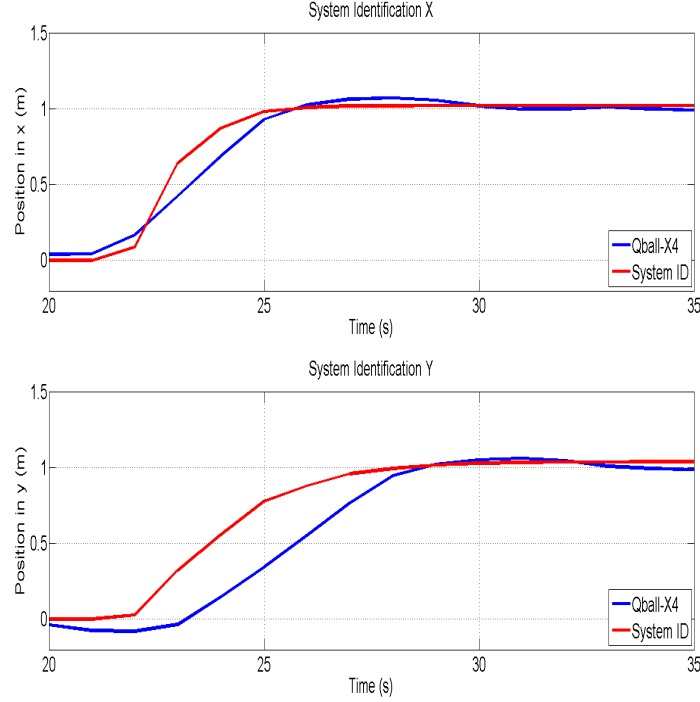


Figure 3.1: Qball-X4 response to a step input in a Cartesian plane and its equivalent linear second order system.

$$X = \begin{bmatrix} 1.7455 & 0 \end{bmatrix} \begin{bmatrix} x \\ \dot{x} \end{bmatrix} \quad (3.16)$$

$$\begin{bmatrix} \dot{y} \\ \ddot{y} \end{bmatrix} = \begin{bmatrix} 0 & 1 \\ -0.4793 & -1.384 \end{bmatrix} \begin{bmatrix} y \\ \dot{y} \end{bmatrix} + \begin{bmatrix} 0 \\ 1 \end{bmatrix} Y_d \quad (3.17)$$

$$Y = \begin{bmatrix} 0.4973 & 0 \end{bmatrix} \begin{bmatrix} y \\ \dot{y} \end{bmatrix} \quad (3.18)$$

where the outputs will be the current positions in  $x$  and  $y$  for each UAV. The state-space representation is linear compared to the system offered in [36]. Notice that we will continue presenting the system dynamics in this thesis in continuous time, but the implementation of these equations is done in discrete time.

### 3.2.2 Encirclement Tactic

The main objective of our designed controller, with regards to the encirclement tactic, is to achieve the required objectives mentioned in the following equations [24]:

$$C1) \lim_{t \rightarrow \infty} |r_i(t) - R_D| = 0 \quad \forall i \leq N \quad (3.19)$$

$$C2) \lim_{t \rightarrow \infty} |\dot{\theta}_i(t) - \dot{\theta}_D| = 0 \quad \forall i \leq N \quad (3.20)$$

$$C3) \lim_{t \rightarrow \infty} |\theta_{i+1}(t) - \theta_i(t)| = \frac{2\pi}{N} \quad \forall i \leq N \quad (3.21)$$

where  $t$  is time;  $N$  is the number of UAVs in the team;  $r_i$  is the radius of the  $i^{th}$  vehicle with respect to the target;  $R_D$  is the desired radius;  $\dot{\theta}_i$  is the angular velocity of the  $i^{th}$  UAV around the target;  $\dot{\theta}_D$  is the desired angular velocity;  $\theta_{i+1}$  is the angle of the leading UAV around the target; and  $\theta_i$  is the angle of the UAV being considered. The above equations represent the system behaviour that must be achieved by the controller: condition *C1* states that each UAV in the team maintains a desired distance from the target, while condition *C2* states that each UAV in the team maintains a desired angular velocity around the target. Finally, condition *C3* states that each member in the team spreads itself evenly in a circular formation around the target. The LMPC controller tries to respects these conditions when accomplishing dynamic encirclement.

Since the control of encirclement will be based on radius and angular velocity, a linearization of the following transformation is necessary for implementing the linear MPC policy:

$$r_i = \sqrt{X_i^2 + Y_i^2} \quad (3.22)$$

$$\omega_i = \dot{\theta}_i = \frac{d}{dt} \left( \arctan \frac{Y_i}{X_i} \right) \quad (3.23)$$

where  $r_i$  is the radius for encirclement of the  $i^{th}$  UAV;  $X_i$  and  $Y_i$  are the current position of the  $i^{th}$  UAV;  $\omega_i$  is the angular velocity of the  $i^{th}$  UAV and  $\theta_i$  is the angle of encirclement of the  $i^{th}$  UAV with respect to the stationary target. It is evident that combining equations (3.15-3.18) with equations (3.22-3.23) will yield a nonlinear system. A transformation matrix is used in the following subsection to ease this complexity.

### 3.2.2.1 Cartesian to Polar transformation

In the last subsection, we are able to identify the model for the Cartesian movement of the Qball-X4 and setup the transformation to the new set of states that will allow us to output radius and angular velocity of each UAV. To complete the transformation we first replace the states  $x$ ,  $y$ ,  $\dot{x}$  and  $\dot{y}$  found in equations (3.15-3.18) with their Polar equivalents:

$$x = r \cos \theta \quad (3.24)$$

$$y = r \sin \theta \quad (3.25)$$

$$\dot{x} = \dot{r} \cos \theta - r \dot{\theta} \sin \theta \quad (3.26)$$

$$\dot{y} = \dot{r} \sin \theta + r \dot{\theta} \cos \theta \quad (3.27)$$

Then, the resultant set of equations characterized by  $[\dot{x} \ \dot{y} \ \ddot{x} \ \ddot{y}]^T$  are multiplied using a transformation matrix  $\mathbf{T}$  as seen in the following:

$$\begin{bmatrix} \dot{r} \\ \dot{\theta} \\ \ddot{r} \\ \ddot{\theta} \end{bmatrix} = \mathbf{T} \begin{bmatrix} \dot{x} \\ \dot{y} \\ \ddot{x} \\ \ddot{y} \end{bmatrix} \quad (3.28)$$

where the transformation matrix  $\mathbf{T}$  is:

$$\mathbf{T} = \begin{bmatrix} \cos \theta & \sin \theta & 0 & 0 \\ \frac{-\sin \theta}{r} & \frac{\cos \theta}{r} & 0 & 0 \\ \omega \sin \theta & \omega \cos \theta & \cos \theta & \sin \theta \\ \frac{\dot{r} \sin \theta}{r^2} - \frac{\omega \cos \theta}{r} & \frac{-\dot{r} \cos \theta}{r^2} - \frac{\omega \sin \theta}{r} & \frac{-\sin \theta}{r} & \frac{\cos \theta}{r} \end{bmatrix}$$

The resultant system is too big to represent here, but the set of equations found in (3.28) have  $[r \ \theta \ \dot{r} \ \dot{\theta}]^T$  as states and  $X_d$  and  $Y_d$  as inputs. The outputs are  $r$  and  $\omega = \dot{\theta}$ , i.e. the radius and angular velocity respectively.

### 3.2.2.2 Linearization using TSL

Since the set of equations in (3.28) is nonlinear, we linearize the system according to different points using TSL. In order to demonstrate TSL, we consider the example of dynamic encirclement at a radius of 1 m as seen in Fig. 3.2. In order to make the

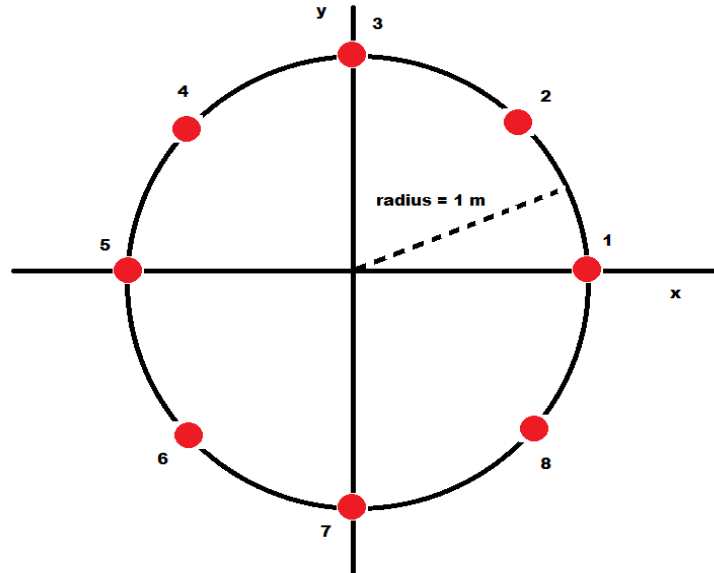


Figure 3.2: Linearization points around a circular path. The radius is 1 m.

linearization error as small as possible, several linearization points need to be found around the path of the vehicle.

As a result, eight distinct linear state-spaces are found which means that eight different Linear Model Predictive (LMP) controllers are used for dynamic encirclement for each UAV in the team. We must note that all controllers use the same cost function for the state prediction and the optimization problem. Piece-wise linearization is the approach used in this thesis in order to create almost seamless transitions between the different controllers. The angle of encirclement is used as an input to the piece-wise system in order to merge the control signal of one LMPC with the other as the UAV encircles its target. It must be noticed that the multiple LMPC controllers still run in real-time but since they all need different data structures, their implementation requires a high usage of the memory available on the UAV microcontroller. Moreover, the UAVs within this formulation are not aware of each other's position and can not adjust according to angle of separation. Accordingly, we set up a new system, more robust and efficient with respect to the TSL linearization. Feedback linearization offers a good solution by offering one linear plant for the LMPC, unlike the eight different ones offered by the TSL method.

### 3.2.2.3 Linearization using FL

In sections 3.2.1 and 3.2.2.1, we discussed the system identification of the model for the motion of the Qball-X4 and also presented the transformation matrix that brings the system from Cartesian coordinates to Polar coordinates. The objective of FL is to linearize equation (3.28) and represent it in the standard state-space form. In order to do this, we first introduce a combination of two new inputs  $u_1$  and  $u_2$  by replacing the inputs  $X_d$  and  $Y_d$  with:

$$\begin{aligned}
X_d = & 0.0000572((-20000\omega\dot{r}\sin(\theta)\cos(\theta)^2) + (12323r\sin(\theta)^2\cos(\theta)) - (20000\omega\dot{r}\sin(\theta)) \\
& + (12320\dot{r}\sin(\theta)^2\cos(\theta)) - (20000u_2r\sin(\theta)) - (26160\omega r\sin(\theta)) \\
& - (10000u_1r\sin(\theta)) - (20000\omega^2r\cos(\theta)^3) + (12320\dot{r}\cos(\theta)^3) + (10000u_1\cos(\theta)) \\
& + (12320r\cos(\theta)^3) + (10000\omega^2r\cos(\theta)) - (10000u_2\cos(\theta)) - (10000r\theta\sin(\theta)))
\end{aligned} \tag{3.29}$$

$$\begin{aligned}
Y_d = & -0.01608((-327\omega r\cos(\theta)) + (250\omega^2r\cos(\theta)^2\sin(\theta)) + (250\omega\dot{r}\cos(\theta)\sin(\theta)^2) \\
& + (154\omega r\cos(\theta)\sin(\theta)^2) - (125\omega^2r\sin(\theta)) - (125u_1\sin(\theta)) + (125u_2\sin(\theta)) \\
& - (250\omega\dot{r}\cos(\theta)) + (154\omega r\cos(\theta)^3) - (125u_1r\cos(\theta)) - (250u_2r\cos(\theta)) \\
& - (125r\theta\cos(\theta)))
\end{aligned} \tag{3.30}$$

This substitution cancels the nonlinearities in equation (3.28) which introduces a linear system with new inputs  $u_1$  and  $u_2$ . We may write the resultant linear system as such:

$$\dot{\bar{X}} = g(r, \theta, \dot{r}, \dot{\theta}, u_1, u_2) \tag{3.31}$$

where  $g$  is a linear function found through FL substitution. The final linear process model may be represented in state-space form:

$$\dot{\bar{X}} = A\bar{X} + BU \quad ; \quad \bar{Y} = C\bar{X} \tag{3.32}$$

where  $U$  is  $[u_1 \ u_2]^T$ ,  $\bar{X}$  is  $[r \ \theta \ \dot{r} \ \dot{\theta}]^T$ ,  $\bar{Y}$  is the output vector holding  $r$  and  $\omega = \dot{\theta}$  and matrices  $A, B, C$  ensure controllability and observability of the state-space. In order to summarize the FL process, Fig. 3.3 shows the linearization scheme used in this approach. Notice that this figure shows a more detailed description of Fig. 2.4.

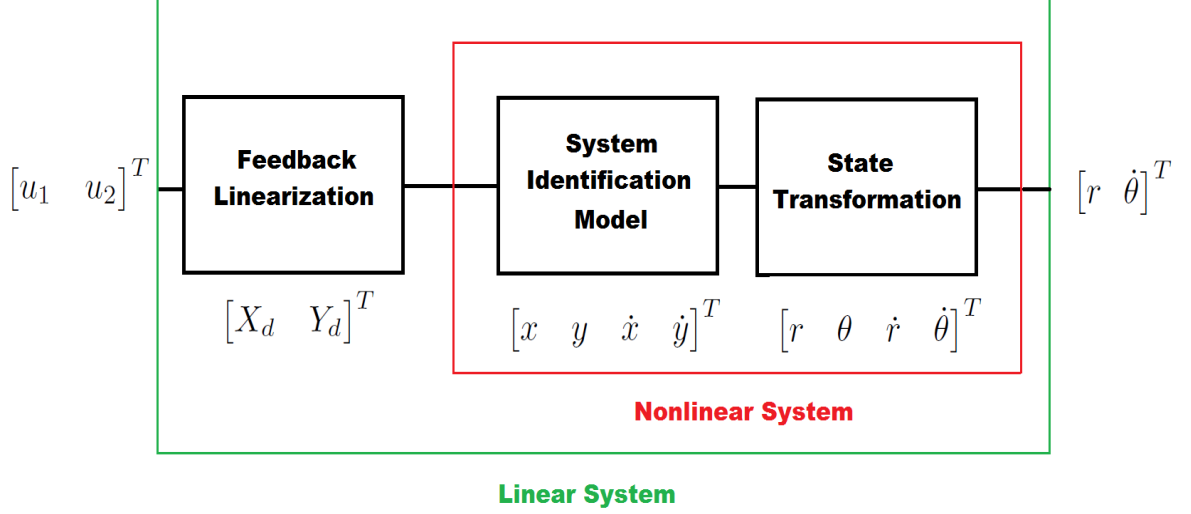


Figure 3.3: Summary of system identification, state transformation and FL.

The substitution shown in equation (3.31) is limited to encirclement around a target found at the origin. In order to accomplish the same task at any point, we introduce the target positions in Cartesian coordinates,  $x_o$  and  $y_o$ , and represent a new substitution:

$$\begin{aligned}
 X_d = & 0.0000572((-20000\omega\dot{r}\sin(\theta)\cos(\theta)^2) + (12323r\sin(\theta)^2\cos(\theta)) \\
 & + (17116x_o\sin(\theta)^2) - (20000\omega\dot{r}\sin(\theta)) + (12320\dot{r}\sin(\theta)^2\cos(\theta)) \\
 & - (20000u_2r\sin(\theta)) - (26160\omega r\sin(\theta)) - (10000u_1r\sin(\theta)) \\
 & - (20000\omega^2r\cos(\theta)^3) + (12320\dot{r}\cos(\theta)^3) + (10000u_1\cos(\theta)) + (17116x_o\sin(\theta)^2) \\
 & + (12320r\cos(\theta)^3) + (10000\omega^2r\cos(\theta)) - (10000u_2\cos(\theta)) - (10000r\theta\sin(\theta))
 \end{aligned} \tag{3.33}$$

$$\begin{aligned}
 Y_d = & -0.000201((20000\omega\dot{r}\sin(\theta)^2\cos(\theta)) + (20000\omega^2r\cos(\theta)^2\sin(\theta)) \\
 & - (10000\omega^2r\sin(\theta)) + (12320\omega r\cos(\theta)\sin(\theta)^2) - (4793\cos(\theta)^2y_o)) \\
 & - (26160\cos(\theta)\omega r) - (1000u_1\sin(\theta)) + (1000\sin(\theta)u_2) \\
 & + (12320\omega r\cos(\theta)^3) - (10000u_1r\cos(\theta)) - (20000u_2r\cos(\theta)) \\
 & - (10000r\theta\cos(\theta)) - (20000\omega\dot{r}\cos(\theta) - (4793y_o\sin(\theta)^2));
 \end{aligned} \tag{3.34}$$

In this way it is possible to encircle targets not located at the origin and moving targets, which makes our solution more general and powerful.

### 3.2.2.4 Angle of Separation

Since our controllers are decentralized, each UAV must control its radius to the target, its angular speed  $w = \dot{\theta}$ , and angle of separation relative to other members. In order to accomplish this, each UAV needs to be cognisant of the leading and lagging UAV in the formation.  $\theta_{lead}$  represents the angular difference between the member being considered and the one in front of it, while  $\theta_{lag}$  represents the angular difference with the one behind it. One last consideration needs to be made before we can have a full solution. Notice that the conditions in (3.19)-(3.21) might not be achieved at the same time. Therefore, we need a way to relax some of them in order to achieve the required behaviour. The condition we chose to relax was the angle of separation  $C3$ .

Let us define the following terms:

$$\Delta\theta_D = 2\pi/N \quad (3.35)$$

$$\Delta\theta_{i,j}(t) = \theta_j(t) - \theta_i(t) \quad (3.36)$$

where  $\theta_i$  represents the angle of the  $i^{th}$  UAV,  $\theta_j$  is the angle of the  $j^{th}$  UAV,  $\Delta\theta_D$  is the desired angular separation between two UAVs, and  $N$  is the number of UAVs in the formation.

Thus, the error between two of the UAVs in a team is given as follows:

$$e_i(t) = \Delta\theta_{i,j}(t) - \Delta\theta_D \quad (3.37)$$

and its time derivative is given as follows:

$$\dot{e}_i(t) = \dot{\theta}_j(t) - \dot{\theta}_i(t) \quad (3.38)$$

Let us further define a suitable Lyapunov candidate function as:

$$\begin{aligned} V(t) &= 1/2(e_1^2(t) + e_2^2(t) + e_3^2(t) + \dots\dots\dots e_N^2(t)) \\ \dot{V}(t) &= e_1(t)\dot{e}_1(t) + e_2(t)\dot{e}_2(t) + \dots\dots\dots e_N(t)\dot{e}_N(t) \end{aligned} \quad (3.39)$$

By choosing the condition

$$\dot{\theta}_j(t) - \dot{\theta}_i(t) = -\gamma e_i(t) \quad (3.40)$$

and by choosing  $\gamma$  as a positive constant, Lyapunov stability is achieved:

$$\dot{V}(t) = -\gamma[e_1(t)^2 + e_2(t)^2 + \dots + e_N(t)^2] \quad (3.41)$$

Moreover, the chosen Lyapunov candidate function allows the errors to decrease as time goes by, despite the fact that the UAVs are allowed to vary their speeds initially to achieve encirclement. We now add the desired angular speed to equation (3.40) using the following equation

$$\dot{\theta}_D = \frac{\dot{\theta}_1(t) + \dot{\theta}_2(t) + \dots + \dot{\theta}_N(t)}{N} \quad (3.42)$$

We can use equations (3.40) and (3.42) to calculate the desired angular speed for each member in the formation.

In general, the desired angular speed for each member in the team is calculated by observing the current angular positions of the leading and lagging UAV in the formation respectively according to the following equation:

$$\dot{\theta}_{D_i}(t) = \frac{3\dot{\theta}_D + \gamma(\theta_{lead\ i}(t) - \theta_{lag\ i}(t))}{3}, \forall i \in [1, N] \quad (3.43)$$

Finally, the state  $\Delta\theta_{i,j}$ , angular separation between two UAVs is added to the linear system presented at the end of section 3.2.2.3 so that it may be included in the cost function. Moreover, the desired angular velocity  $\dot{\theta}_{D_i}$  is fed back as a reference to the process model.

### 3.2.3 Formation Flight dynamics

In sections 3.2.2.2 and 3.2.2.3, we have linearized the nonlinear dynamics pertaining to the encirclement tactic. Now, we propose a linear system, based on error equations created from equations (3.15)-(3.18), to describe the formation flight dynamics. The UAVs form a linear formation and advance in a leader-follower manner while maintaining desired distance between each team member and matching the speed of others. Fig. 3.4 shows the three required configurations to be accomplished in this thesis.

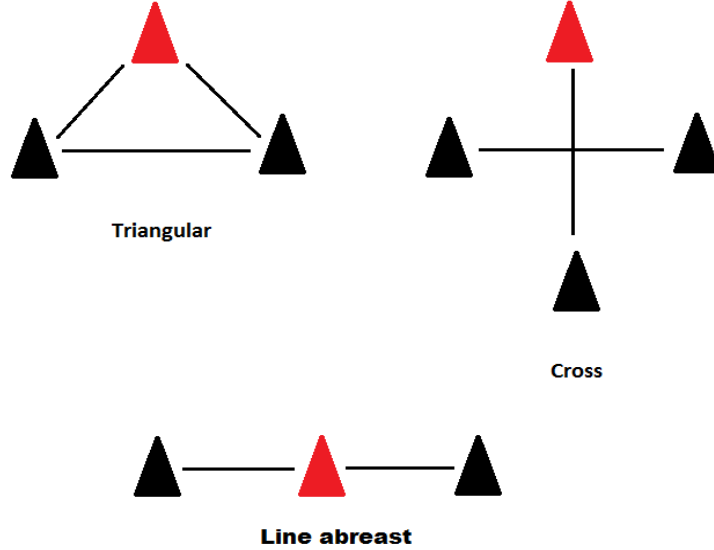


Figure 3.4: The triangular, cross and line abreast UAV formations. Notice that the red UAV represents the team leader.

By subtracting equations for UAV 1 from the same equations for UAV 2, we get the following error dynamics in state-space form:

$$\begin{bmatrix} \dot{E}_x \\ \ddot{E}_x \end{bmatrix} = \begin{bmatrix} 0 & 1 \\ -1.71 & -2.61 \end{bmatrix} \begin{bmatrix} E_x \\ \dot{E}_x \end{bmatrix} + \begin{bmatrix} 0 & 0 \\ -1 & 1 \end{bmatrix} \begin{bmatrix} X_{d2} \\ X_{d1} \end{bmatrix} \quad (3.44)$$

$$\bar{Y}_x = [1.7455 \quad 0] \begin{bmatrix} E_x \\ \dot{E}_x \end{bmatrix} \quad (3.45)$$

$$\begin{bmatrix} \dot{E}_y \\ \ddot{E}_y \end{bmatrix} = \begin{bmatrix} 0 & 1 \\ -0.47 & -1.38 \end{bmatrix} \begin{bmatrix} E_y \\ \dot{E}_y \end{bmatrix} + \begin{bmatrix} 0 & 0 \\ -1 & 1 \end{bmatrix} \begin{bmatrix} Y_{d2} \\ Y_{d1} \end{bmatrix} \quad (3.46)$$

$$\bar{Y}_y = [0.4973 \quad 0] \begin{bmatrix} E_y \\ \dot{E}_y \end{bmatrix} \quad (3.47)$$

where  $E_x$  and  $E_y$  are the errors in  $x$  and  $y$  respectively between UAV 1 and 2 while  $\dot{E}_x$  and  $\dot{E}_y$  are their respective time derivatives.  $\bar{Y}_x$  and  $\bar{Y}_y$  are the output vectors for the error dynamics in  $x$  and  $y$  respectively. LMPC is used to maintain these errors at a desired value. The choice of leader UAV helps us form a line abreast or a triangle formation.

### 3.3 Tactics Switching Logic

In order to accomplish the task in a decentralized manner, each UAV in the team will take its own formation or encirclement decisions. Each member in the team has a sensing and a communications radius: the sensing radius is responsible for detecting the target while the communications radius is responsible for detecting the other vehicles in the team. When a target is within the sensing radius, the UAV will decide based on the target's threat level and importance if it should encircle or not. Moreover, if other vehicles are in the communications radius when the target is detected, a packet of information is sent to all other UAVs within this range. This packet includes: external threat of the target, its importance and encirclement decision of the sender UAV. When the UAV on the receiving end gets the information, it goes through the same decision making process as the sender UAV. Once the UAV decides to encircle, we combine the controller commands for formation and encirclement in a piece-wise manner to complete the switch. The algorithm shown in 1 summarizes the switching logic. The target threat level and importance thresholds along side the range to target may change depending on the situation. these thresholds are values ranging from zero to one.

---

#### Algorithm 1 Tactics Switching Logic

---

```

if Receiving target information from other UAVs then
  if Target threat level <0.5 and Target importance >0.5 then
    if Range to target <5 then
      Encircle the target
    end if
  end if
else {Range to target <Sensing radius}
  if Range to other vehicles <Communications radius then
    Send target information to other vehicles
  end if
  if Target threat level <0.5 and Target importance >0.5 then
    if Range to target <5 then
      Encircle the target
    end if
  end if
end if

```

---

## 3.4 Conclusion

In this chapter, we discussed the identification of a second order system for the low-level control of the Qball-X4 quadrotor in section 3.2.1 and all subsequent transformations and derivations until we found the necessary linear models. Throughout the encirclement tactic, we show the controller conditions for encirclement, the cartesian to polar transformation and various linearizations through TSL and FL. In section 3.2.3, we showcase the linear model derived to describe the formation tactic. Finally, in section 3.3, the switching logic used by each UAV is described. We have formulated two linear systems describing the encirclement and formation tactics, to be used alongside LMPC.

## Simulation Results

In this Chapter we outline all the simulation results necessary to show the success of our designed controllers. Running the system in MATLAB *Simulink* safely will allow us to move to the Qball-X4 platform. We begin by showing the results for encirclement of one, two and three UAVs for stationary and moving target. We then apply an autonomous logic system to each UAV that allows the team to accomplish the tactics switching policy from formation to encirclement. For each of these simulation results, FL or TSL is used for the linearization of the dynamic equations.

### 4.1 Encirclement using TSL

This section covers the results based on the LMPC and TSL formulations highlighted in section 3.2.2.2.

#### 4.1.1 One UAV encircling a stationary target using TSL

A UAV, positioned initially at  $(1, 0)$ , successfully encircles a stationary target located at the origin. The simulation is run for 80 seconds. Fig. 4.1 shows the overall movement of the UAV during encirclement. We can clearly see that the combination of the piece-wise system and the eight LMP controllers is working properly because the UAV converges very closely to the ideal circle. In Fig. 4.2, it is evident that the LMP controllers maintain the radius close to 1m with a steady-state error of less than 10%. From the second half of Fig. 4.2, the angle of encirclement goes from 0 to  $\pi$ rad and from  $-\pi$  to 0rad, thus completing a circle. The angular velocity of the UAV's movement is 0.0801rad/s which is close to the desired 0.1rad/s. The same simulation, with an initial UAV position of  $(-1, 0)$ , was implemented showing positive results.

#### 4.1.2 Two UAVs encircling a stationary target using TSL

Two UAVs with initial positions  $(1, 0)$  and  $(-1, 0)$  encircle a stationary target located at the origin. This simulation was also run for 80 seconds. Fig. 4.3 summarizes dynamic encirclement for the two-UAV team. Firstly, the radii of both vehicles is maintained at 1m with a steady-state error of less than 10%. Secondly, as expected from running the single UAV test, UAV 1 has its angle of encirclement as in Fig. 4.2 while UAV 2 has its angle from  $-\pi$  to  $\pi$  rad. Both vehicles complete one cycle around the target with no perturbations. Thirdly, the angle of separation between them is maintained around  $\pi$ rad which means that the collision avoidance system was not triggered. The LMPC policy was successful at controlling both UAVs at the desired radius and with proper angular separation.

#### 4.1.3 Three UAVs encircling a stationary target using TSL

Three UAVs with starting positions  $(1, 0)$ ,  $(-0.5, 0.86)$  and  $(-0.5, -0.86)$ , encircle a stationary target at the origin. Fig. 4.4 shows how all three radii are maintained close to 1m with a steady-state error of less than 10%. moreover, we can see that the angle of encirclement for UAV 1 starts at 0rad, for UAV 2 starts at  $\frac{2\pi}{3}$ rad and for UAV 3 starts at  $-\frac{2\pi}{3}$ rad. All UAVs run for 80 seconds completing one cycle around the target. The challenge with running this number of vehicles is making sure that the angle of separation between all three is maintained and that no collisions occur. Looking at Fig. 4.5 we can see that the angles between all three vehicles are maintained around  $\frac{2\pi}{3}$ rad which means that no collision occurred. The applied controllers are successful at controlling the UAVs in dynamic encirclement.

## 4.2 Encirclement using FL

This section covers the results based on the LMPC and FL formulations highlighted in section 3.2.2.3.

#### 4.2.1 One UAV encircling a stationary target using FL

Now, we use the combination between FL and LMPC to accomplish the task of dynamic encirclement. The objective of the LMP controller here is to maintain the vehicle at 2 m from the target with an angular speed of 0.15 rad/s. In Fig. 4.6, we show the UAV successfully encircling a stationary target while in Fig. 4.7, we see the radius and angular speed of the vehicle. Finally, Fig. 4.8 shows the UAV converging to the desired requirements despite different starting positions.

#### 4.2.2 Three UAVs encircling a stationary target using FL

The success of one UAV encircling the stationary target prompted us to apply the system on a scalable multi-UAV platform. The objective here is to show that the UAVs may accomplish dynamic encirclement by controlling their own radius with respect to the target, their angular velocity and the angular separation considering the leading and lagging UAV in the team. In other words we take the formulation shown in Section 3.2.2.3, and apply it to three UAVs working together on the task of encirclement. Using multiple vehicles is a suitable and robust testbed for the designed system.

##### 4.2.2.1 Case #1: UAVs at standard initial positions

A set of three UAVs with initial positions  $(2, 0)$ ,  $(-1, 1.732)$  and  $(-1, -1.732)$  successfully encircle a stationary target located at the origin as seen in Fig. 4.9. This simulation was also run for 120 seconds. The main parameters used in simulation are desired radius of 2 m, angular velocity of 0.15 rad/s and angular separation between the three UAVs is  $\Delta\theta_D = \frac{2\pi}{3}$  rad.

Fig. 4.10 shows that the team of UAVs is able to successfully encircle the target. The angular separation between the three vehicles is shown in Fig. 4.11, where the vehicles maintain their desired angular separation at  $\frac{2\pi}{3}$  rad.

#### 4.2.2.2 Case #2: UAVs at different initial positions

The robustness of our simulation is shown by different initial positions and angles for the UAVs. The team successfully converges to the desired radius around the target as seen in Fig. 4.12. The first UAV starts from a distance 2 m from the target with angle 0 rad, UAV 2 starts at a distance 1.5 m with angle separation of  $\frac{5\pi}{6}$  rad, while UAV 3 starts at 2.5 m with angle separation of  $\frac{7\pi}{6}$  rad. The radii of encirclement and the angular velocities of the three vehicles are shown in Fig. 4.13, while the angles of separation between the three UAVs are shown in Fig. 4.14. Despite different positions, the team of UAVs successfully converges to all required values.

#### 4.2.3 Three UAVs encircling a moving target using FL

Using the formulation for moving target shown in Section 3.2.2.3, the UAVs accomplish encirclement of a moving target.

##### 4.2.3.1 Case #1: UAVs encircling a target moving in a straight line

A set of three UAVs with initial positions (10, 0), (5, 10) and (0, 0) successfully encircle a moving target with initial position at (5,5) as seen in Fig. 4.15. This simulation runs for 320 seconds. The main parameters used in simulation are desired radius of 5 m, angular velocity of 0.15 rad/s and angular separation between the three UAVs is  $\Delta\theta_D = \frac{2\pi}{3}$  rad. The moving target is moving at 0.1 m/s.

Fig. 4.16 shows that the team of UAVs is able to successfully encircle the moving target with the desired angular velocity. The angular separation between the three vehicles is shown in Fig. 4.17, where the vehicles maintain their desired angular separation at  $\frac{2\pi}{3}$  rad.

##### 4.2.3.2 Case #2: UAVs encircling a target moving in a sinusoidal motion

The robustness of our simulation is shown by successful encirclement around a sinusoidally moving target. The target is following a sine wave with amplitude 2 m and frequency 0.015 Hz. The team successfully converges to the desired radius around

the moving target as seen in 4.18. The first UAV starts from (10,0), UAV 2 starts at (5,10) with angle separation of  $\frac{2\pi}{3}$  rad from UAV1, while UAV 3 starts at the origin with angle separation of  $\pi$  rad from UAV1. The radii of encirclement and the angular velocities of the three vehicles are shown in Fig. 4.19, while the angles of separation between the three UAVs are shown in Fig. 4.20. Despite different positions, the team of UAVs successfully converges to all required values.

## 4.3 Formation

This section deals with the linear system highlighted in section 3.2.3.

### 4.3.1 Three UAVs in formation flights

The UAV team successfully accomplishes leader-follower formation while maintaining required distance and speed between team members. Line-of-breast, triangular and cross formations are observed in simulation.

#### 4.3.1.1 Case #1: Triangular formation

The starting positions of the UAVs, in two dimensional Cartesian coordinates are for UAV 2, (0, 4), for UAV L, (0, 0) and for UAV 3, (-4, 0). The height through out the experimentation is maintained at 0.5 m using a process model of the Qball-X4 found through system identification algorithms. The UAVs take off, adjust to the proper height and distance and then converges to the required speed based on UAV L. The bird's eye view may be seen in Fig. 4.21. The distances in  $x$  and  $y$  between UAV L and 2 are successfully maintained at 3 m using LMPC and this may be seen in Fig. 4.22. Moreover, the distances between UAV L and 3 are also maintained at the required value of 3 m as seen in Fig. 4.23. The required speed to be maintained while in formation is 0.2 m/s. The speeds of all UAVs, matching the required value, may be seen in Fig. 4.24.

#### 4.3.1.2 Case #2: Cross formation

The success of a triangular formation flight test prompted us to try the cross formation. The UAV successfully accomplishes this formation as seen in Fig. 4.25. The distances between UAVs 2, 3 and the leader are 3 m as seen in Case #1 while UAV 4 maintains 6 m with the leader. The correct position of UAV 4 with respect to UAV L may be observed in Fig. 4.26. The speeds of all UAVs are seen in Fig. 4.27 and converge to the required speed of 0.2 m/s in the x direction.

### 4.4 Tactics Switching

The control strategy discussed in section 3.3 is successfully implemented in simulation on a multi-UAV team consisting of three vehicles. The objective of these simulations is to show that the LMPC policy designed is fit for a leader-follower formation and dynamic encirclement. Our requirements are a desired separation distance of 5m between the three UAVs during the formation phase, a radius of encirclement of 10m and an angular separation of  $\frac{2\pi}{3}$  rad during the encirclement phase.

#### 4.4.1 Case #1: One UAV encircling a stationary target

A set of three UAVs with initial positions  $(0, 4)$ ,  $(0, 0)$  and  $(0, 4)$  successfully form a line abreast formation with a desired distance of 5m between each other. The target is located at  $(35, -2)$  but the UAVs are not aware of it in the beginning of the flight test. UAV1 senses the target first and informs the other UAVs in its communication radius of the presence of the target. UAV1 takes the decision to switch to the encirclement tactic while the other two members in the team take the decision to continue in the formation tactic. This simulation runs for 240 seconds and its overall result may be seen in Fig. 4.28. The main parameters used in simulation are desired separation distance of 5m, desired radius of 10 m and encirclement angular velocity of 0.15 rad/s. Fig. 4.29 represents the speed of each UAV in the team during the formation flight phase where we can see that each UAV matches the other flockmate's

speed of 0.2 m/s. Moreover, Fig. 4.30 shows the desired radius and angular velocity for UAV1 during the encirclement phase. During both tactics, the UAVs converge to the proper requirements highlighted above.

#### 4.4.2 Case #2: Three UAVs encircle a stationary target

A team of three UAVs flying in a line abreast formation with a distance of 5m between each other switch to a dynamic encirclement tactic around a moving target with a desired radius of encirclement of 10 m, angular velocity of 0.05 rad/s and an angular separation of  $\frac{2\pi}{3}$  rad. The initial positions of the UAVs are (0, 4), (0, 0) and (0, -4) and the target is located at (35,-5). The objective here is to show that the UAVs may accomplish dynamic encirclement by controlling their own radii with respect to the target, their angular velocities and the angle of separation considering the leading and lagging UAV in the team. Using multiple vehicles in the solution is a suitable and robust testbed for the designed system. This simulation was run for 600 seconds. Fig. 4.31 shows the overall performance of the team. The desired radii and angular velocities are respected as seen in Fig. 4.32. Finally, Fig. 4.33 shows that the UAVs converge to the desired angle of separation while orbiting the moving target.

## 4.5 Conclusion

The simulation results show that the UAVs converge to the proper references and accomplish dynamic encirclement, formation and tactics switching. We can see that the result using TSL for one UAV in Fig. 4.1 and 4.2 has a bigger steady-state error in the radius than the result using FL shown in Fig. 4.6 and 4.7. Moreover, the solution using FL is more robust than that using TSL since we successfully tested the system with UAVs at different positions as seen in Fig. 4.9 and 4.12, and with moving targets as seen in Fig. 4.15. Fig. 4.18 shows another validation of the FL robustness, the UAVs successfully encircling a sinusoidally moving target. Formation, on the

other hand, does not require linearization and offers positive results and robustness. The UAVs, when operating under the leader-follower category, can successfully fly in triangle and cross formations as seen in Fig. 4.21 and 4.25. Combining both control policies along side a switching algorithm, we can see that the switching from one tactic to the other is done with no major perturbations and with good robustness as seen in Fig. 4.28 and 4.31. The experimental results, applied on the Qball-X4, will be shown in the next chapter.

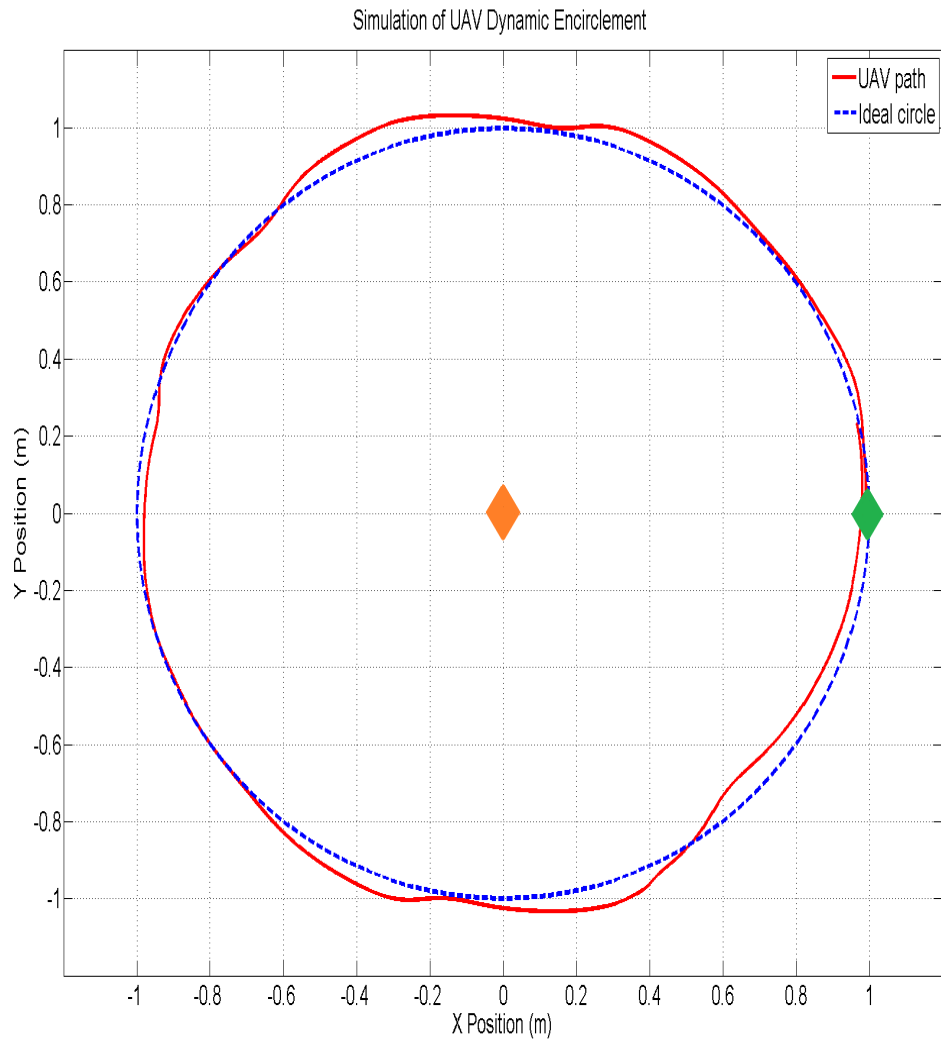


Figure 4.1: Single UAV encircling a stationary target in anti-clockwise direction. The green diamond represents the UAV's starting position of  $(1, 0)$  while the dashed blue line shows a reference circle. The orange diamond represents the stationary target at the origin.

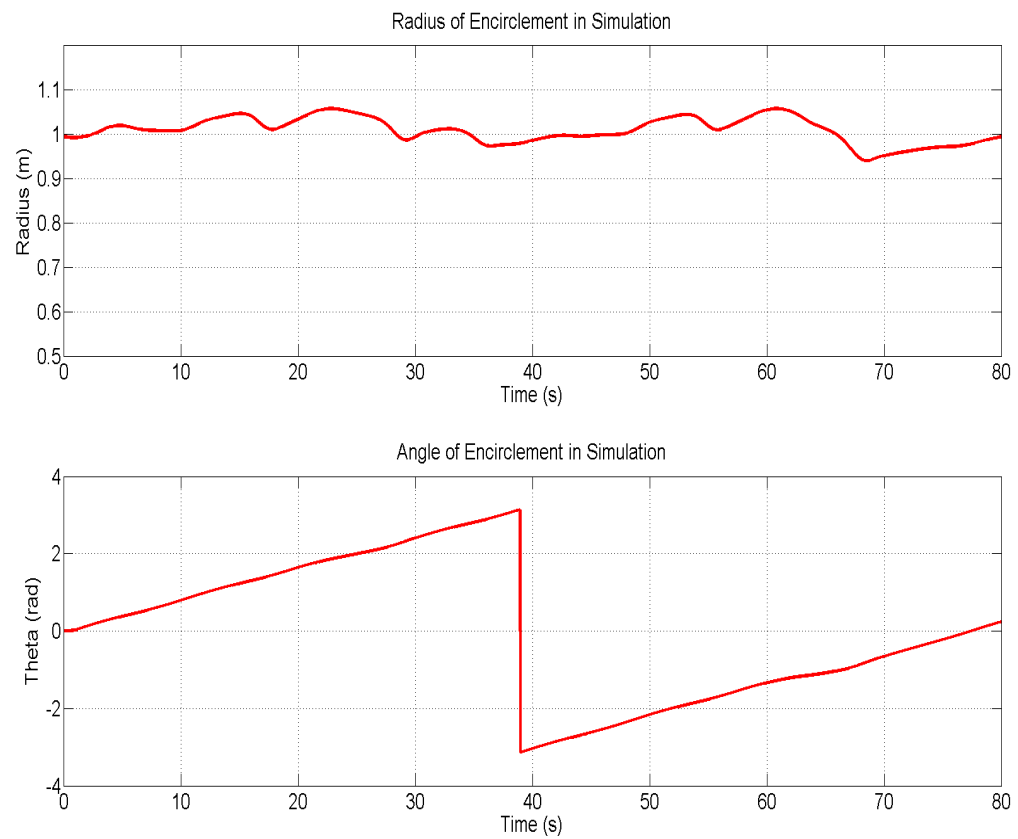


Figure 4.2: Radius and angle of encirclement for a single UAV around a stationary target. Notice that the radius steady-state error is less than 10 %.

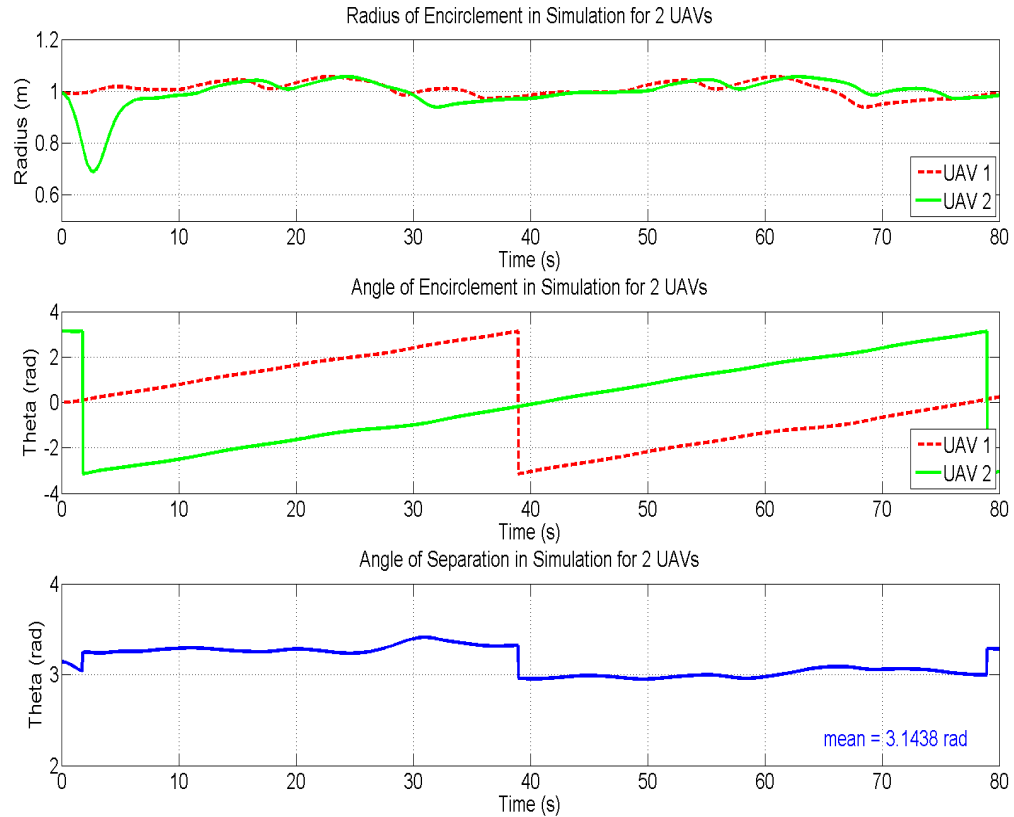


Figure 4.3: Radii, angle of encirclement and angle of separation for the case of 2 UAVs, starting at  $(1, 0)$  and  $(-1, 0)$ , encircling a stationary target. The dashed red line represents UAV 1 while the green line represents UAV 2. The blue line shows the separation angle between both UAVs.

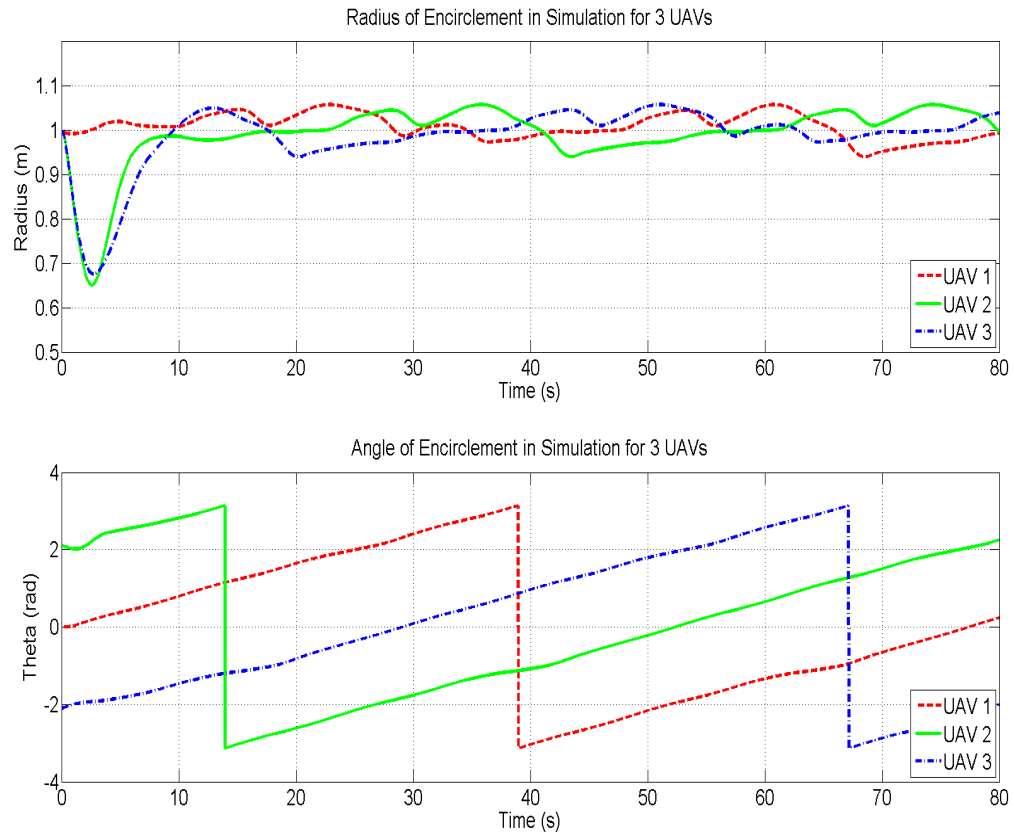


Figure 4.4: Radii and angle of encirclement for the case of 3 UAVs, starting at  $(1, 0)$ ,  $(-0.5, 0.86)$  and  $(-0.5, -0.86)$ , encircling a stationary target. The dashed red line, green line and dashed blue line represent UAV 1, 2 and 3 respectively.

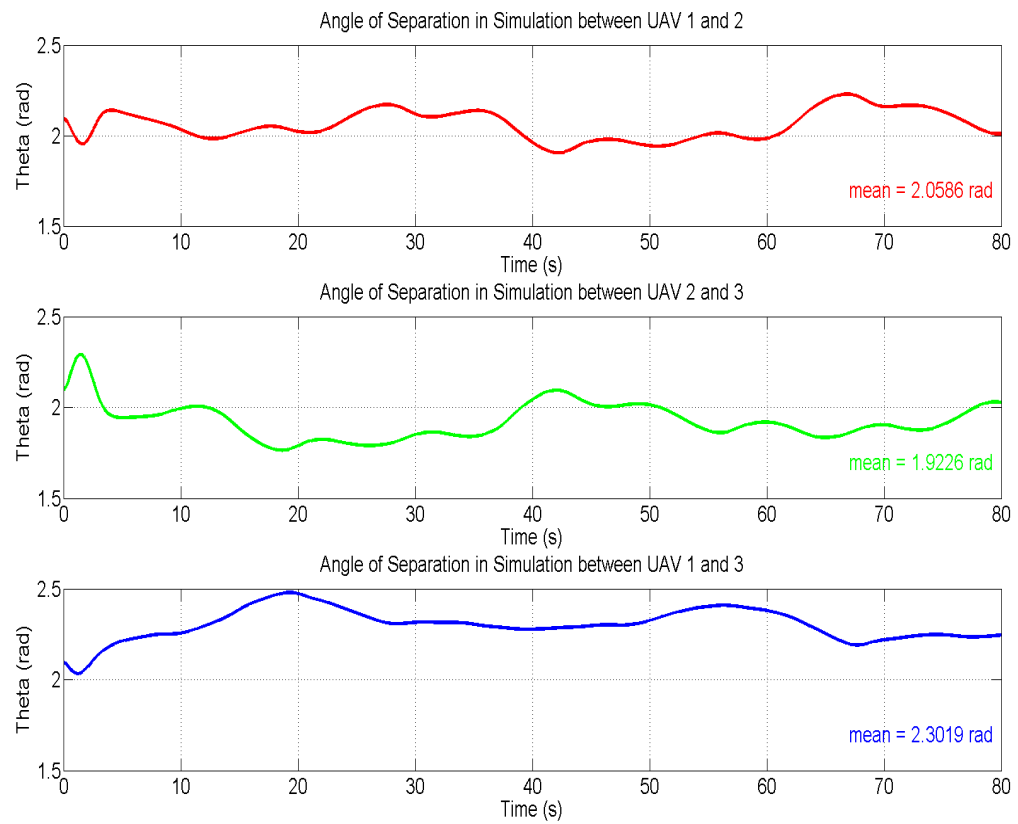


Figure 4.5: Angle of separation between the 3 UAVs. Notice that all the means are close to  $\frac{2\pi}{3}$  rad.

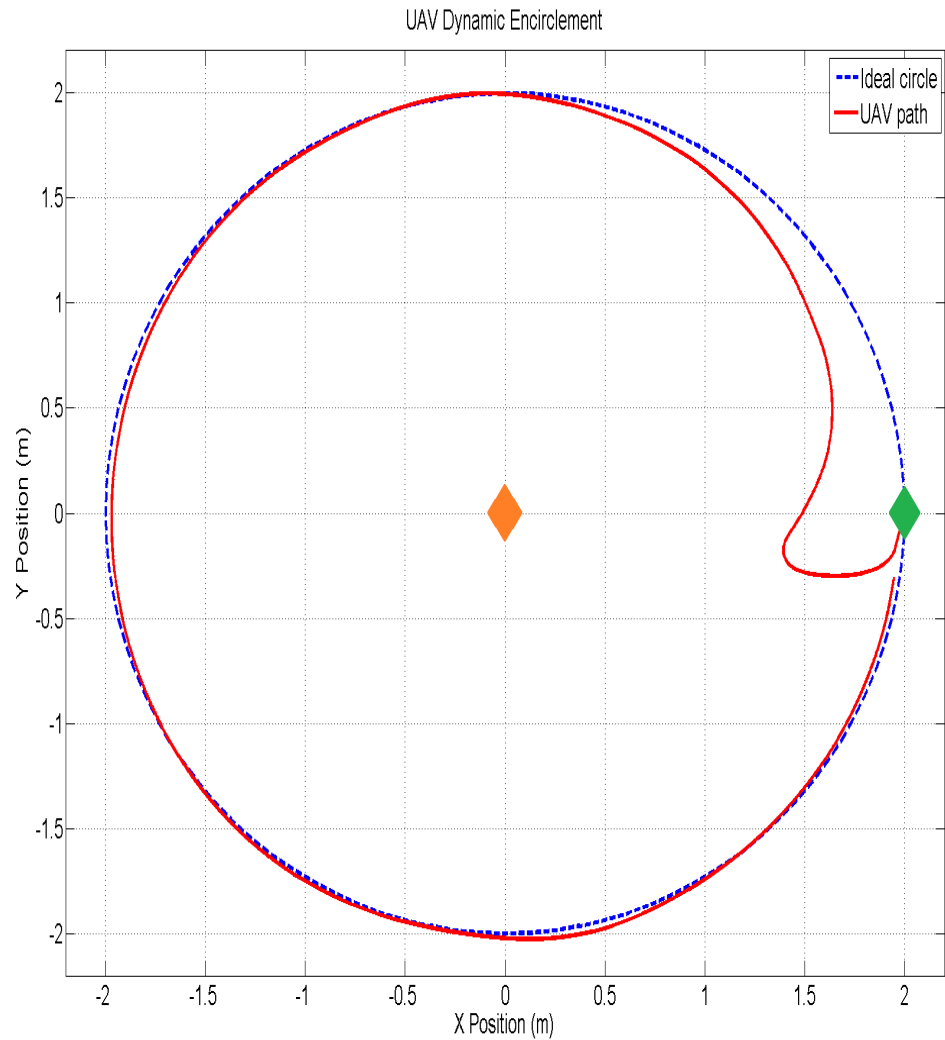


Figure 4.6: Single UAV encircling a stationary target in anti-clockwise direction. The green diamond represents the UAV's starting position of  $(2, 0)$  while the dashed blue line shows a reference circle. The orange diamond represents the stationary target at the origin.

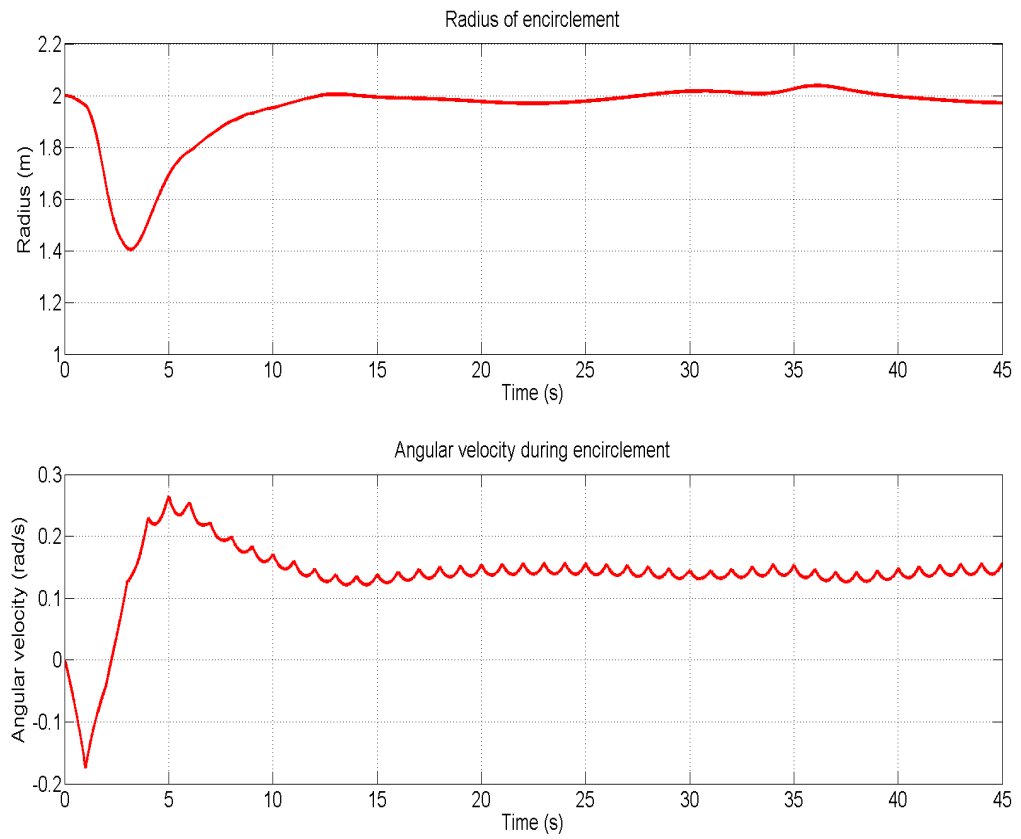


Figure 4.7: Radius and angular speed for a single UAV encircling a stationary target using FL.

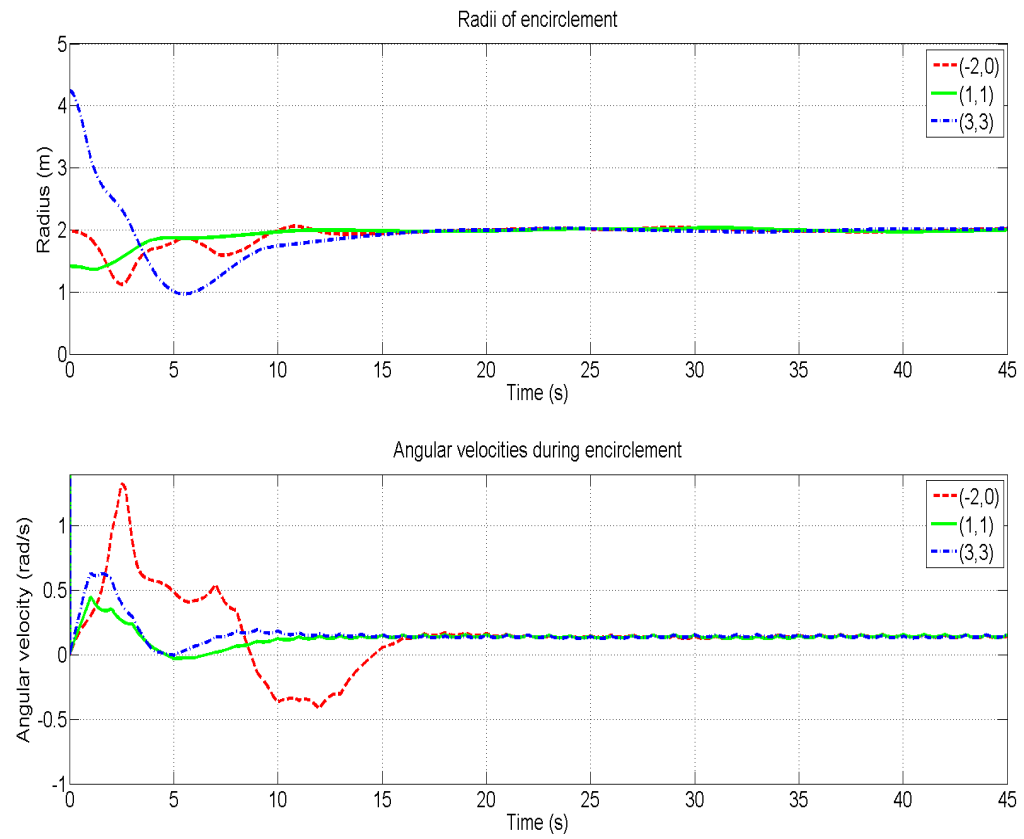


Figure 4.8: Radii and angular speeds for one UAV with different initial positions.

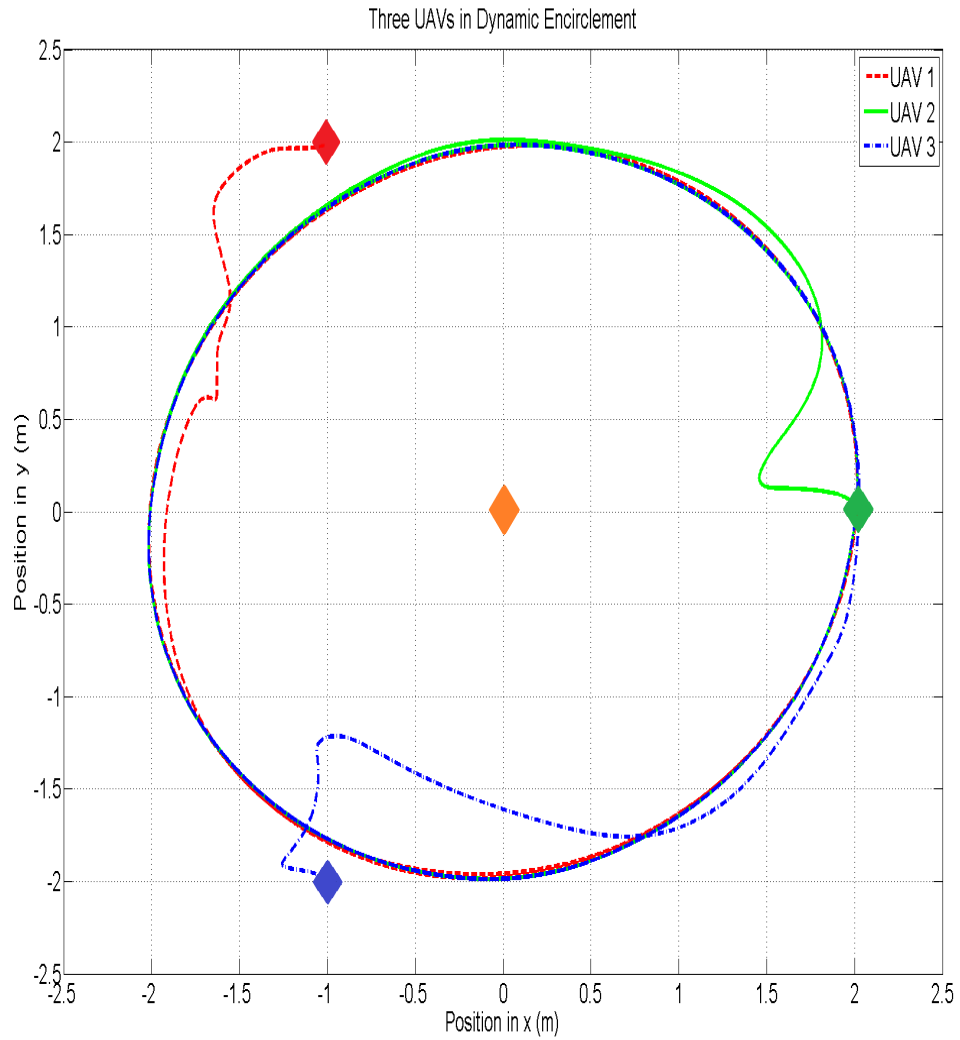


Figure 4.9: Three UAVs, for Case #1, encircling a stationary target using FL. Each UAV is represented by a red, green or blue diamond while the target is shown as an orange diamond.

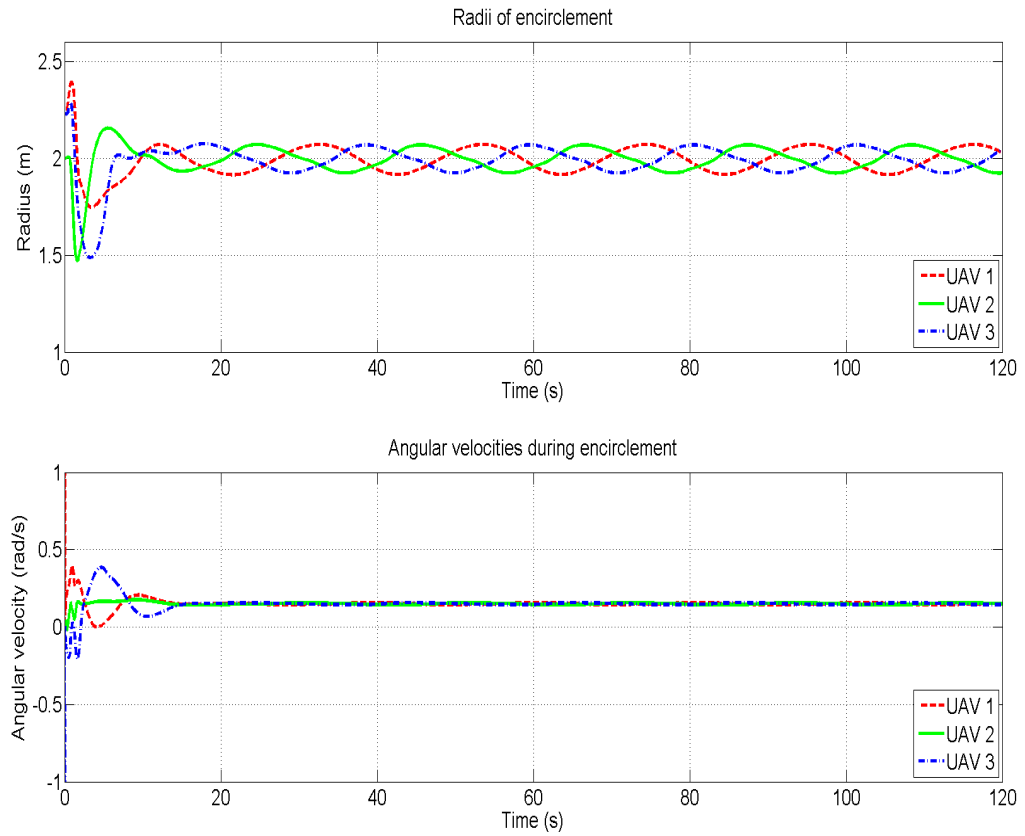


Figure 4.10: The radii of encirclement and angular velocities for three UAVs encircling a stationary target at the origin using FL. UAV 1 is shown in red and is initialized at  $(2,0)$ , UAV 2 is shown in green and is initialized at  $(-1,1.732)$  with angle  $\frac{2\pi}{3}$  rad from UAV 1, while UAV 3 is shown in blue and is initialized at  $(-1,-1.732)$  with angle  $\frac{4\pi}{3}$  rad from UAV 1.

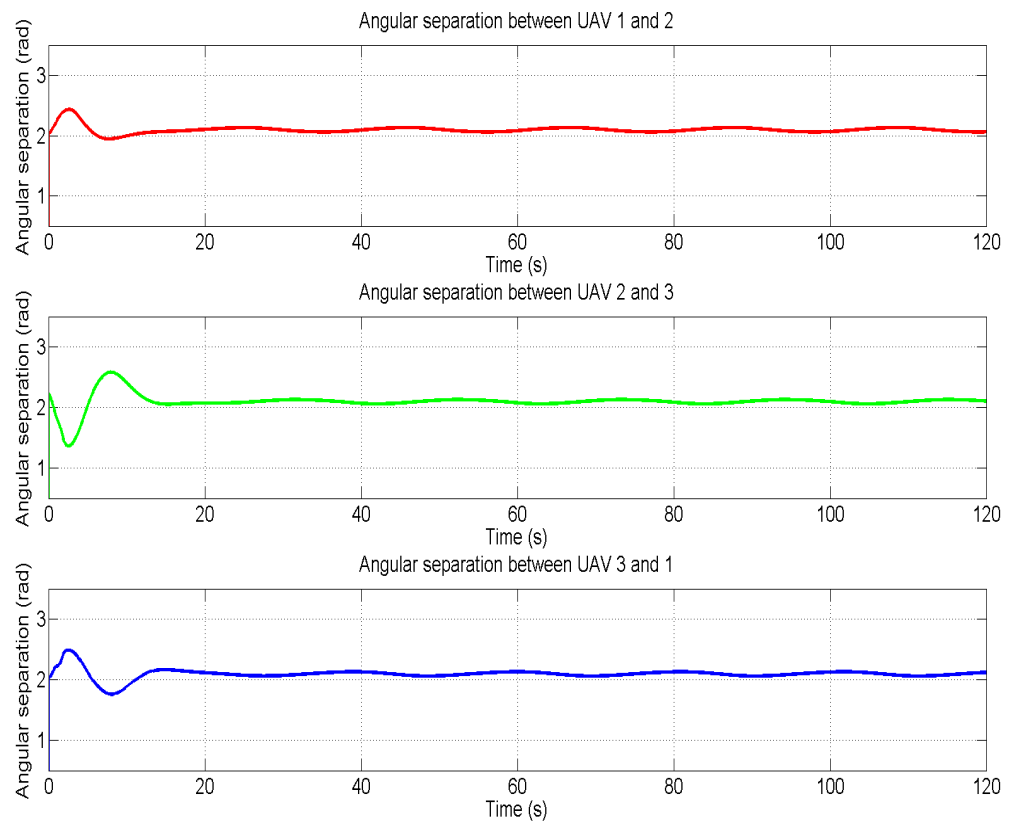


Figure 4.11: Angular separation for three UAVs encircling a stationary target using FL.

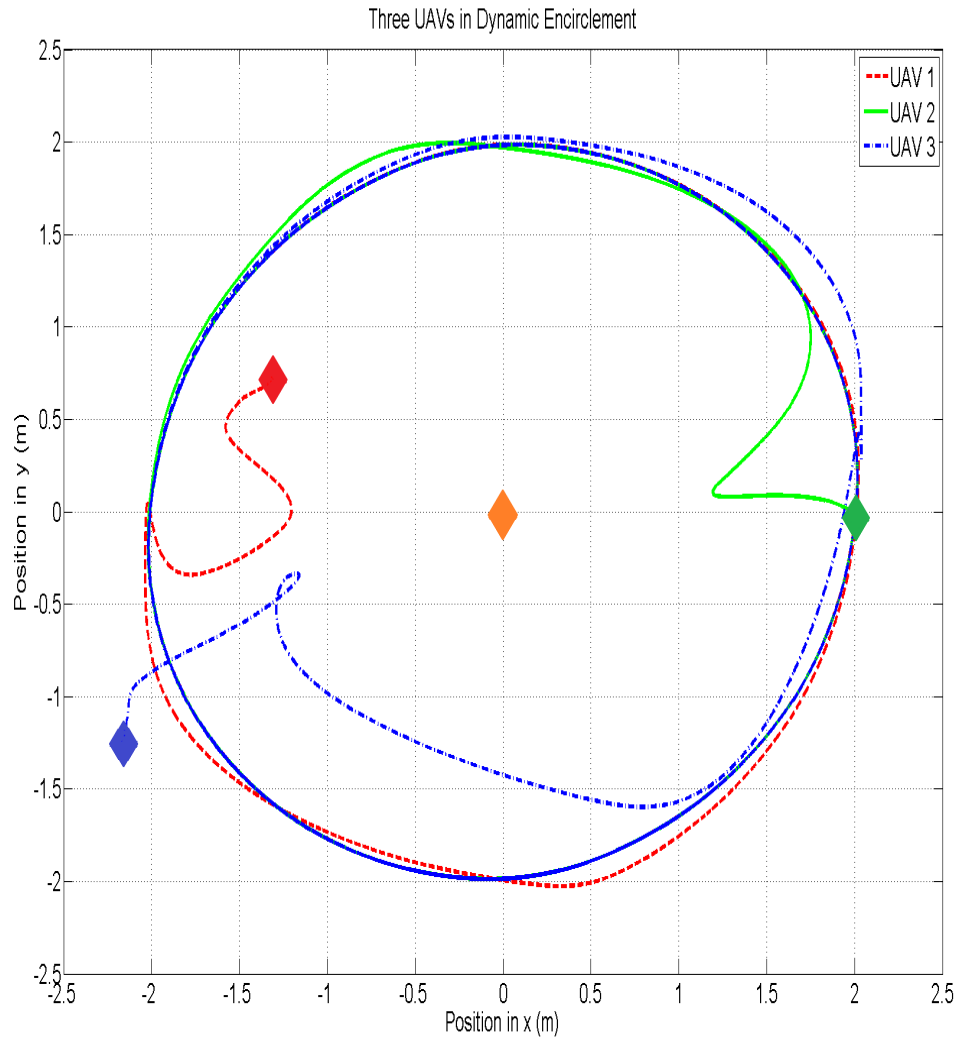


Figure 4.12: Three UAVs, for Case #2, encircling a stationary target. Each UAV is represented by a red, green or blue diamond while the target is shown as an orange diamond.

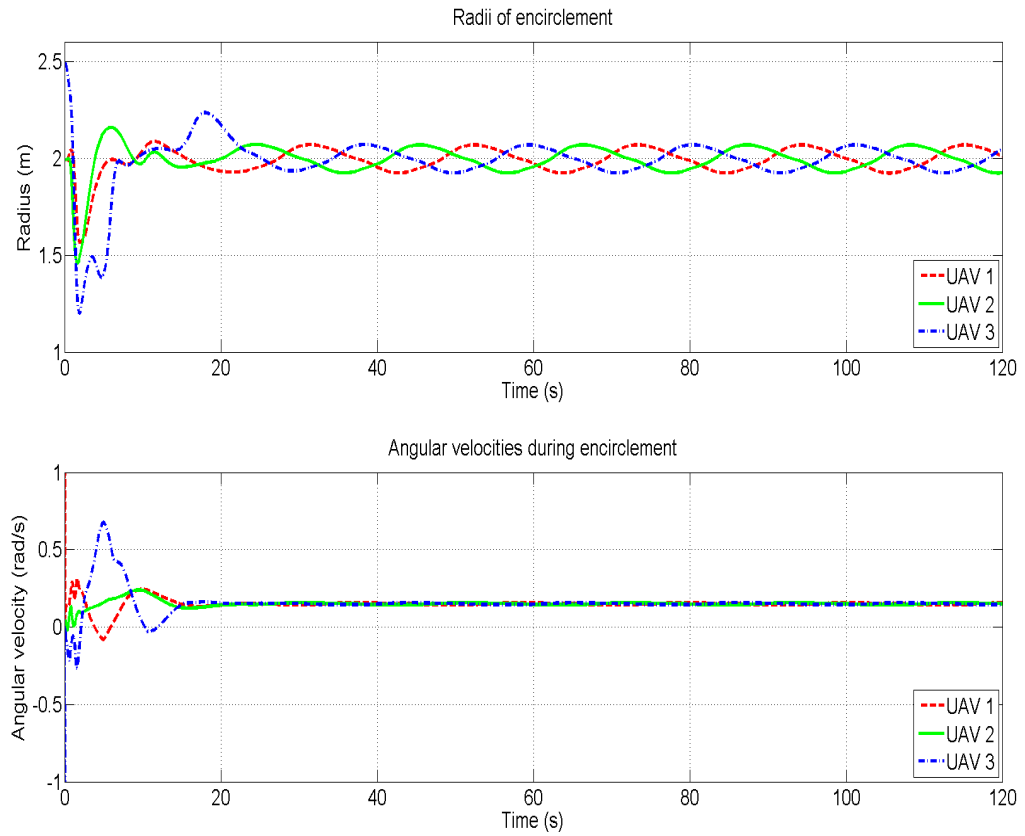


Figure 4.13: The radii of encirclement and the angular velocities for three UAVs encircling a stationary target at the origin. UAV 1 is shown in red and is initialized at  $(2,0)$ , UAV 2 is shown in green and is initialized at 1.5 m from the target with angle  $\frac{5\pi}{6}$  rad from UAV 1, while UAV 3 is shown in blue and is initialized at 2.5 m from the target with angle  $\frac{7\pi}{6}$  rad from UAV 1.

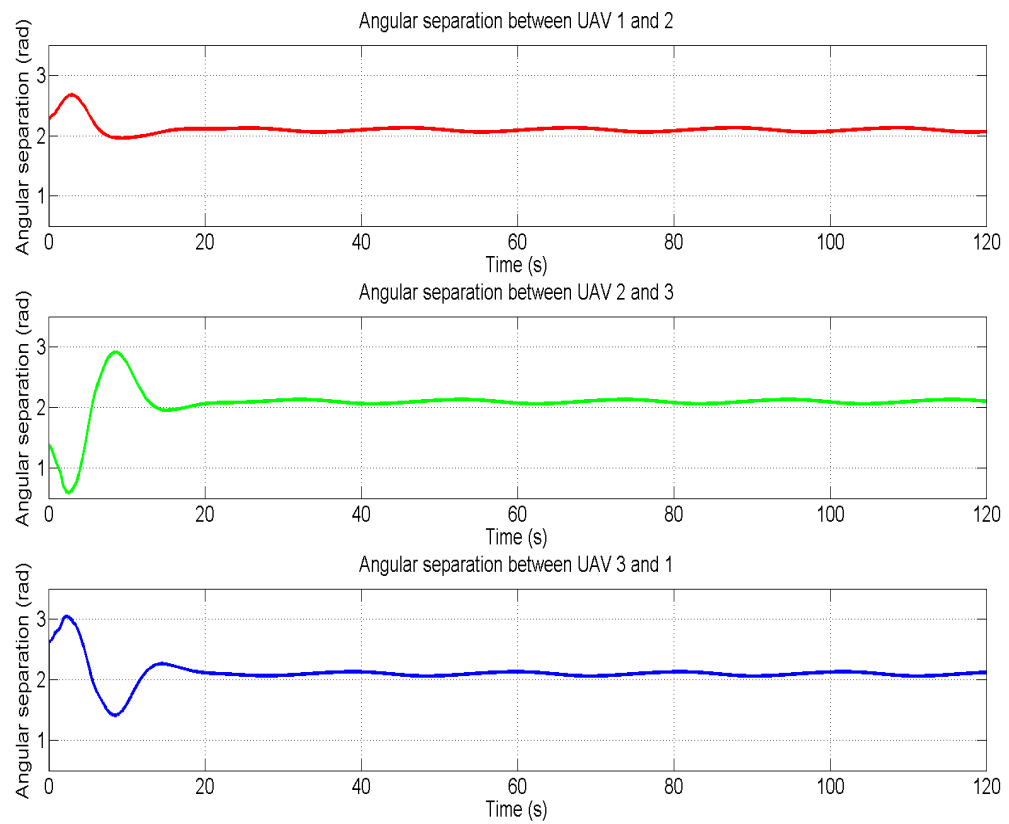


Figure 4.14: Angular separation for three UAVs encircling a stationary target starting at different locations and angles. The UAVs converge to a separation of  $\frac{2\pi}{3}$

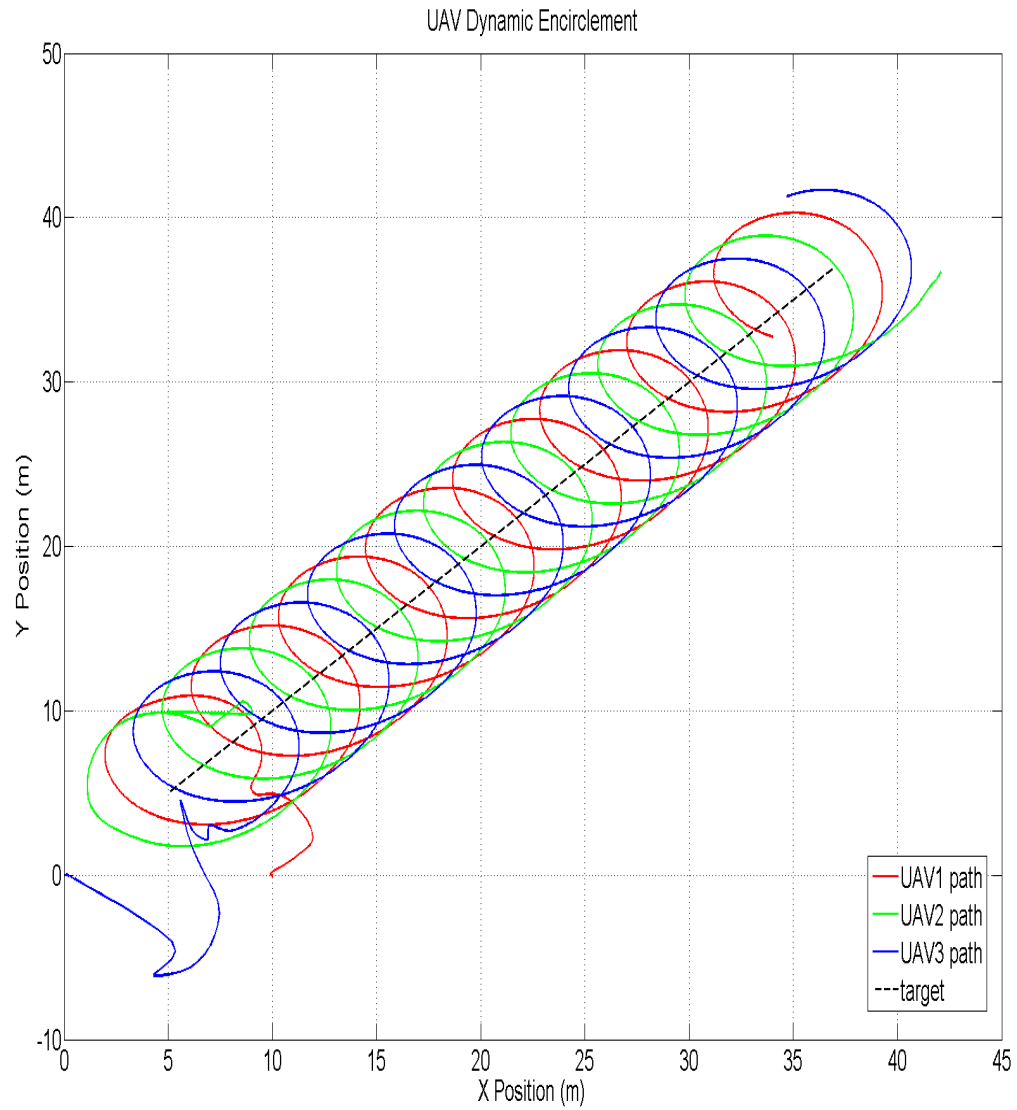


Figure 4.15: Three UAVs, for Case #1, encircling a moving target. Each UAV is represented by a red, green or blue line while the moving target is shown as a black dashed line.

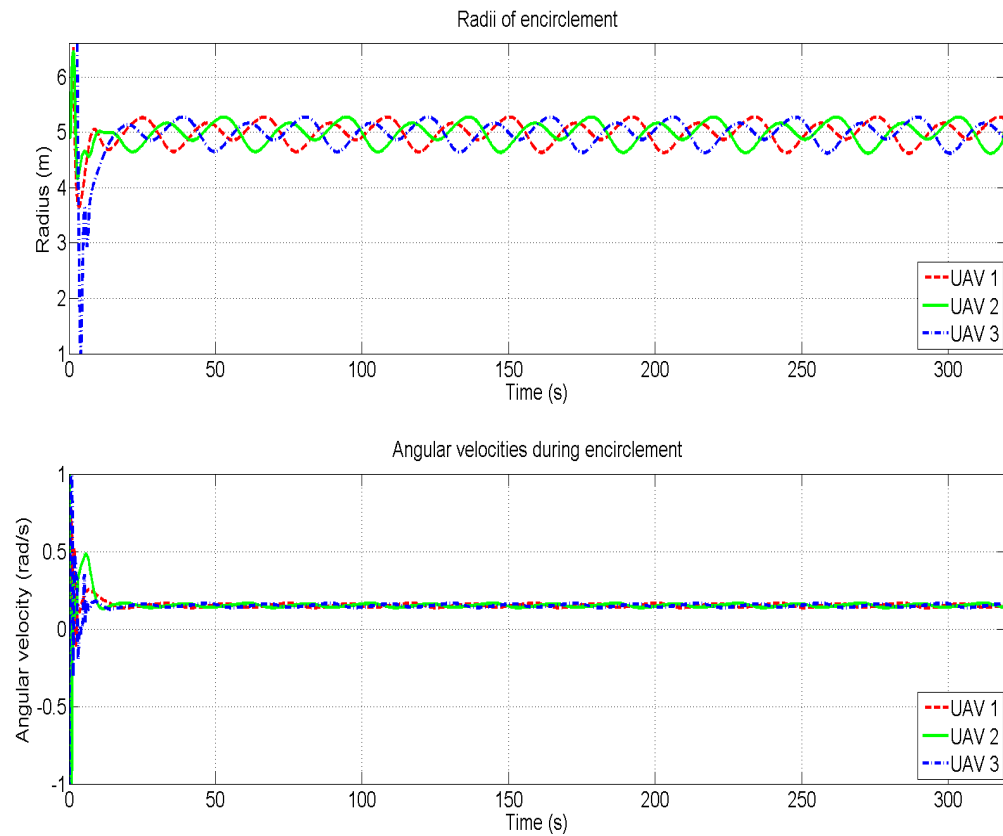


Figure 4.16: The radii of encirclement and angular velocities for three UAVs encircling a target moving in a straight line, starting at (5,5). UAV 1 is shown in red and is initialized at (10,0), UAV 2 is shown in green and is initialized at (5,10) with angle  $\frac{2\pi}{3}$  rad from UAV 1, while UAV 3 is shown in blue and is initialized at the origin with angle  $\pi$  rad from UAV 1.

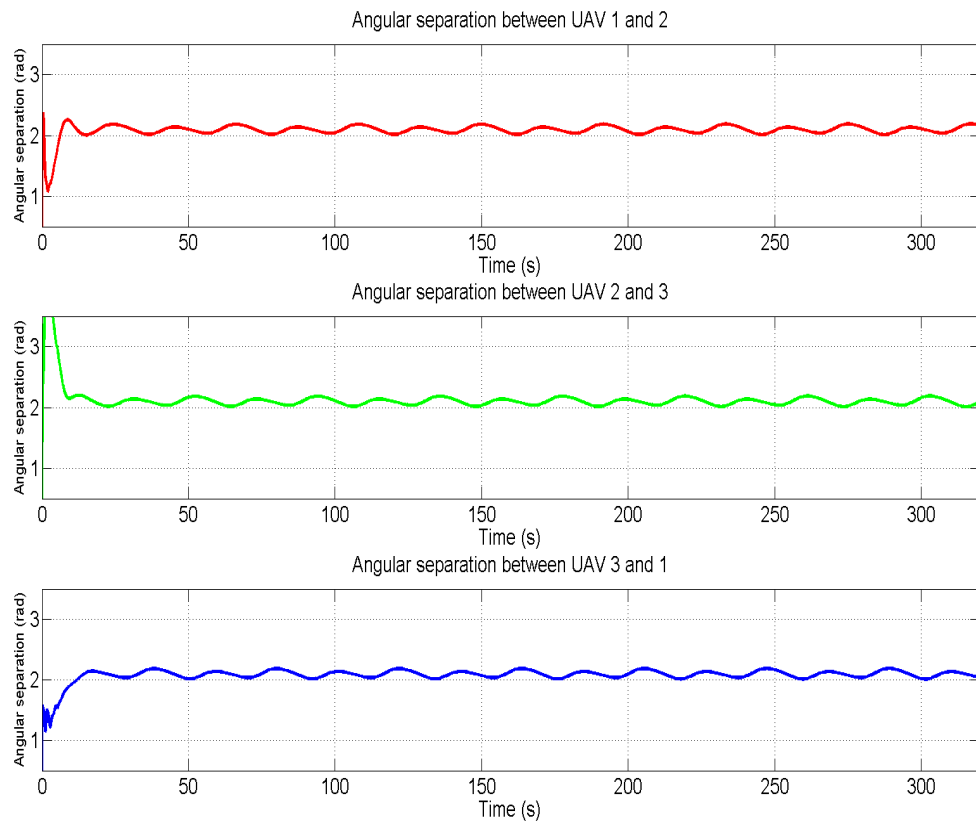


Figure 4.17: Angular separation for three UAVs encircling a target moving in a straight line.

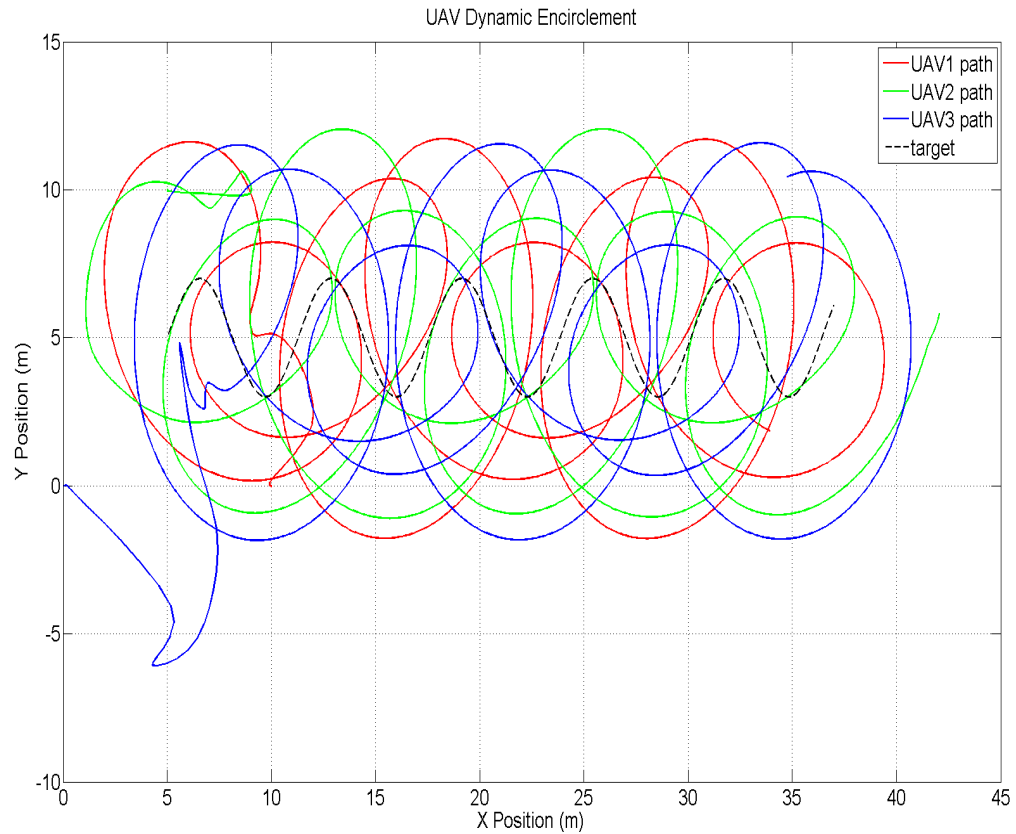


Figure 4.18: Three UAVs, for Case #2, encircling a moving target. Each UAV is represented by a red, green or blue line while the moving target is shown as a black dashed line.

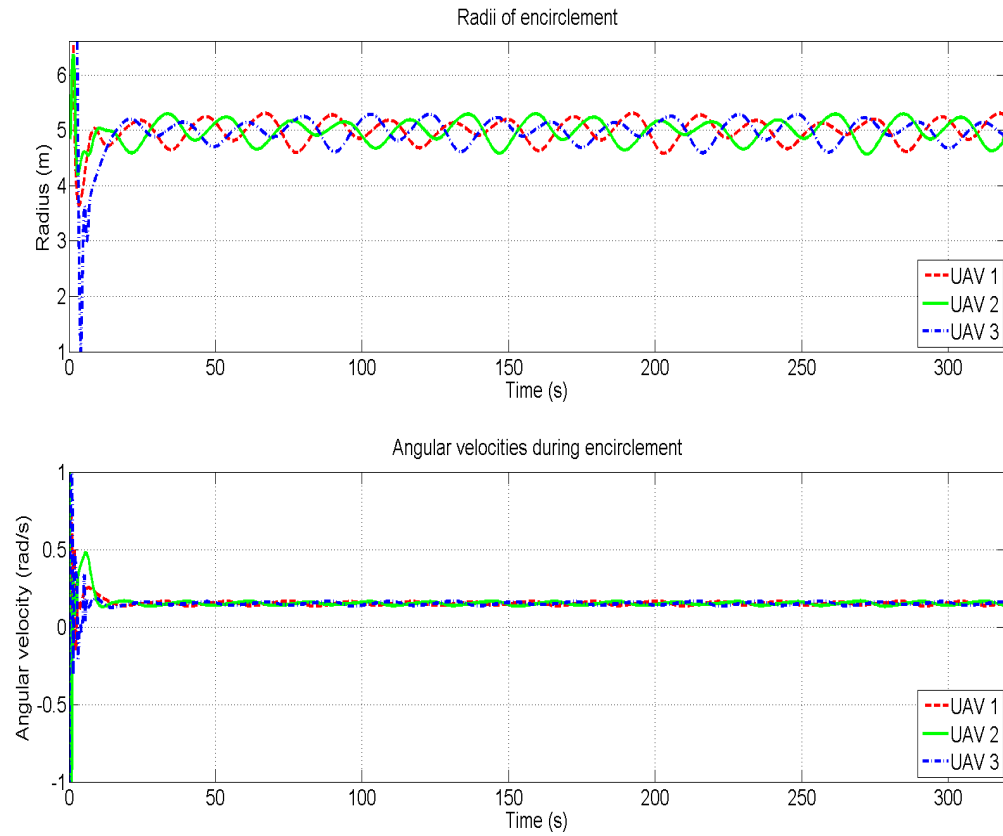


Figure 4.19: The radii of encirclement and the angular velocities for three UAVs encircling a sinusoidally moving target starting at (5,5). UAV 1 is shown in red and is initialized at (10,0), UAV 2 is shown in green and is initialized at (5,10) with angle  $\frac{2\pi}{3}$  rad from UAV 1, while UAV 3 is shown in blue and is initialized at the origin with angle  $\pi$  rad from UAV 1.

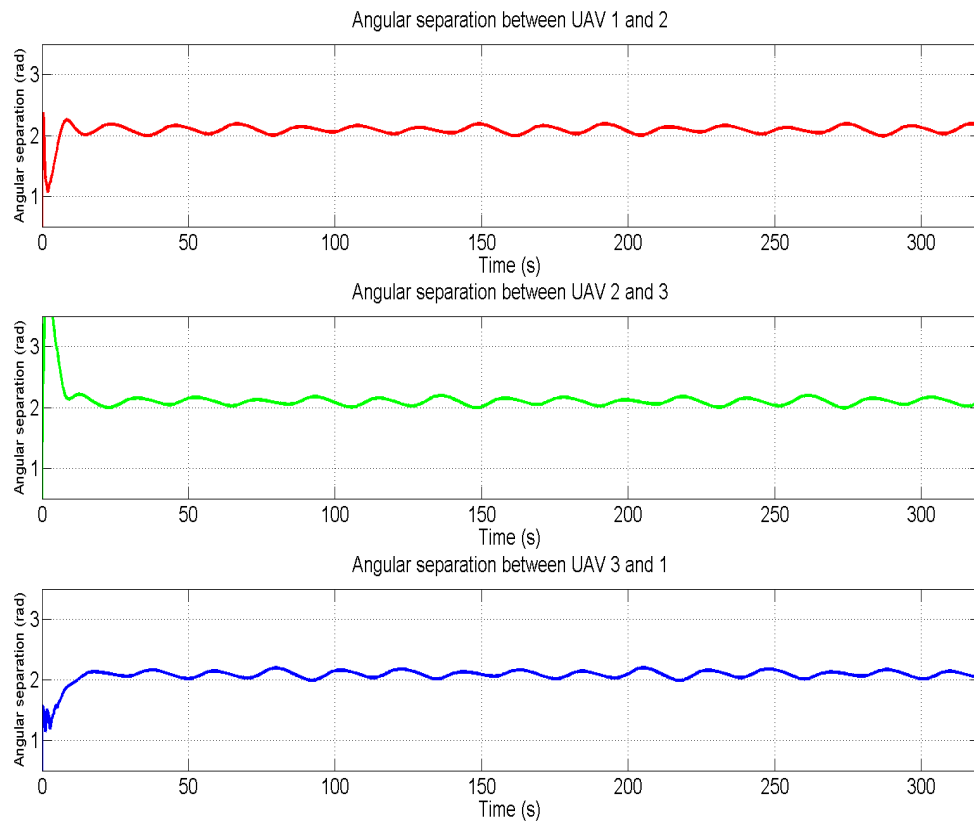


Figure 4.20: Angular separation for three UAVs encircling a sinusoidally moving target starting at (5,5). The UAVs converge to a desired angle of separation of  $\frac{2\pi}{3}$

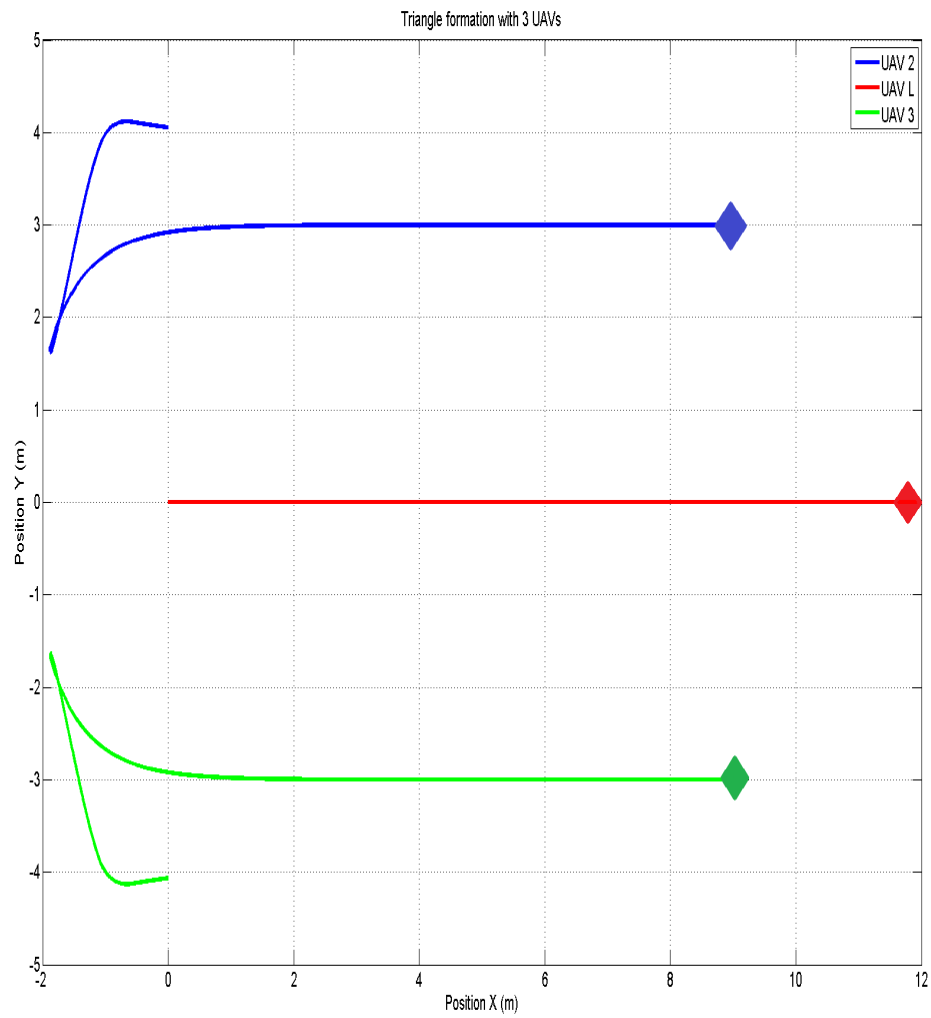


Figure 4.21: UAV team members in triangular formation flying towards the positive x direction. They maintain required distance and speed with each other.

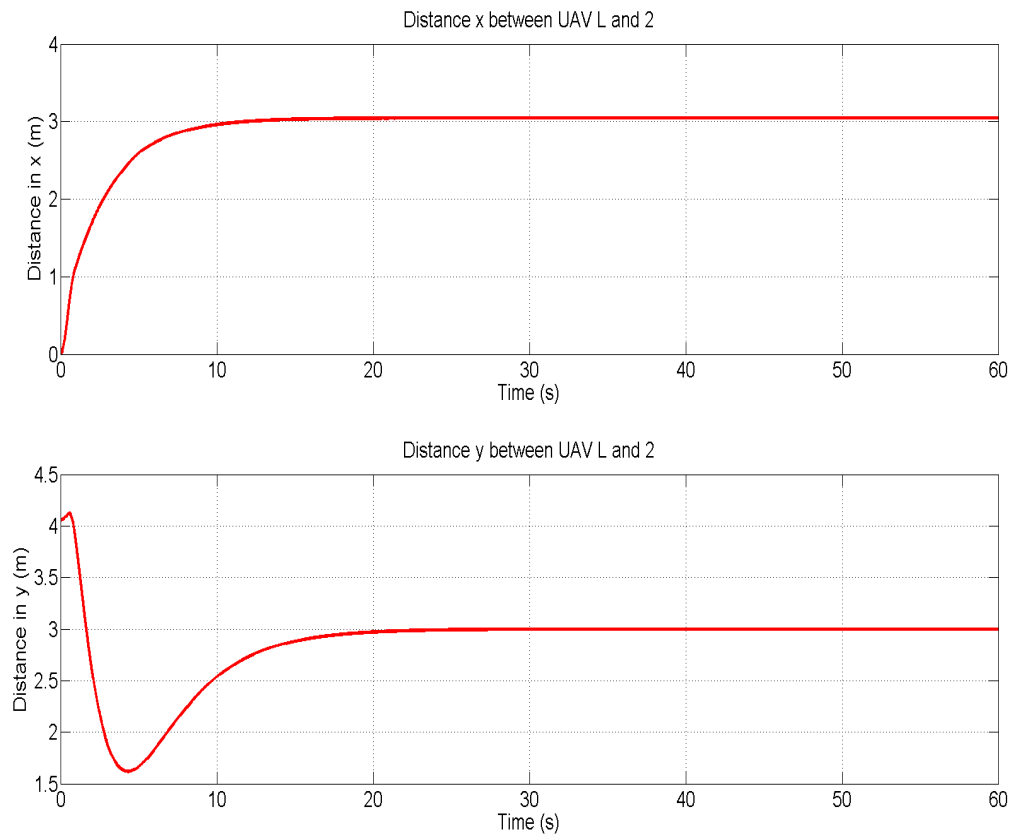


Figure 4.22: The distance in x and y between UAV 2 and UAV L. The distance matches the required value of 3 m.

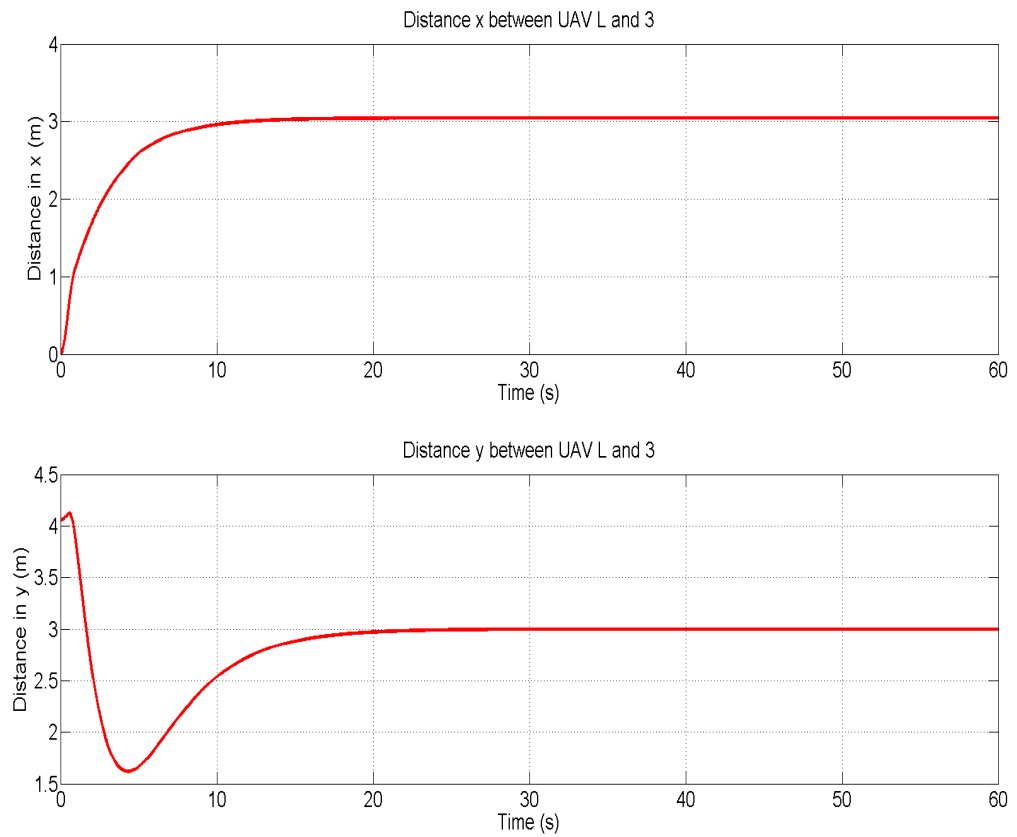


Figure 4.23: The distance in x and y between UAV 3 and UAV L. The distance matches the required value of 3 m.

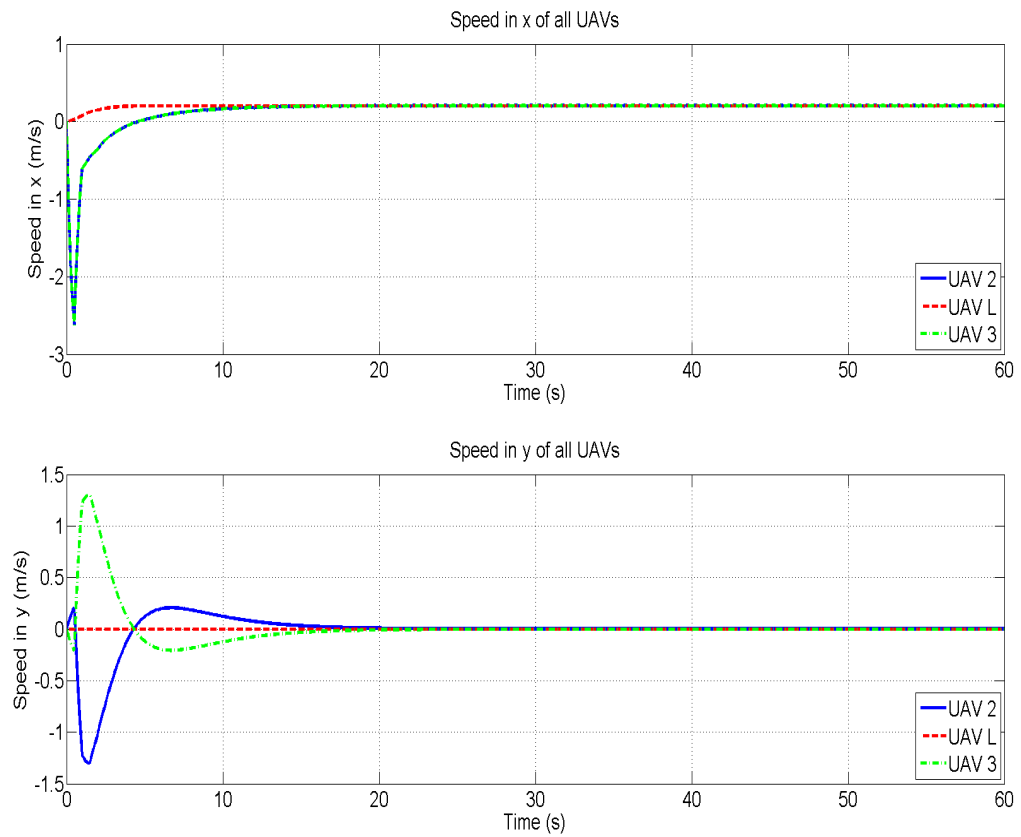


Figure 4.24: The speeds of UAV members during the triangular formation. Since the team travels in the positive x direction, the speed in y converges to 0 m/s.

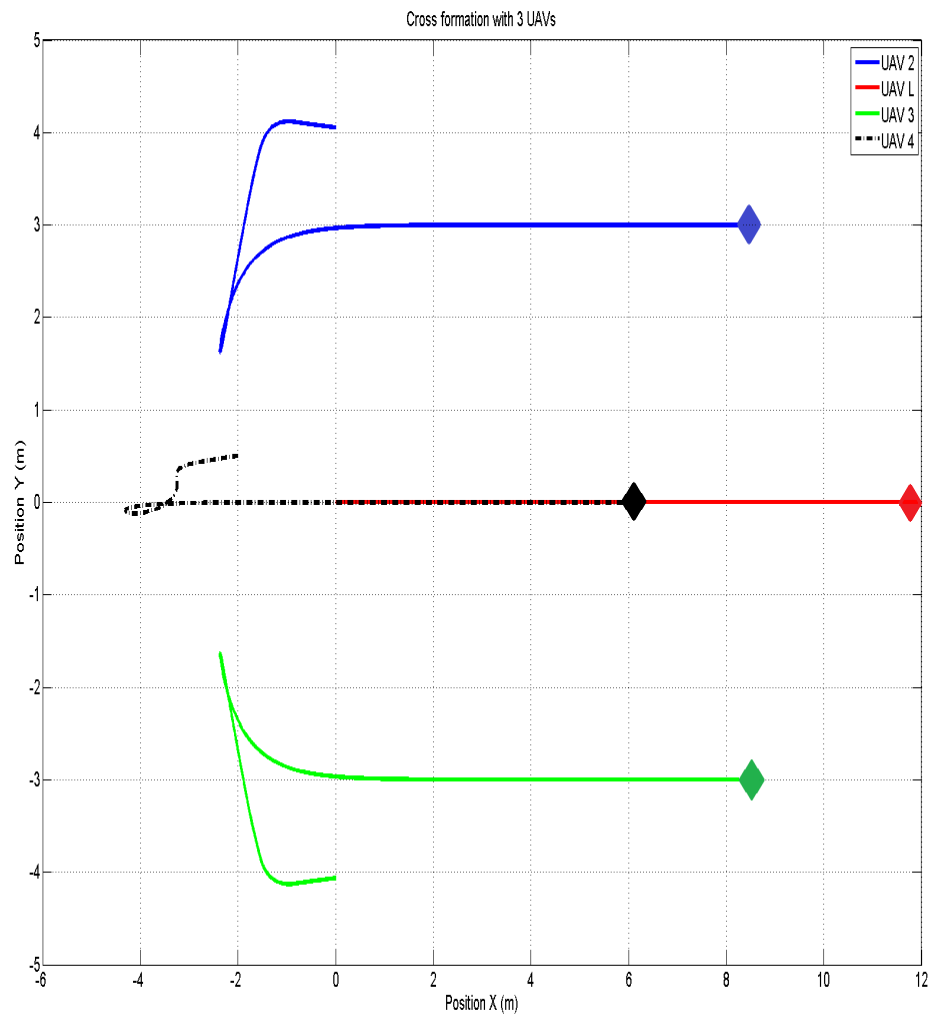


Figure 4.25: UAV team members in cross formation flying towards the positive x direction. They maintain required distance and speed with each other.

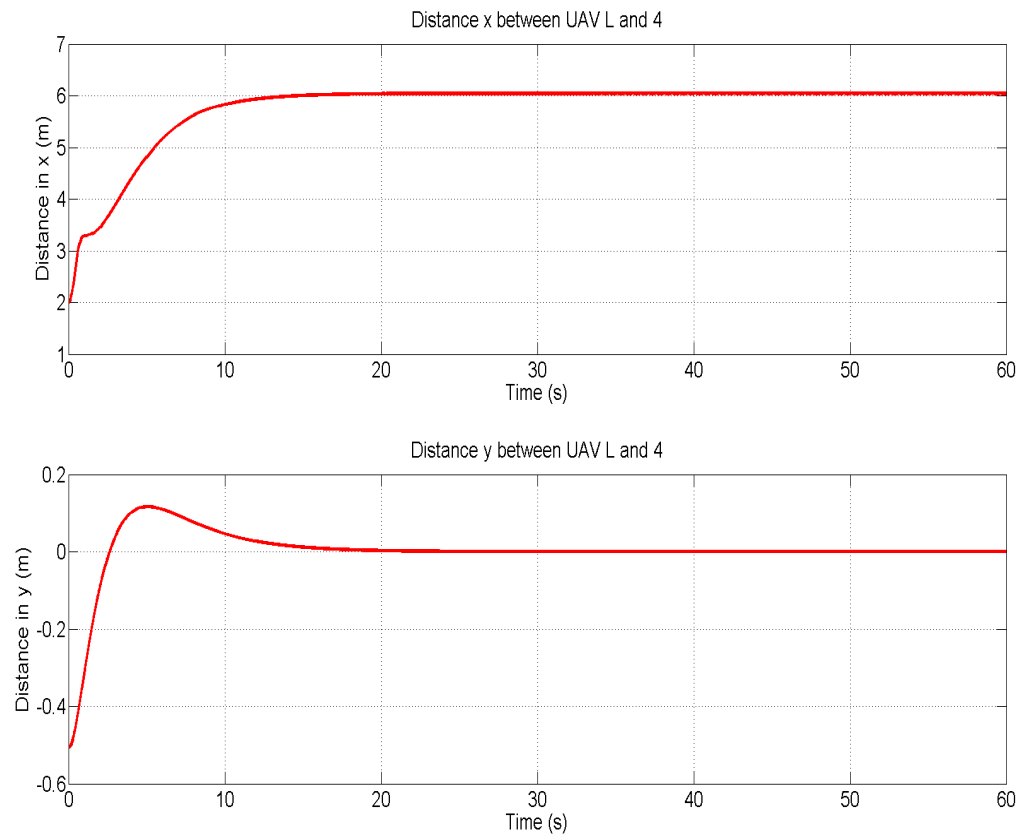


Figure 4.26: UAV team members in cross formation flying towards the positive  $x$  direction. They maintain required distance and speed with each other.

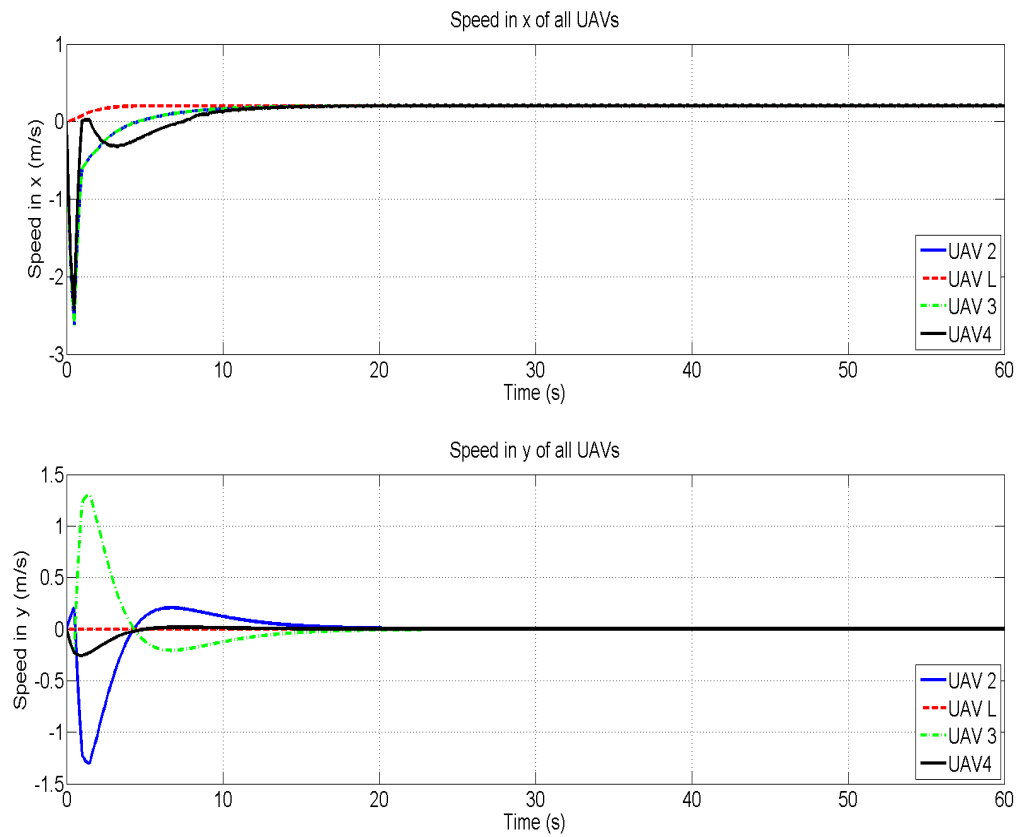


Figure 4.27: The speeds of UAV members during the cross formation. Since the team travels in the positive x direction, the speed in y converges to 0 m/s.

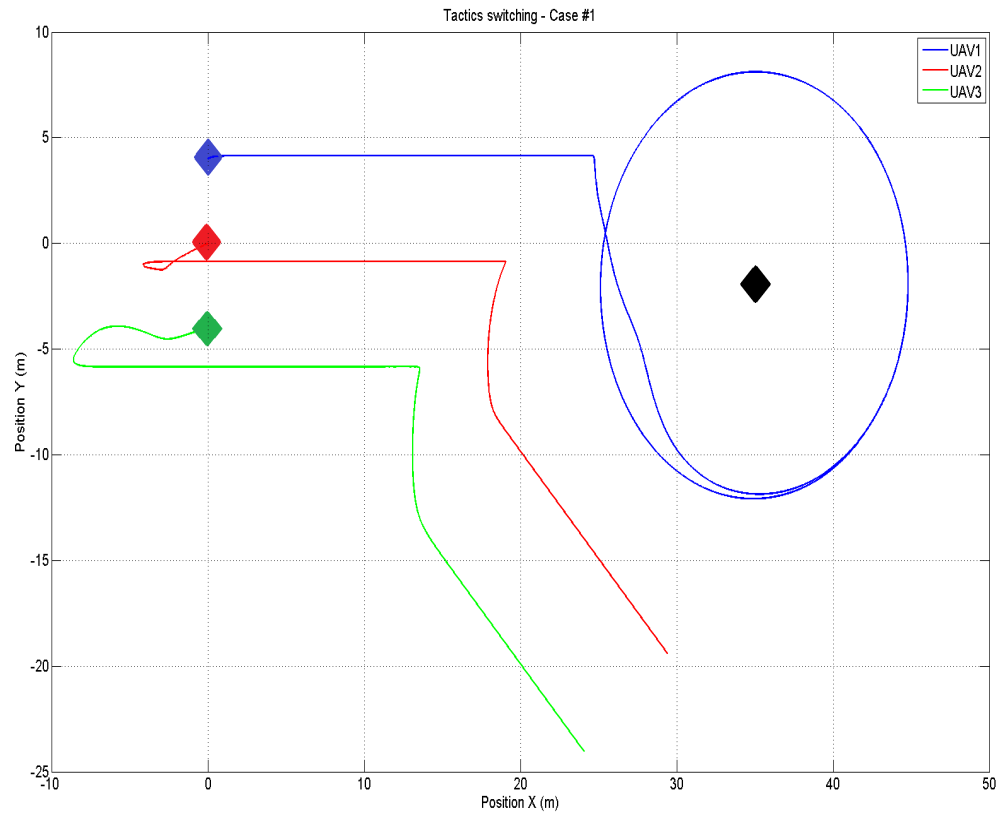


Figure 4.28: UAV team members switching from formation flight to dynamic encirclement tactic while maintaining the required separating distance during the formation phase and the desired radius and angular velocity during the encirclement phase. UAV 1, 2 and 3 are represented by the blue, red and green diamonds respectively while the target is the black diamond.

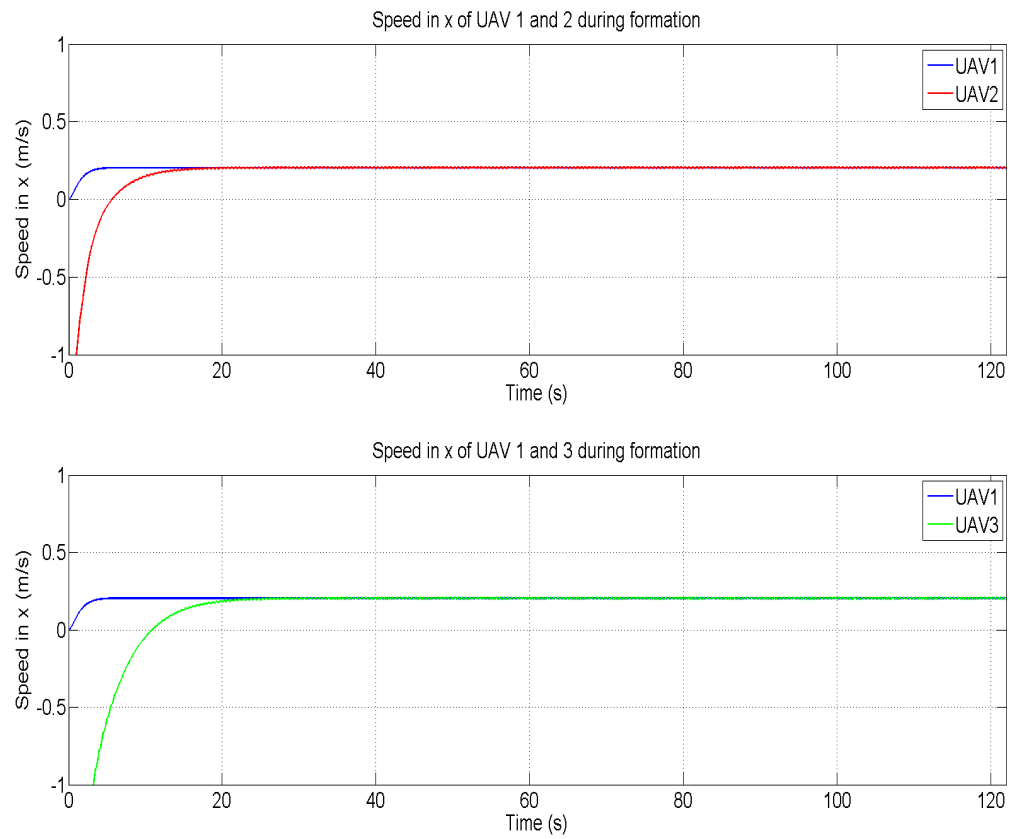


Figure 4.29: The speed of the UAV team in the x-direction during formation phase.

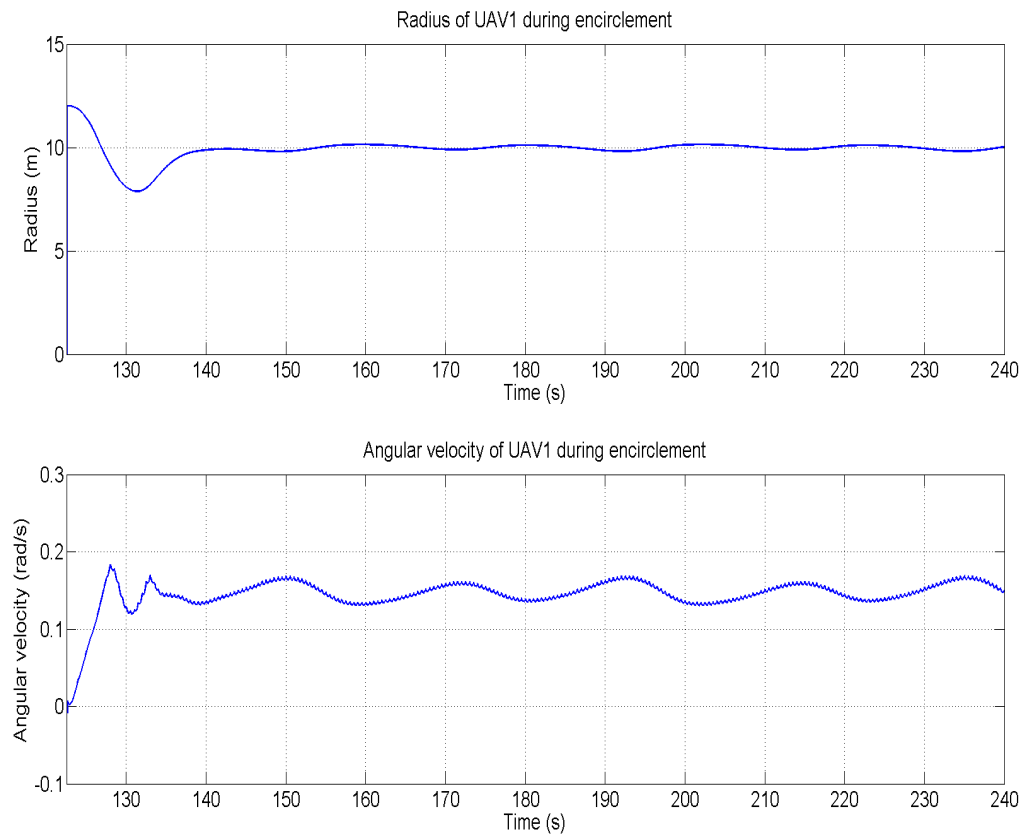


Figure 4.30: The radius of encirclement and angular velocity for UAV1 encircling a stationary target at  $(35,-2)$ .

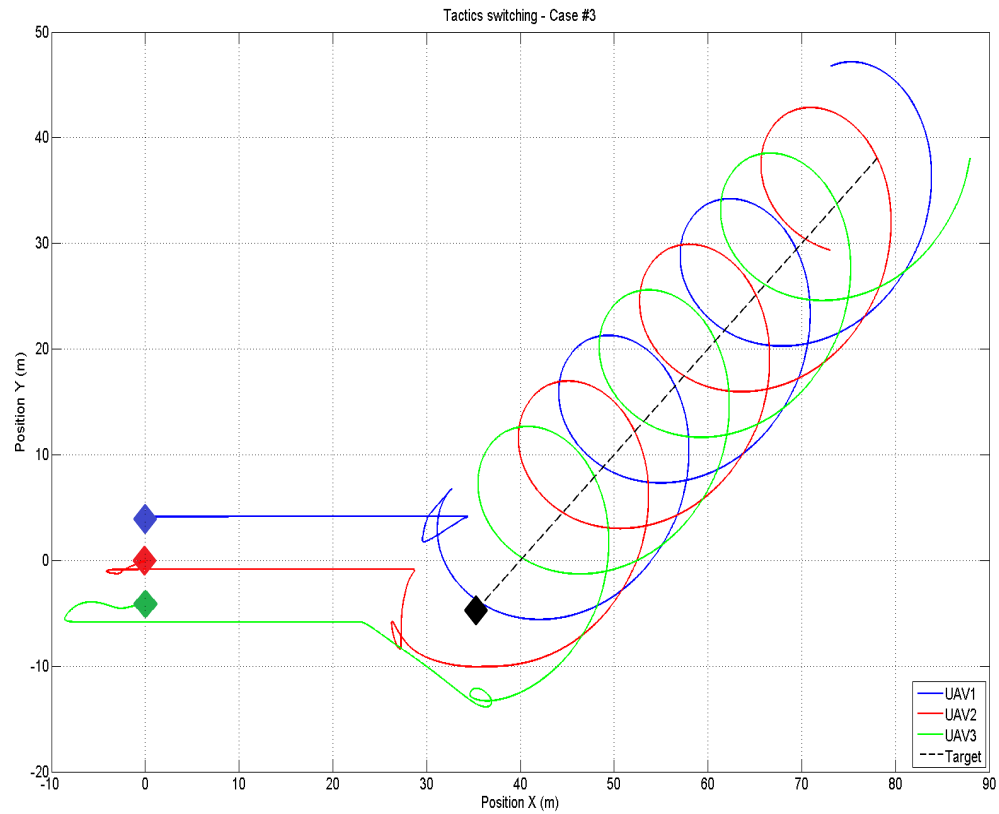


Figure 4.31: Three UAVs, switch from the formation tactic to encirclement tactic around a moving target. UAV 1, 2 and 3 are represented by the blue, red and green diamonds respectively while the target is the black diamond.

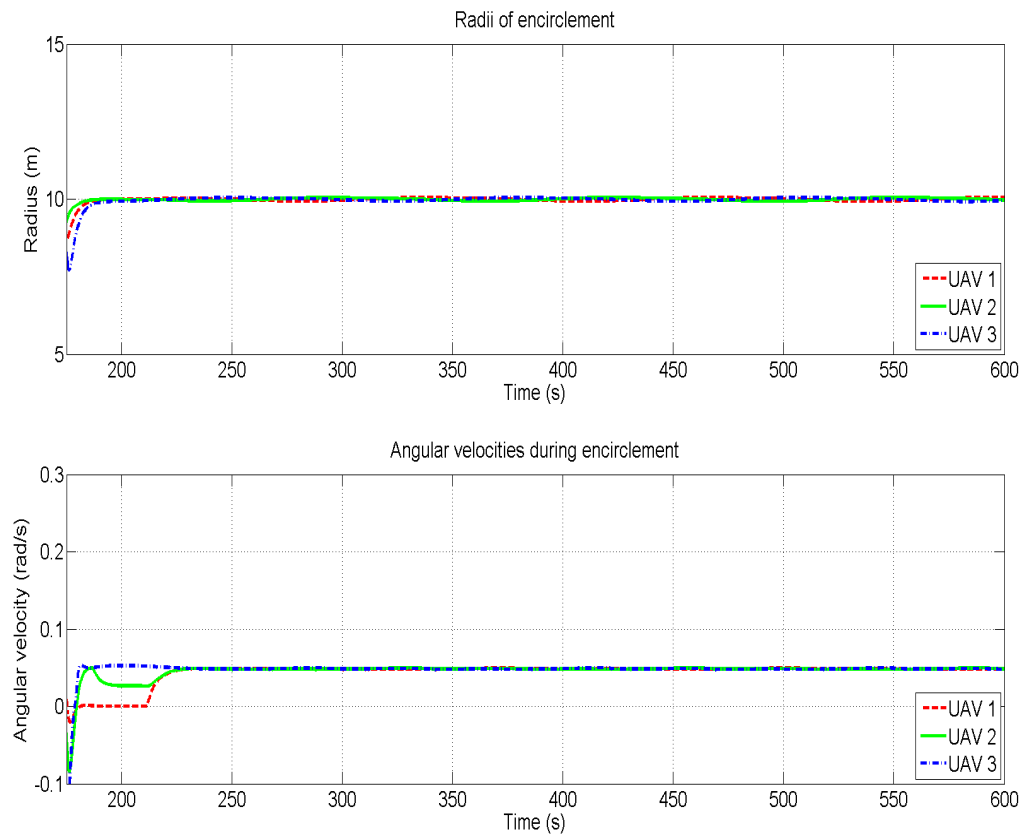


Figure 4.32: The radii of encirclement and angular velocities for three UAVs encircling a target moving in a straight line, starting at  $(35, -5)$ .

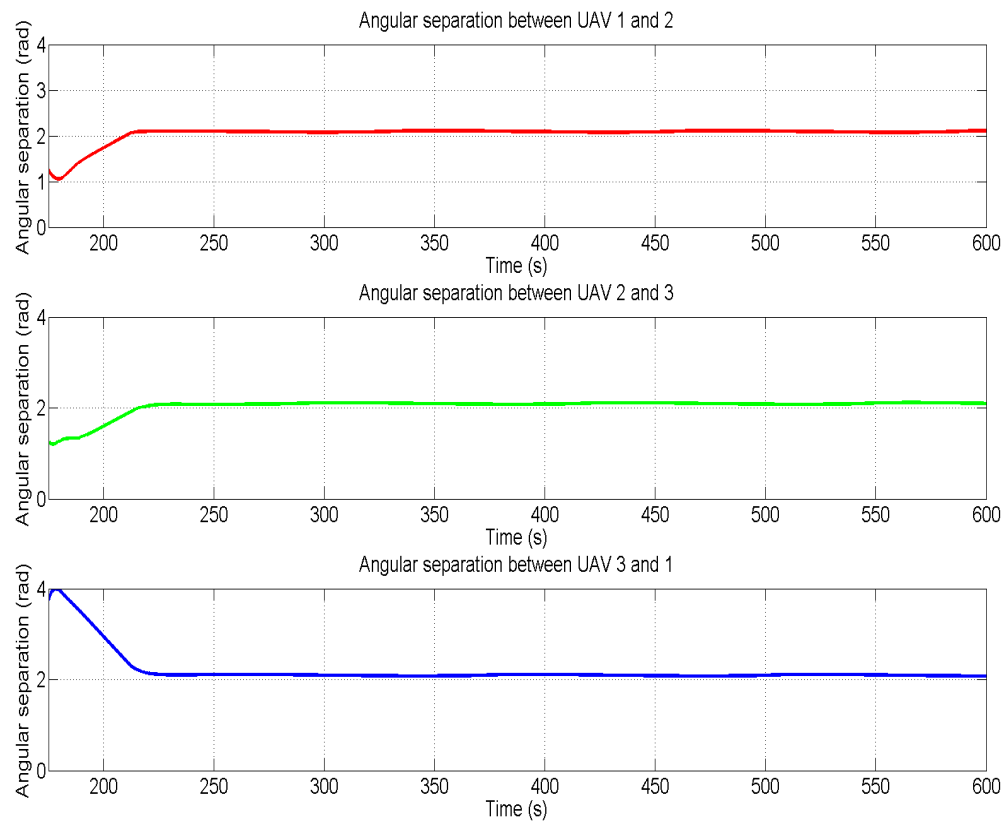


Figure 4.33: Angular separation for three UAVs encircling a target moving in a straight line. All vehicles converge to an angle of separation of  $\frac{2\pi}{3}$  rad.

## Experimental Results

In this chapter, we show the experimental results implemented based on the models explained in Chapter 3. We begin first with a quick description of the Qball-X4 quadrotor followed by an introduction to the experimental area. We then show all the real-world flight tests accomplished starting with one UAV using TSL and including both formation and encirclement tactics. Finally, we combine the tactics into switching flight tests where the stability of the vehicles is shown.

### 5.1 Encirclement using TSL

This section deals with the LMPC and TSL formulations found in section 3.2.2.2.

#### 5.1.1 One UAV encircling a stationary target

This subsection deals with the LMPC policy derived in section 3.1 which is implemented successfully on the Qball-X4.

The reference radius and speed are 1m and 0.1047 rad/s respectively. The experiment runs for approximately 85 seconds. Again, 20 seconds are allotted to the UAV as stabilization time in order to improve the results. This stabilization time consists of the UAV taking off and hovering at the origin. Without the delay, the UAV would have lag time and a slight initial error before converging to the desired reference. The height of the UAV during implementation is maintained at 0.6 m

Fig. 5.1 shows in red the dynamic encirclement of the Qball-X4 around a stationary target. The result converges to the ideal path and respects the constraints highlighted in Section IV. Steady-state error is present in Fig. 5.1 because of the prediction horizon chosen, however, this choice of horizon still maintains algorithmic efficiency. This is a necessary compromise in order to allow real-time implementation of the control scheme. Furthermore, the noise from the PID controllers used and

the OptiTrack sensors contribute to the steady-state error. The protective layer on the Qball, as seen in Fig. 2.5, influences flight dynamics slightly, which adds to the error. The control horizon remains five during all experiments to ensure stability of the UAV. Fig. 5.2 shows the actual UAV position, broken down to its  $x$  and  $y$  components. We can clearly see that the UAV positions converges to the desired path while maintaining the proper height.

The LMPC cost, shown in Fig. 5.3, shows the performance of the LMPC in tracking the reference signal. The lower the MPC cost, the better the performance. This figure shows how the cost in  $x$  is decreasing with time, improving the controller performance as the experiment continues. This means that with time, the lowering of the LMPC cost signals convergence to the ideal path and therefore better performance. The cost in  $y$  is small to begin with, since the UAV is at desired  $y$  at the start of experiment. A small spike is present at 60 seconds due to small disturbance of the UAV during testing. This does not affect performance since the cost at 60 seconds is 0.036 which is very small.

Finally, Fig. 5.4 summarizes the objective of the Linear Model Predictive (LMP) controller. We can clearly see that the radius is maintained very close to the ideal radius of 1m. Furthermore, the speed of the UAV is maintained at an average of 0.1139 rad/s, very close to the required 0.1047 rad/s. This is found by calculating the slopes of the angular position  $\theta$  found in Fig. 5.4. The angular velocity of the UAV is almost the required one of 0.1m/s. The Qball-X4 successfully encircled the stationary target while maintaining the required radius and angular velocity.

### 5.1.2 One UAV encircling a stationary target using TSL

A Qball-X4, positioned initially at  $(1, 0)$  successfully encircles a stationary target located at the origin. We run the vehicle during this test for 75 seconds and its height is maintained at 0.6m. Fig. 5.5 shows the overall movement of the Qball-X4 around the target. We can see the Qball-X4 accomplishes one cycle while maintaining the desired radius. Looking at Fig. 5.6, the radius of the UAV stays around 1m with a steady state-error of about 15%. The increase in error and the jittery behavior seen

in Fig. 5.5 is due to the ground disturbance generated by the indoor flying UAV. The spike seen at 10 seconds in Fig. 5.6 is due to the takeoff of the vehicle where multiple controllers, such as the LMPC dynamic encirclement and the height controller, are all commanding the UAV at the same time. Despite the small increase in the steady-state error, the LMPC policy succeeds in controlling the vehicle in dynamic encirclement. Compared to simulation, seen in Fig. 4.2, the Qball-X4 encircles its target with an angle from 0 to  $\pi$  and from  $-\pi$  to 0 as seen in the second half of Fig. 5.6.

### 5.1.3 Two UAVs encircling a stationary target using TSL

Two Qball-X4 quadrotors, initially positioned at  $(1, 0)$  and  $(-1, 0)$  encircle a stationary target located at the origin. Fig. 5.7 summarizes the flight of both quadrotors. Firstly, the radii are maintained around the desired value of 1m with a small amount of a disturbance due to the wind generated by both UAV in the lab environment. Secondly, similar to the simulation results, the two vehicles complete one cycle around the target as can be seen in the angle of encirclement graph in Fig. 5.7. Thirdly, the separation angle between both quadrotors is 3.17 rad. The collision avoidance system and the LMP controllers managed to accomplish the task of dynamic encirclement using two Qball-X4. These results show that LMPC policy was implemented properly on the UAVs in real-time in order to accomplish the desired task.

## 5.2 Encirclement using FL

This section deals with the LMPC and FL formulations found in section 3.2.2.3.

### 5.2.1 One UAV encircling a stationary target using FL

A Qball-X4, positioned initially at  $(0, 1.5)$  successfully encircles a stationary target located at the origin. The flight test lasted 60 seconds with a 20 second stabilization period where the UAV is allowed to reach its desired height of 0.6 m without lateral

movement. The desired radius of encirclement is 1.5 m with an angular velocity of 0.15 rad/s.

The overall movement of the Qball-X4 is shown in Figure 5.8, while the radius and angular velocity of the Qball-X4 are shown in Figure 5.9. Despite the small increase in the steady-state error, the combination between the decentralized LMPC and feedback linearization policy succeeds in controlling the vehicle in dynamic encirclement. We repeat the experiment for different radii (1 m and 1.8 m) with the same desired angular velocity; all tests show positive results. The success of one UAV encircling the stationary target for different radii of encirclement prompted us to apply the system on a scalable multi-UAV platform.

### 5.2.2 Two UAVs encircling a stationary target using FL

Two Qball-X4 quadrotors, initially positioned at  $(0, 2)$  and  $(0, -1)$  encircle a stationary target located at the origin. The flight test lasted 140 seconds with a 20 second stabilization period where the UAV is allowed to reach its desired height of 0.6 m without lateral movement. Figure 5.10 show that the radii are maintained around the desired value of 1.5 m with a small amount of a disturbance due to the wind generated by both UAVs in the lab environment, while the angular speed converge to the desired angular speed of 0.15 rad/sec. Also, the separation angle between both quadrotors converges to the required angle of separation as shown in Figure 5.11. These results show that the designed LMPC policy was implemented properly on the UAVs in real-time in order to accomplish the desired task.

### 5.2.3 Three UAVs encircling a stationary target using FL

Three Qball-X4 quadrotors are used to encircle a stationary target located at the origin. Similar to the previous experiments, Figure 5.12 shows that the radii are maintained around the desired value of 1.5 m with a little amount of a disturbance

due to the wind generated from the rotors of the three UAVs in the lab environment. Also, the angular speed of the three quadrotors converge to the desired angular speed 0.15 rad/sec. The angles of separation between the three UAVs are shown in Figure 5.13, where the angles converge to the desired separation angle  $2\pi/3$  rad.

### 5.3 Formation

This section deals with the linear system found in section 3.2.3.

#### 5.3.1 Three UAVs in a line abreast formation

The initial positions for the UAVs are, for UAV 2  $(-2.3, 2.5)$ , for UAV L  $(0, 2.5)$  and for UAV 3  $(2.3, 2.5)$ . The UAVs, travelling in the negative  $y$  direction, successfully accomplish line abreast during a flight test of 120 seconds. The required distance between the members is 1.7 m while the speed is 0.1 m/s. The distance in  $x$  between UAV 2, 3 and UAV L is shown in Fig. 5.14. The distance in  $y$  needs to be 0 m and is seen in Fig. 5.15. The speed of UAV 2 in the  $y$  direction is 0.0934 m/s while the speed of UAV 3 is 0.0948 m/s. This shows that the UAVs match the speed of UAV L flying at a speed of 0.1036 m/s.

### 5.4 Tactics switching

This section deals with the formulation found in section 3.3. In the final stages of this thesis, we combine the different tactics in order to validate our designs on actual Qball-X4 quadrotors. First, three UAVs maintain a line abreast formation going in the negative  $y$  direction. Once at the end of the experimental area, the UAVs change direction with the middle UAV considered as the leader. The target is located at  $(0, 1)$  with the UAVs having a sensor radius of 2 m. The required distance for the formation flight is 1.7 m between UAVs while the desired radius of encirclement is 1 m and the angular velocity is 0.15 rad/s. Fig. 5.16 shows the distance achieved in the  $x$  direction: we can see that the distance of 1.7 m is achieved. Fig. 5.17 shows

the convergence in the  $y$  direction. Finally, Fig. 5.18 shows the radius and angular velocity of the vehicle: the UAV successfully encircles the stationary target.

## 5.5 Conclusion

The experimental results demonstrate the ability of using the proposed LMPC for real-time implementation of the system which is not allowed in the case of NMPC, found in [36], due to the non-convexity of the optimization control problem. Notice that, the experimental results are noisy if compared with the simulation results. The main reason for the noisy response is the wind disturbance effect produced from the rotors of each quadrotor on the other during flying in the lab environment. However, the system is still robust to the disturbances and converges to the desired behavior. The TSL solution, as seen in Fig. 5.5, is similar to the FL solution as seen in Fig. 5.8, but the implementation of the FL solution is easier since it does not require the use of multiple controllers as explained in sections 3.2.2.2 and 3.2.2.3. Due to this ease in implementation and robustness of the proposed solution, we use FL in two and three UAV encirclement as seen in Fig. 5.10 and 5.12. The angle of separation respects the  $2\pi/N$  reference in both cases. Similar to our simulation results, formation and tactics switching is done successfully with the UAV team switching in a stable manner. The encircling UAV during the tactics switching converges to the proper references as seen in Fig. 5.18.

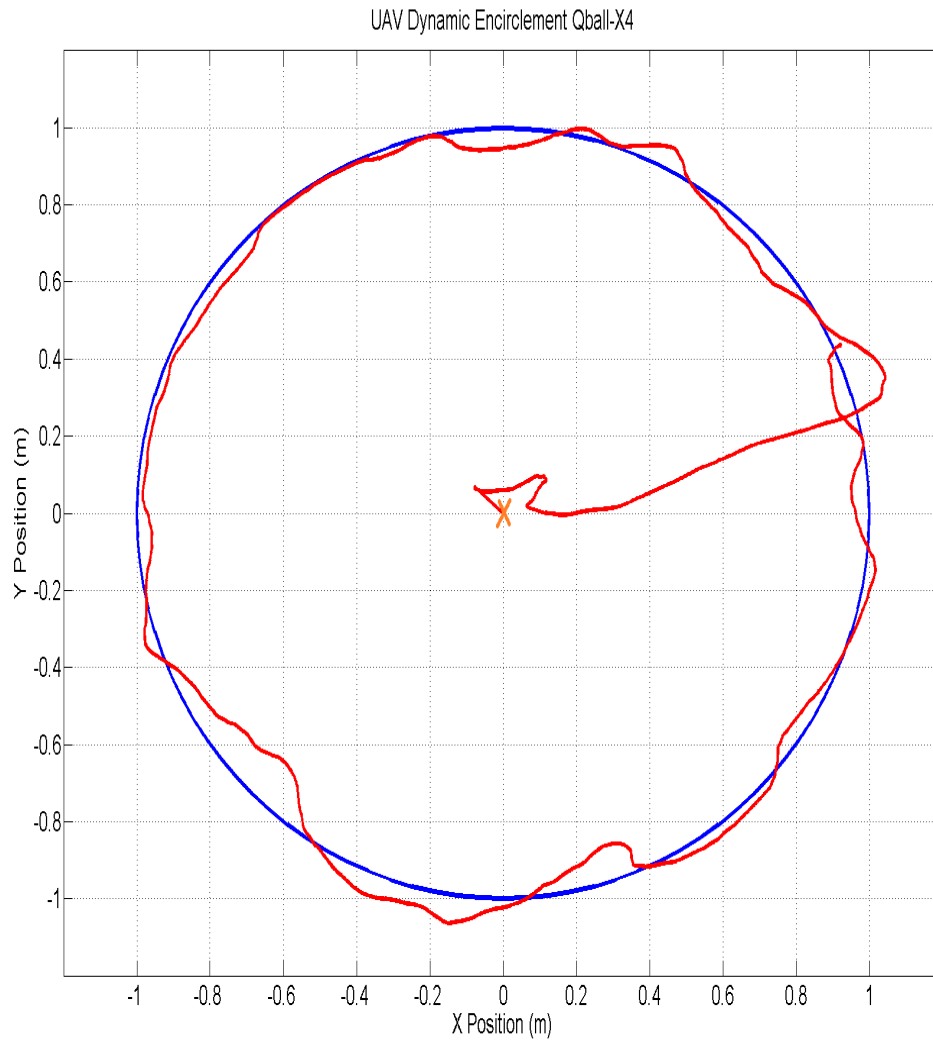


Figure 5.1: Path completed by the Qball-X4 quadrotor for the encirclement of a stationary target. The vehicle takes off from a stationary position at  $(0m, 0m)$  (represented by the orange 'x'). The blue line consists of the ideal circular path, while the red line is the UAV's actual path.

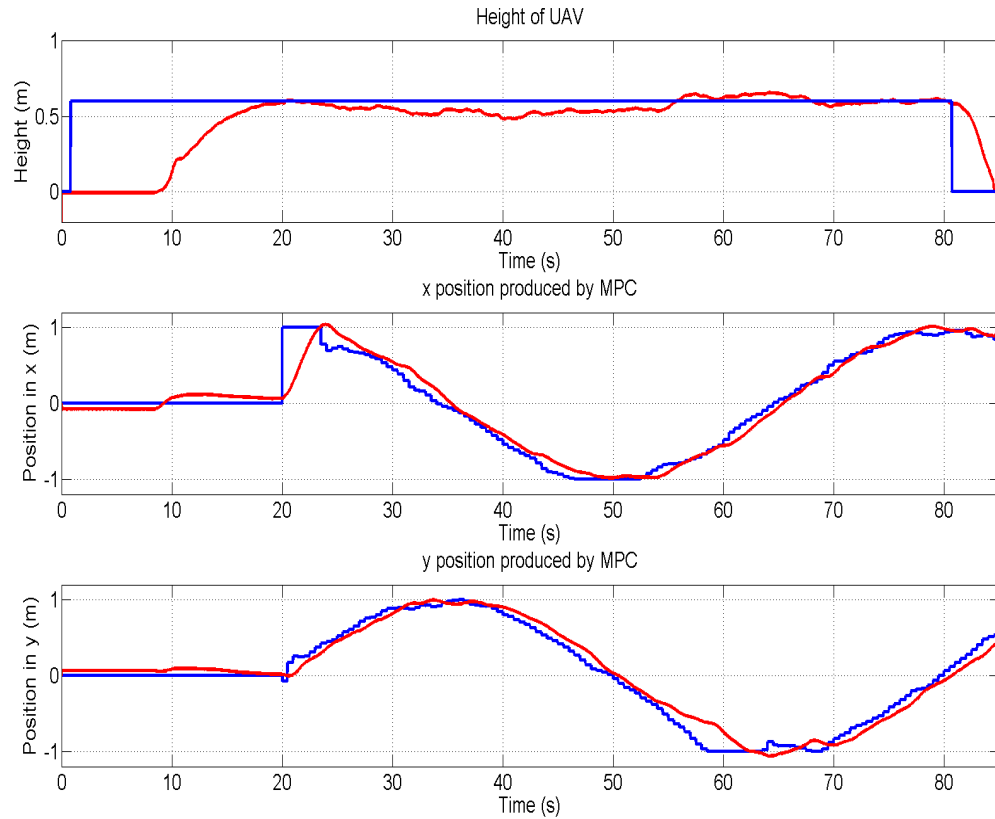


Figure 5.2: Height of Qball-X4 along side actual UAV  $x$  and  $y$  positions. The height during testing is maintained at  $0.6m$ . The green line in the height plot shows the actual height of the UAV. The red lines in the position plots represent the  $x$  and  $y$  paths completed by the UAV. The blue lines represent the path produced as a result of the chosen radius and angular velocity.

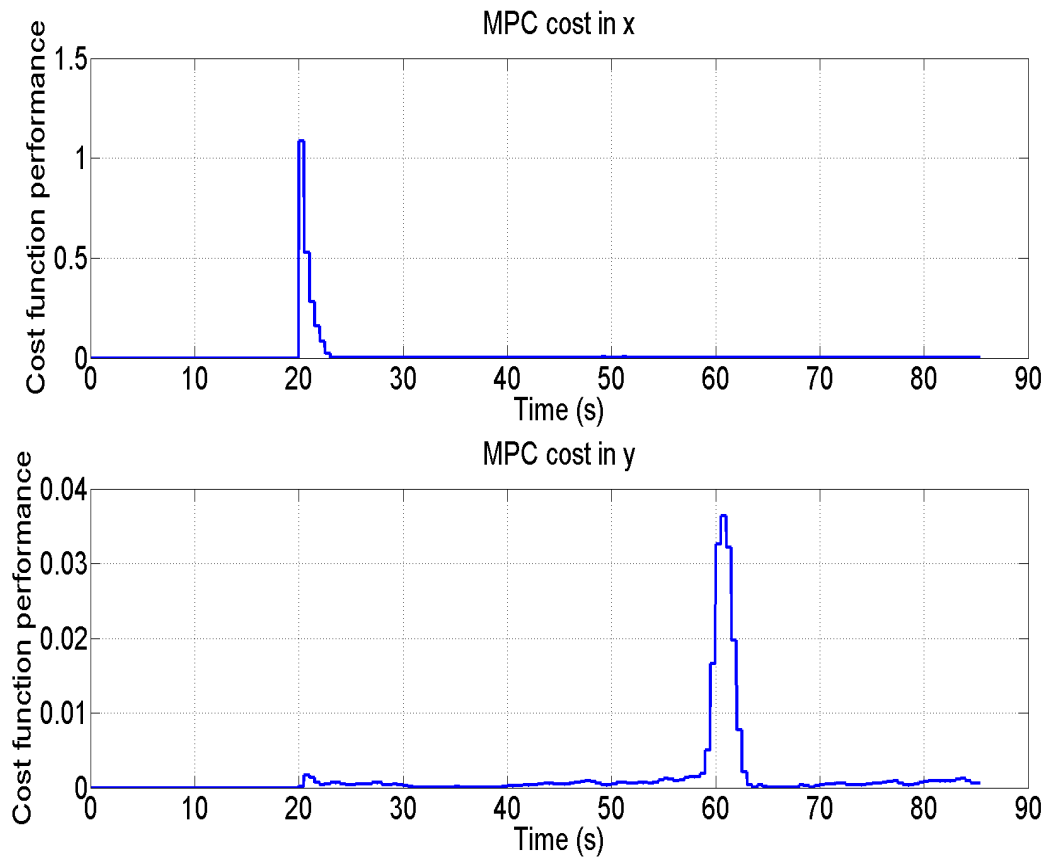


Figure 5.3: MPC cost function performance and control signal. Notice that the MPC cost becomes smaller with time. The MPC control signal represents the two manipulated variables calculated with similar weights.

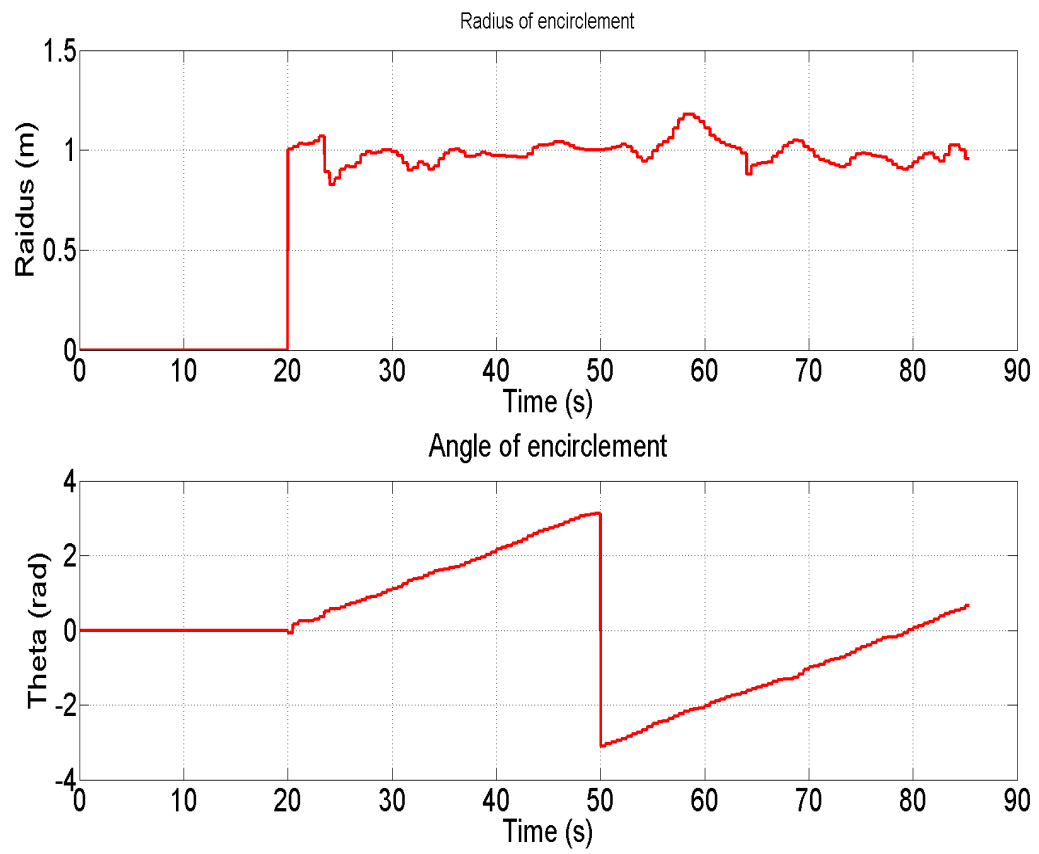


Figure 5.4: Radius and speed of the UAV. The blue lines represent the desired radius of  $1m$  and desired speed of  $0.1047m/s$ .

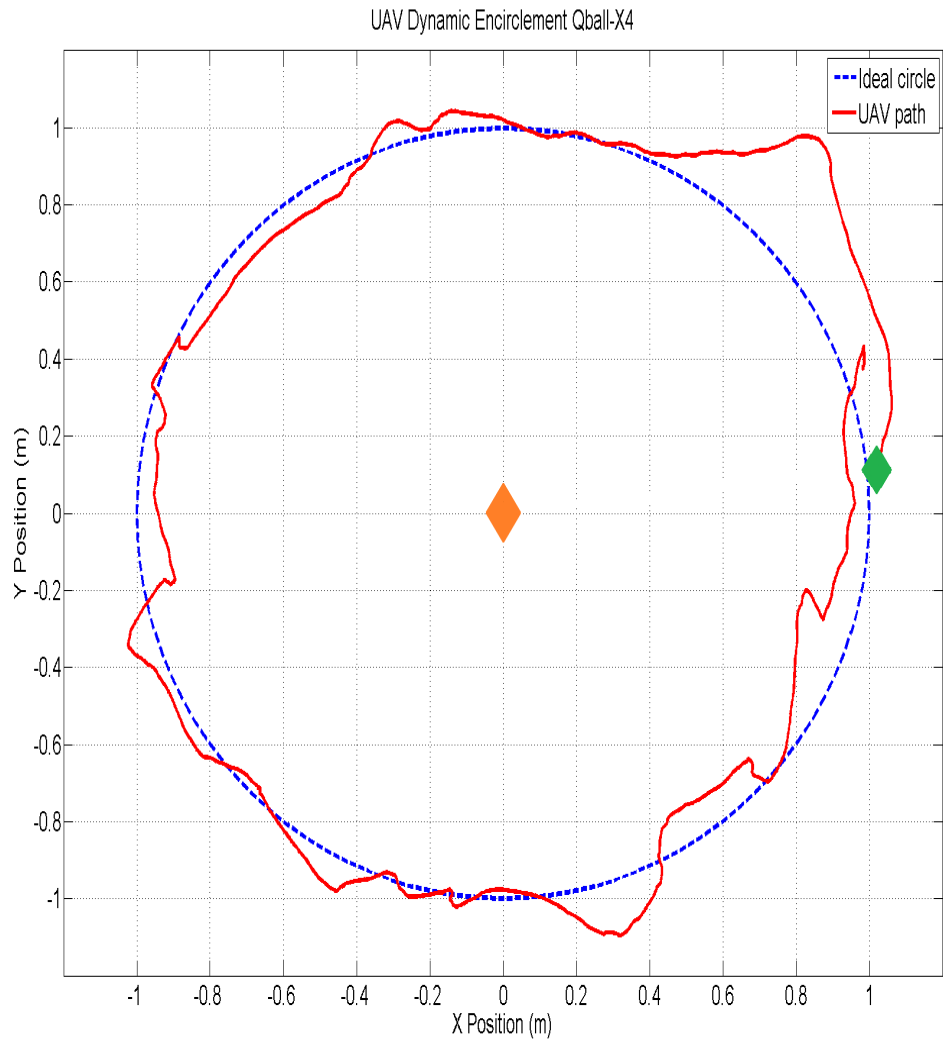


Figure 5.5: Single Qball-X4 encircling a stationary target in anti-clock wise direction. The green diamond represents the UAV's starting position of  $(1, 0)$  while the dashed blue line shows a reference circle. the orange diamond represents the stationary target at the origin.

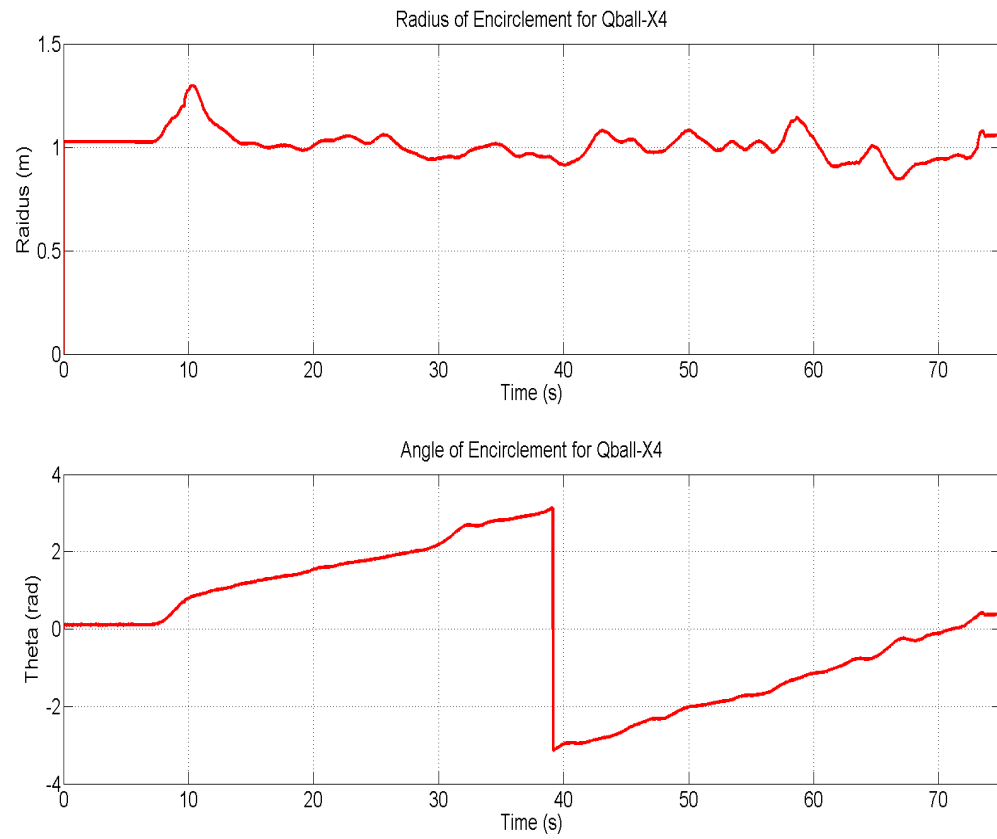


Figure 5.6: Radius and angle of encirclement for a single Qball-X4 around a stationary target. Notice that the radius steady-state error is less than 15 %.

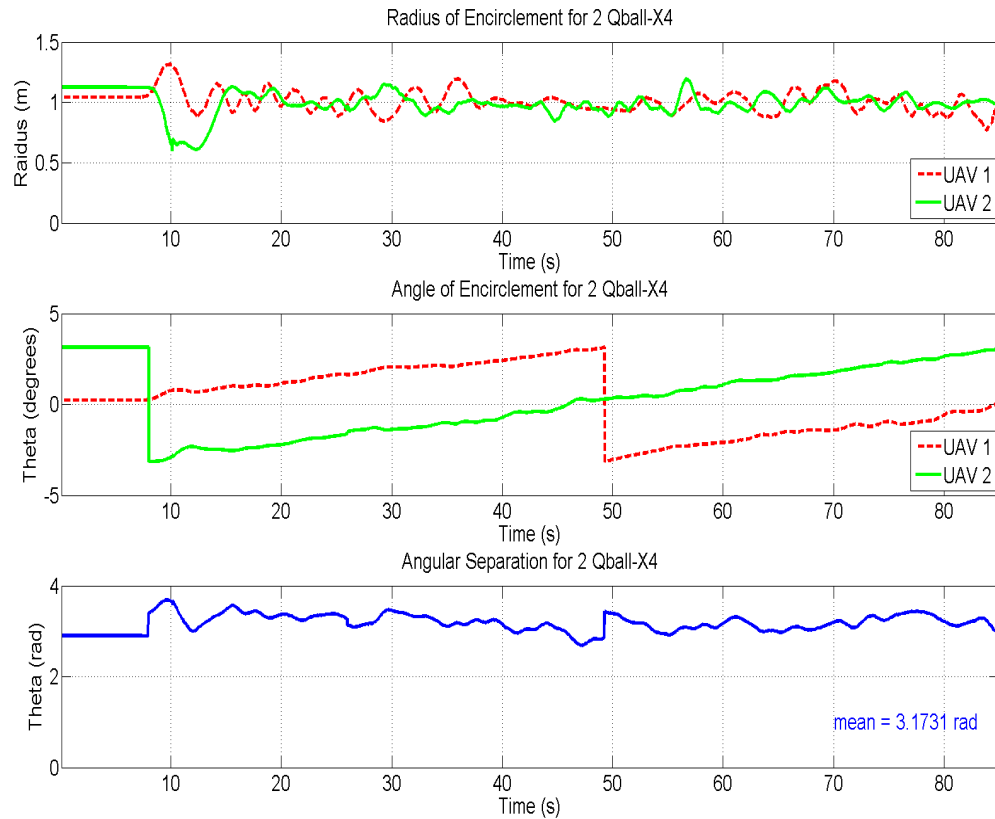


Figure 5.7: Radii, angle of encirclement and angle of separation for the case of 2 Qball-X4, starting at  $(1,0)$  and  $(-1,0)$ , encircling a stationary target. The dashed red line represents Qball 1 while the green line represents Qball 2. The blue line shows the separation angle between both UAVs.

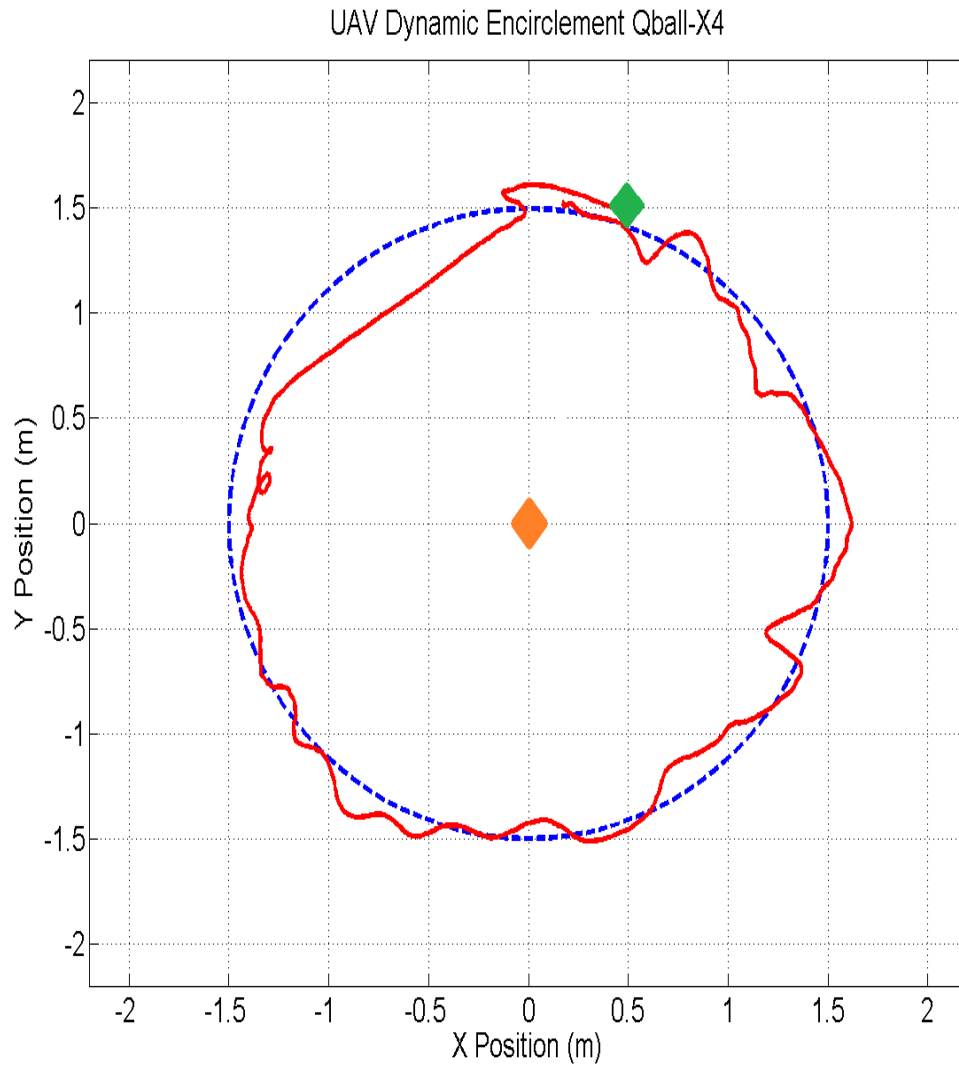


Figure 5.8: Single UAV encircling a stationary target in anti-clockwise direction. The green diamond represents the UAV's starting position of  $(0, 1.5)$  while the dashed blue line shows a reference circle. The orange diamond represents the stationary target at the origin.

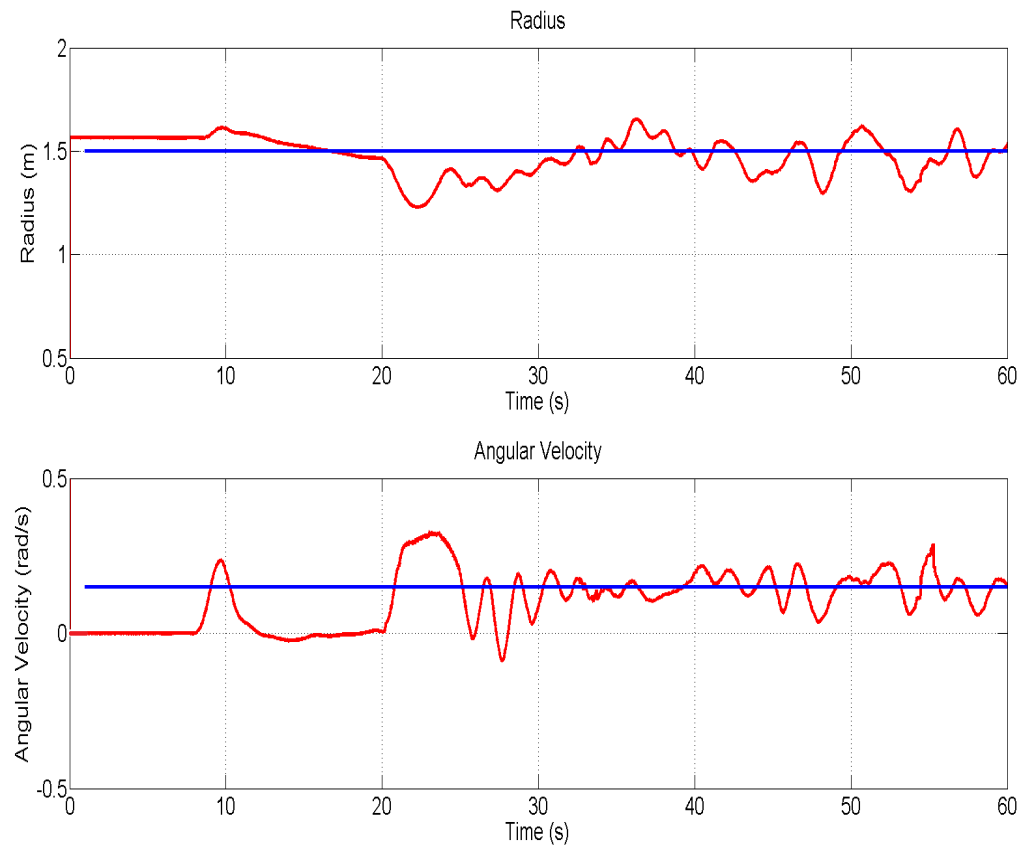


Figure 5.9: Radius and angular velocity of Qball-X4 encircling a stationary target. The blue line represents the desired radius and angular velocity.

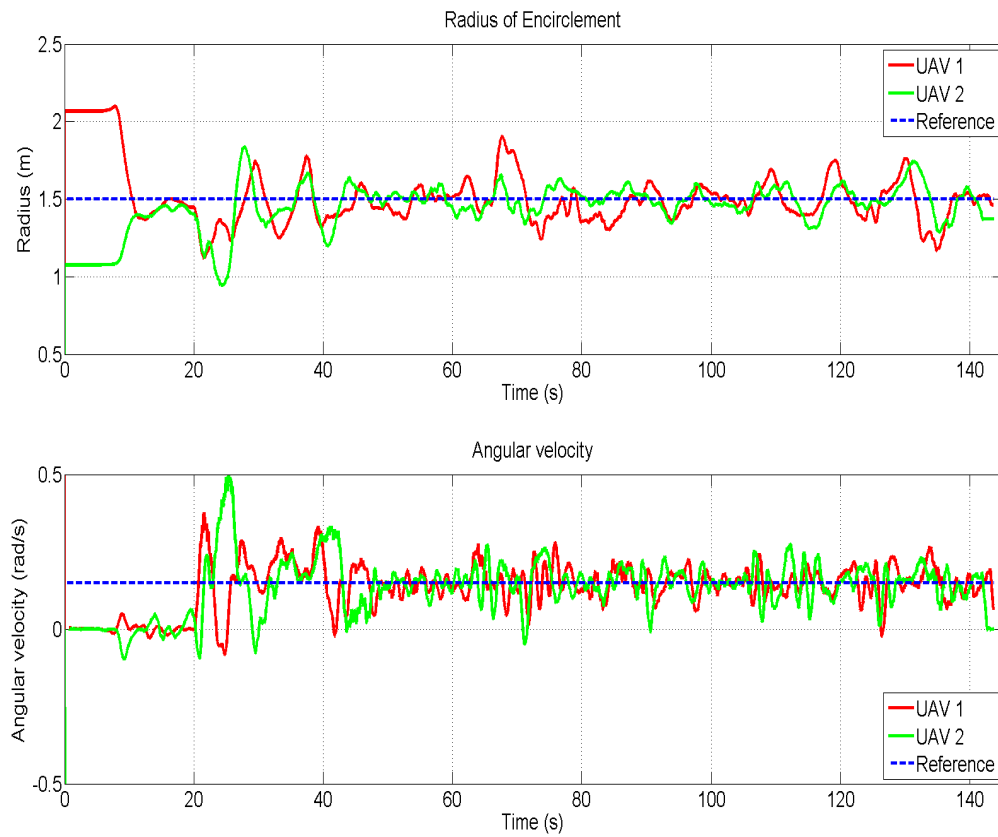


Figure 5.10: The radii of encirclement and the angular velocities for two UAVs encircling a stationary target at the origin.

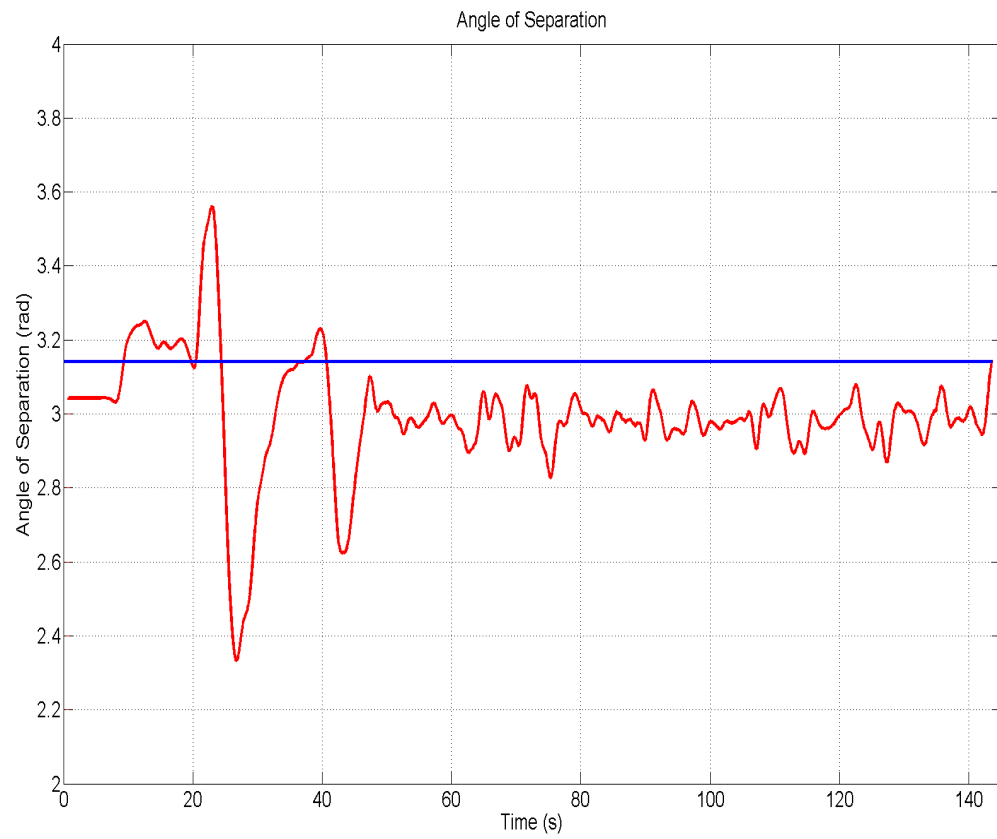


Figure 5.11: Angular separation for two UAVs encircling a stationary target. The UAVs converge to a separation of almost  $\pi$

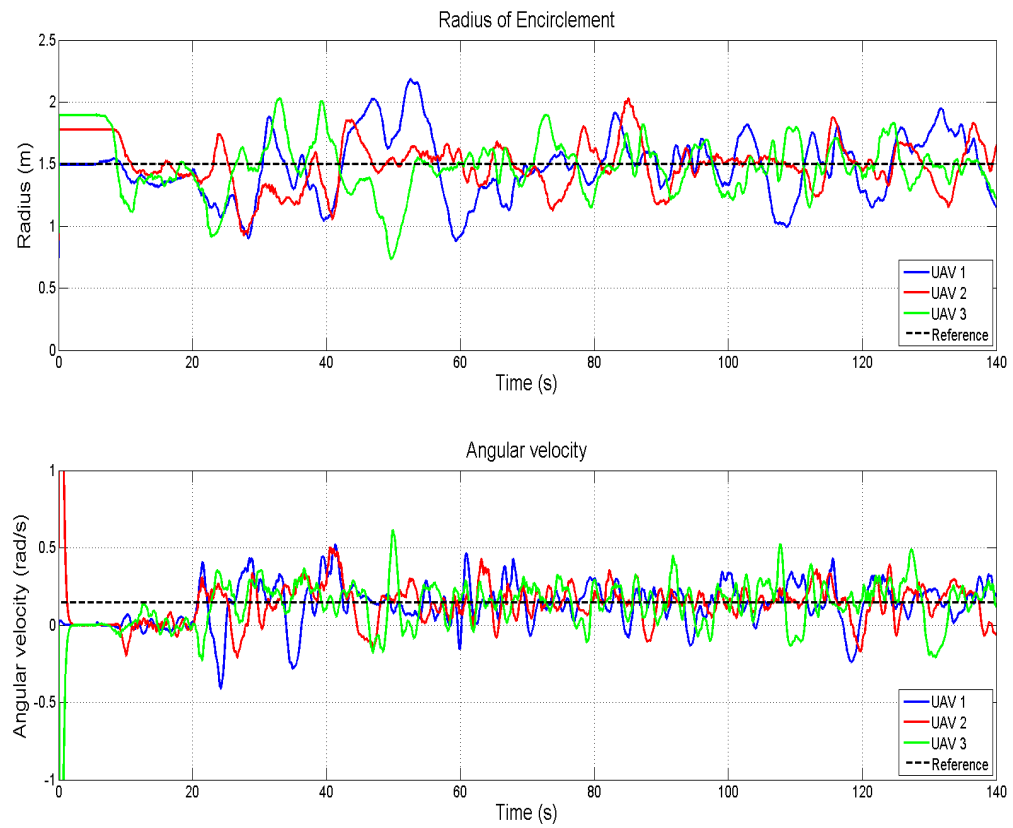


Figure 5.12: The radii of encirclement and the angular velocities for three UAVs encircling a stationary target at the origin.

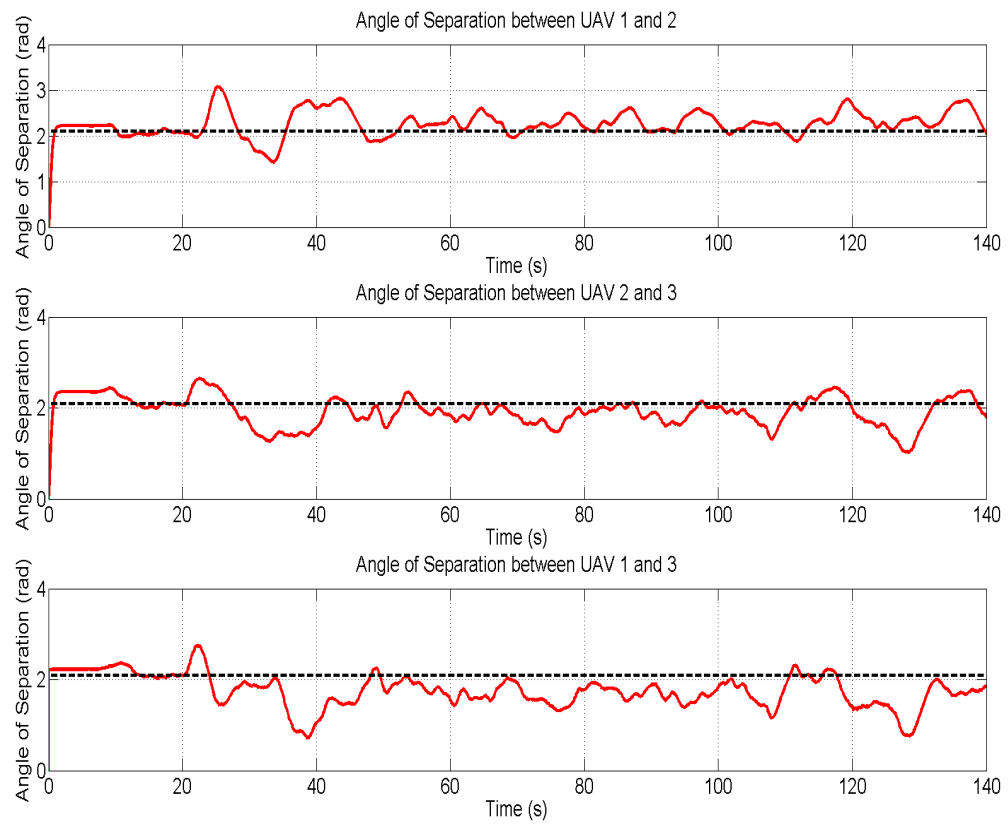


Figure 5.13: Angular separation for two UAVs encircling a stationary target. The UAVs converge to a separation of almost  $2\pi/3$

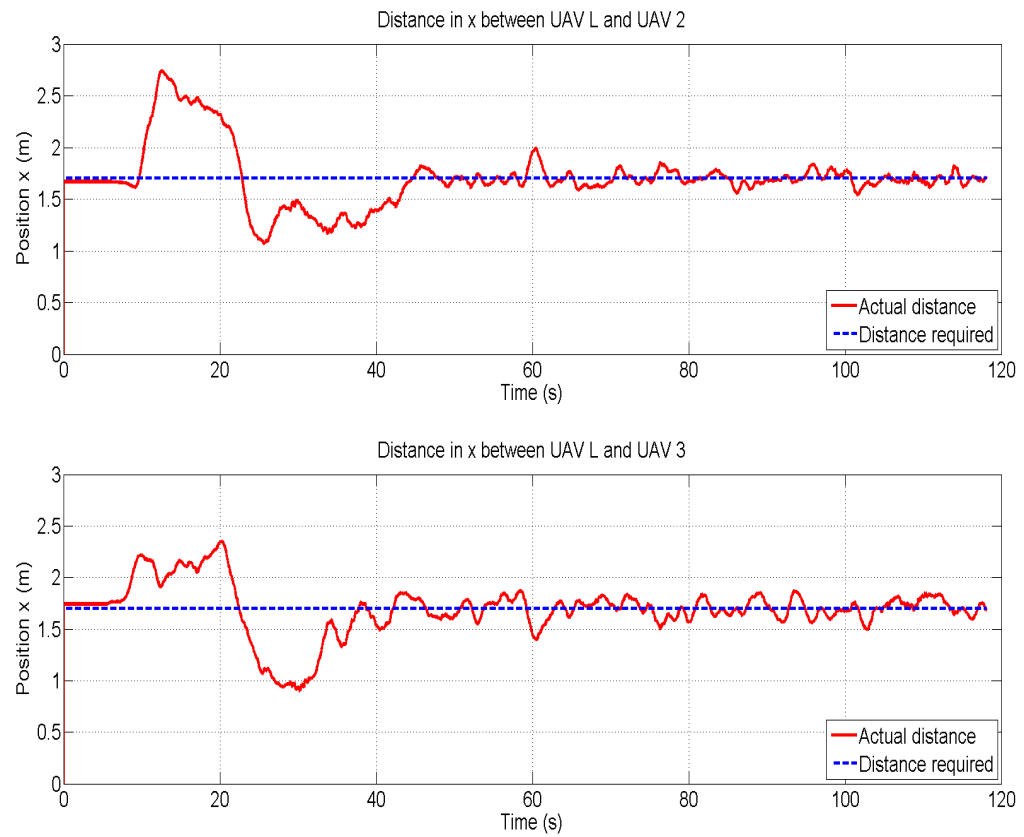


Figure 5.14: Distances in x between UAV 2, 3 and the leader going in the negative y direction. The required distance is 1.7 m

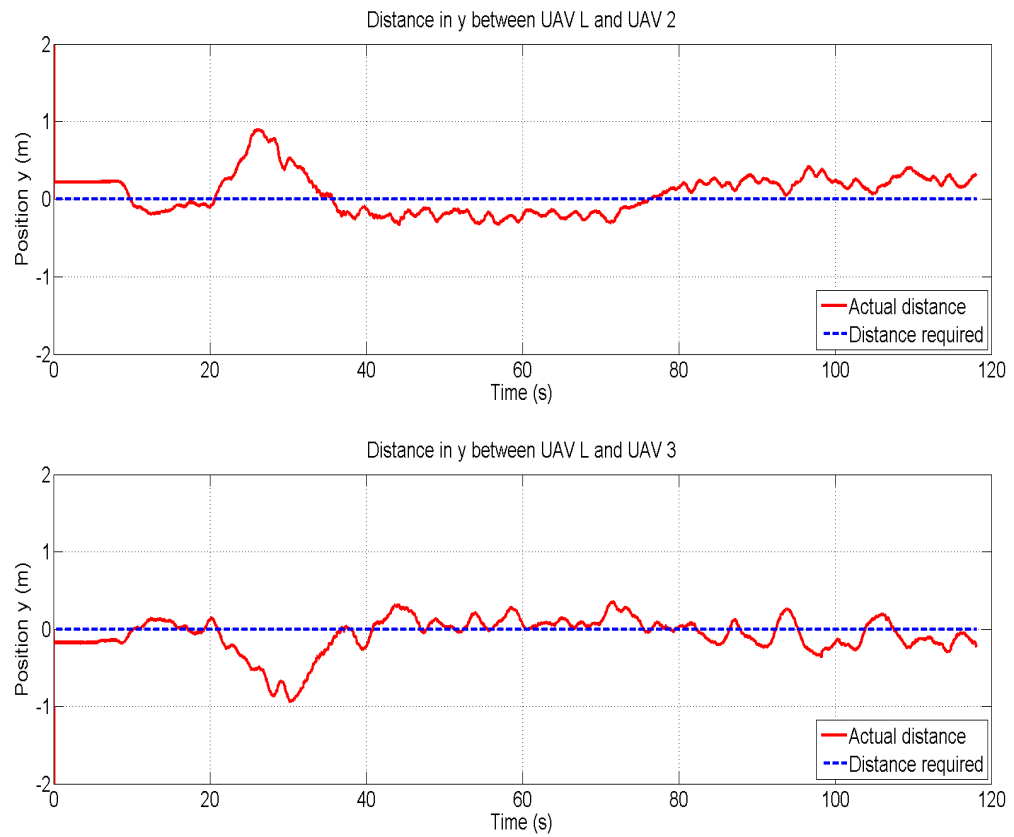


Figure 5.15: Distances in y between UAV 2, 3 and the leader going in the negative y direction. The required distance is 0 m

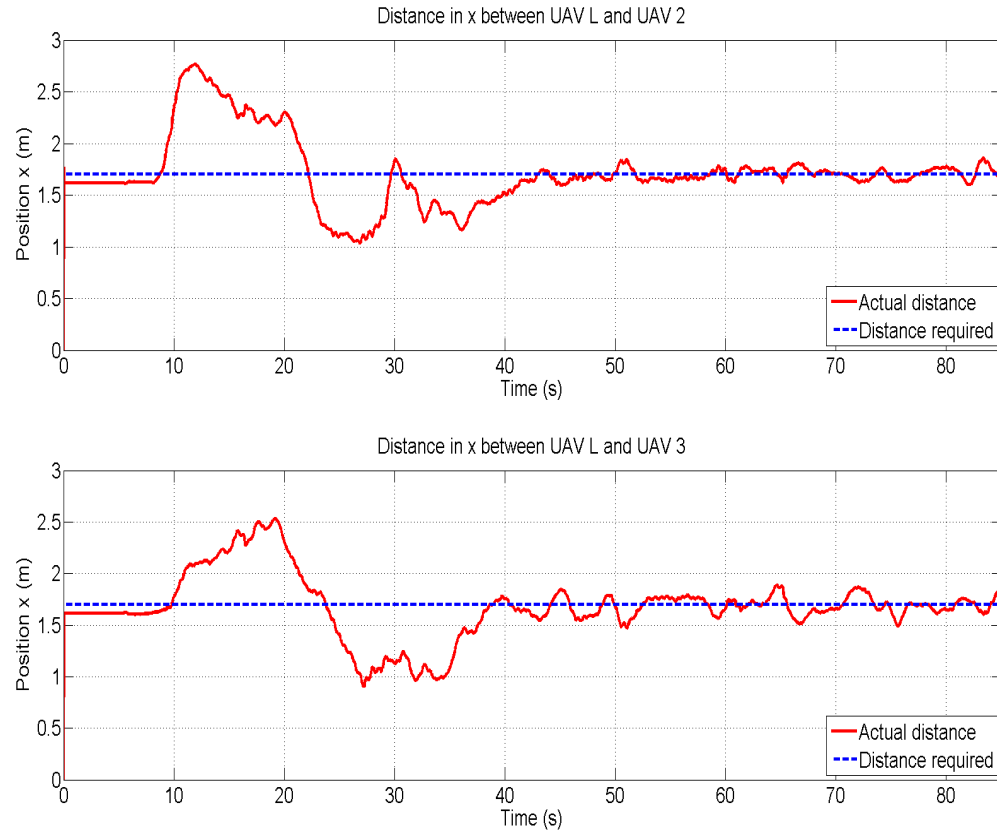


Figure 5.16: Distances in x between UAV 2, 3 and the leader going in the negative y direction. The required distance is 1.7 m. This is part of a tactic switching flight test where UAV L decides to encircle the target

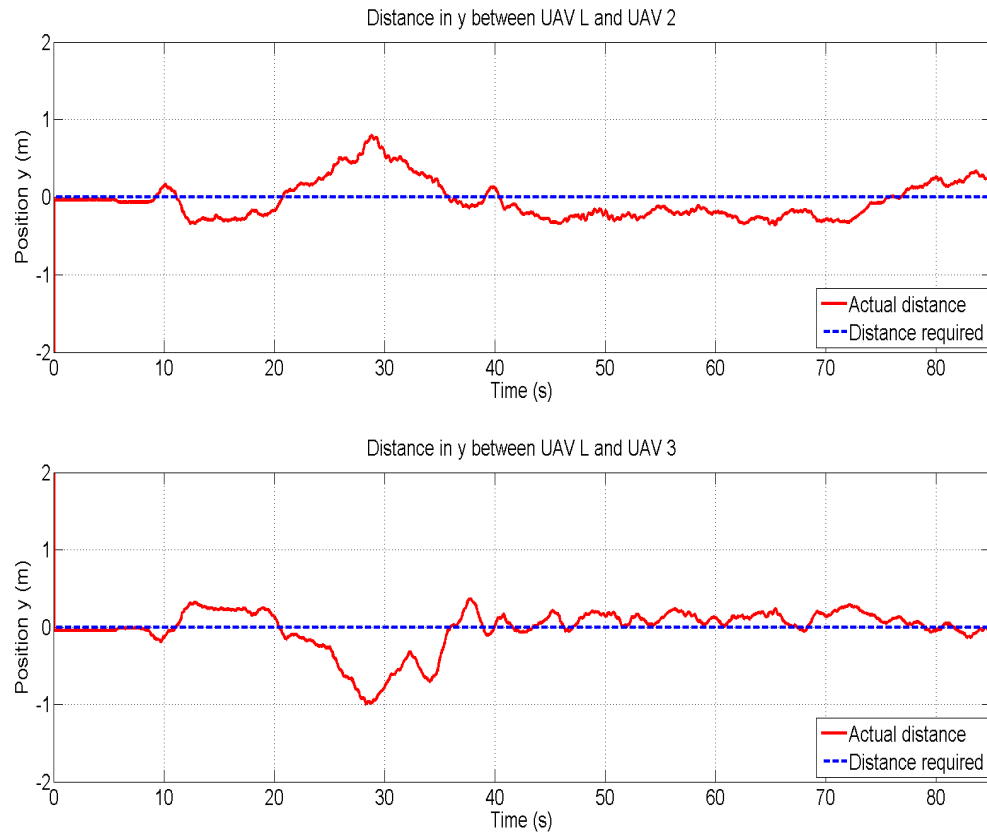


Figure 5.17: Distances in  $y$  between UAV 2, 3 and the leader going in the negative  $y$  direction. The required distance is 0 m. This is part of a tactic switching flight test where UAV L decides to encircle the target

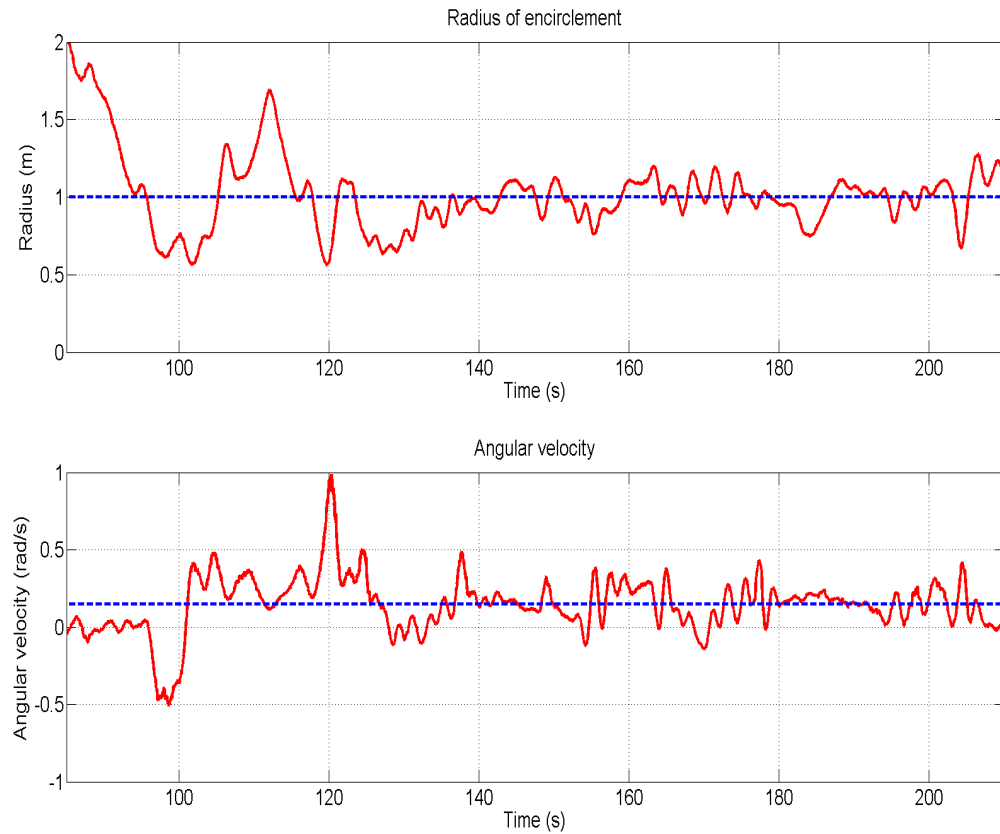


Figure 5.18: The radius of encirclement and the angular velocity for one UAV encircling a stationary target found at  $(0,1)$ . This is part of a tactic switching flight test where UAV L decides to encircle the target

## Chapter 6

# Conclusion

The use of UAVs, such as surveillance, search and destroy and photogrammetry, are continuing to grow. Solving cooperative robotic tasks with the use of scalable UAV teams is becoming the preferred solution for various UAV and control communities. As this trend continues, more complex control systems, such as MPC, are used to solve these multi-variable tasks under heavy constraints. The need for real-time implementation of designed controllers on actual vehicles is pushing the community towards linearization methods such FL. Accomplishing tasks with decentralized methods of control in uncertain environments proves to be a challenge for the future.

In Chapter 3, we formulate an LMPC strategy capable of dealing with the formation and encirclement tactics for a three-member UAV team. The solution operates as a decentralized control method where each member makes decisions based on the presence of the target and other team members. Real-time control is shown through the issuing of control signals every 0.5 seconds. In Chapter 4, the designed controllers and decision making processes are validated for the cases of triangle, cross and line abreast formations, along side encirclement of a stationary and moving target. Moreover, simulations of tactic switching are also presented, showing stable switching from formation to encirclement. In Chapter 5, we take the controllers and implement them on a three-UAV team of Qball-X4 and show the successful flights of line abreast formation, encirclement of a stationary target and the switching from one to the other. We show that despite wind disturbance created by the vehicles' motors, the LMPC is able to adjust vehicle behavior in order to meet the proper requirements of distance, radii, velocities and angles of separation. In this thesis, we show the convergence of behavior with a small steady-state error, demonstrating the effectiveness of the designed controllers and algorithms and their successful implementation on real vehicles.

## 6.1 Contributions

The contributions of this thesis are as follows: The problem of safely switching from formation flight to encirclement of a stationary and moving target is achieved using LMPC applied on a team of three UAVs. First, system identification, based on a least-squares algorithm, is used to identify the Qball-X4 quadrotor's Cartesian movement. We observed that the resulting models are similar to the quadrotor's behavior. Second, TSL and FL are used to linearize the tactics models, allowing for real-time implementation of the designed controllers on real-world vehicles. Third, LMPC successfully controls the quadrotor aircrafts during their formation flights, maintaining distance and matching speeds with other vehicles. Furthermore, the controllers respect the desired radii, angular velocities and angles of separation between team members during the encirclement tactic. Finally, we show that the control strategies may be implemented successfully on a multi-UAV team composed of Qball-X4 aircrafts.

We also provided extensive simulation and experimental results, dealing with both the formation and the encirclement tactics. We successfully implement line abreast in simulation and in real-life while cross and triangle are shown only in simulation. The encirclement of a stationary and moving targets using one, two and three vehicles are shown where the UAVs successfully reach the desired radii and angular velocities. No collisions are reported due to the angles of separation being accounted for by the LMPC cost function. The controller performance is observed with a small steady-state error while the switching from one tactic to another is done safely.

## 6.2 Future work

Cooperative robotic tasks and environments will continue to grow in complexity and the uses of UAVs will be ever so relevant. With this in mind, the combination of LMPC and FL will be considered a feasible solution for future uses of UAVs since it allows for real-time implementation on real-vehicles. We foresee the use of LMPC along side learning based algorithms to adjust for model and environment uncertain-

ties. Accordingly, the linearized process models only consider first order derivation; as such learning algorithms would help alleviate the small difference between the nonlinear models and their linearized counterparts. Moreover, accounting for wind disturbance and possible ground effects may be done using these same methods. As an example of possible strategies we name, Learning Based MPC (LBMPC) and reinforcement learning algorithms combined with the control policies outlined in this thesis.

Applying LMPC and the tactic switching system described here on outdoor flying vehicles is a future area of research. This way, the system may be tested in more complex environments. Multi-UAV outdoor mapping and photogrammetry along side an outdoor traveling salesman problem are some areas of focus.

### 6.3 Conclusion

Our work has shown that LMPC, combined with FL and TSL, is an effective control system for multi-UAV formation flights and encirclement of stationary and moving target. These control strategies are applied in real-time on Qball-X4 quadrotors and the switching from one tactic to another is shown to be stable and effective.

## References

- [1] Kostas Alexis, Christos Papachristos, George Nikolakopoulos, and Anthony Tzes. Model predictive quadrotor indoor position control. In *19th Mediterranean Conference on Control and Automation*, pages 1247–1252, June 2011.
- [2] M. Alighanbari and J.P. How. Cooperative task assignment of unmanned aerial vehicles in adversarial environments. In *Proceedings of the 2005 American Control Conference*, pages 4661–4666 vol. 7, 2005.
- [3] Abdel Ilah Alshbatat and Qais Alsafasfeh. Cooperative decision making using a collection of autonomous quad rotor unmanned aerial vehicle interconnected by a wireless communication network. *AWERProcedia Information Technology and Computer Science*, 1, 2012.
- [4] G. Arslan, J.R. Marden, and J.S. Shamma. Autonomous vehicle-target assignment: A game-theoretical formulation. *Journal of Dynamic Systems, Measurement, and Control*, 129:584, 2007.
- [5] A. Bemporad and C. Rocchi. Decentralized linear time-varying model predictive control of a formation of unmanned aerial vehicles. In *2011 50th IEEE Conference on Decision and Control, European Control Conference (CDC-ECC)*, pages 7488–7493, 2011.
- [6] A Benallegue, A Mokhtari, and L Fridman. Feedback linearization and high order sliding mode observer for a quadrotor uav. In *International Workshop on Variable Structure Systems, 2006. VSS'06.*, pages 365–372. IEEE, 2006.
- [7] B. Bethke, J.P. How, and J. Vian. Group health management of UAV teams with applications to persistent surveillance. In *American Control Conference, 2008*, pages 3145 –3150, Jun. 2008.
- [8] S. Bhattacharya and T. Başar. Game-theoretic analysis of an aerial jamming attack on a UAV communication network. In *American Control Conference (ACC), 2010*, pages 818 –823, Jun. 2010.
- [9] E. Bone and C. Bolkom. Unmanned aerial vehicles: Background and issues for congress. DTIC Document, 2003.
- [10] F. Bourgault, T. Furukawa, and H.F. Durrant-Whyte. Coordinated decentralized search for a lost target in a bayesian world. In *Proceedings of the 2003 IEEE/RSJ International Conference on Intelligent Robots and Systems (IROS 2003)*, volume 1, pages 48–53. IEEE, 2003.

- [11] M. Bryson and S. Sukkarieh. Decentralised trajectory control for multi-UAV SLAM. In *Proceeding of the 4th International Symposium on Mechatronics and its Applications (ISM07)*, Sharjah, U.A.E., Mar. 2007.
- [12] G. Cai, K.Y. Lum, B.M. Chen, and T.H. Lee. A brief overview on miniature fixed-wing unmanned aerial vehicles. In *2010 8th IEEE International Conference on Control and Automation (ICCA)*, pages 285–290. IEEE, 2010.
- [13] Eduardo F. Camacho and Carlos Bordons. *Model Predictive Control*. Springer-Verlag, London, 2007.
- [14] J. Campbell, J. Hamilton, M. Iskandarani, and S.N. Givigi. A systems approach for the development of a quadrotor aircraft. In *2012 IEEE International Systems Conference (SysCon)*, pages 1–7, March 2012.
- [15] Jr. Cruz, J.B., Genshe Chen, D. Garagic, Xiaohuan Tan, Dongxu Li, Dan Shen, Mo Wei, and Xu Wang. Team dynamics and tactics for mission planning. In *Proceedings of the 42nd IEEE Conference on Decision and Control 2003*, volume 4, pages 3579 – 3584 vol.4, Dec. 2003.
- [16] KD Do and J. Pan. Nonlinear formation control of unicycle-type mobile robots. *Robotics and Autonomous Systems*, 55(3):191–204, 2007.
- [17] William B. Dunbar and Richard M. Murray. Model predictive control of coordinated multi-vehicle formations. In *IEEE Conference on Decision and Control*, March 2002.
- [18] Zhou Fang, Zhang Zhi, Liang Jun, and Wang Jian. Feedback linearization and continuous sliding mode control for a quadrotor uav. In *27th Chinese Control Conference CCC 2008*, pages 349–353. IEEE, 2008.
- [19] Ahmed T Hafez, Anthony J Marasco, Sidney N Givigi, Alain Beaulieu, and Camille Alain Rabbath. Encirclement of multiple targets using model predictive control. In *American Control Conference (ACC), 2013*, pages 3147–3152. IEEE, 2013.
- [20] S. Hara, T.H. Kim, Y. Hori, and K. Tae. Distributed formation control for target-enclosing operations based on a cyclic pursuit strategy. In *Proceedings of the 17th IFAC World Congress*, pages 6602–6607, 2008.
- [21] Michael A. Henson and Dale E. Seborg. *Nonlinear Process Models*. Prentice Hall, United States, 1997.
- [22] J.P. How, C. Fraser, K.C. Kulling, L.F. Bertuccelli, O. Toupet, L. Brunet, A. Bachrach, and N. Roy. Increasing autonomy of uavs. *Robotics & Automation Magazine, IEEE*, 16(2):43–51, 2009.

- [23] M. Iskandarani, A. Hafez, S. Givigi, A. Beaulieu, and A. Rabbath. Using multiple quadrotor aircraft and linear model predictive control for the encirclement of a target. In *IEEE International Conference SYSCON 2013*, pages 1–7. IEEE, 2013.
- [24] H. Kawakami and T. Namerikawa. Cooperative target-capturing strategy for multi-vehicle systems with dynamic network topology. In *American Control Conference, 2009. ACC'09.*, pages 635–640. IEEE, 2009.
- [25] Hiroki Kawakami and Toru Namerikawa. Virtual structure based target-enclosing strategies for nonholonomic agents. In *2008 IEEE Multi-Conference on Systems and Control*, pages 1043–1048, September 2008.
- [26] V.R. Khare, F.Z. Wang, S. Wu, Y. Deng, and C. Thompson. Ad-hoc network of unmanned aerial vehicle swarms for search & destroy tasks. In *4th International IEEE Conference on Intelligent Systems IS'08*, volume 1, pages 6–65. IEEE, 2008.
- [27] H.J. Kim, D.H. Shim, and S. Sastry. Decentralized non-linear model predictive control of multiple flying robots in dynamic environments. In *IEEE Conference on Decision and Control*, December 2003.
- [28] Tae-Hyoung Kim and Toshiharu Sugie. Cooperative control for target-capturing task based on a cyclic pursuit strategy. *Automatica*, 43:1426–1431, 2007.
- [29] T.H. Kim, S. Hara, and Y. Hori. Cooperative control of multi-agent dynamical systems in target-enclosing operations using cyclic pursuit strategy. *International Journal of Control*, 83(10):2040–2052, 2010.
- [30] Y. Lan, G. Yan, and Z. Lin. Distributed control of cooperative target enclosing based on reachability and invariance analysis. *Systems & Control Letters*, 59(7):381–389, 2010.
- [31] J.R.T. Lawton, R.W. Beard, and B.J. Young. A decentralized approach to formation maneuvers. *IEEE Transactions on Robotics and Automation*, 19(6):933–941, 2003.
- [32] N. Lechevin, C.A. Rabbath, and M. Lauzon. A decision policy for the routing and munitions management of multiformations of unmanned combat vehicles in adversarial urban environments. *IEEE Transactions on Control Systems Technology*, 17(3):505–519, May. 2009.
- [33] Daewon Lee, H Jin Kim, and Shankar Sastry. Feedback linearization vs. adaptive sliding mode control for a quadrotor helicopter. *International Journal of Control, Automation and Systems*, 7(3):419–428, 2009.
- [34] R.V. Lopes, R.K.H. Galvao, A.P. Milhan, V.M. Becerra, and T. Yoneyama. Modelling and constrained predictive control of a 3dof helicopter. In *XVI Congresso Brasileiro de Automática, Salvador, Brazil, Paper*, volume 123, pages 429–434, 2006.

- [35] A.J. Marasco. Control of Cooperative and Collaborative Team Tactics in Autonomous Unmanned Aerial Vehicles Using Decentralized Model Predictive Control. Master's thesis, Royal Military College - Canada, 2012.
- [36] Anthony J Marasco, Sidney N Givigi, and Camille Alain Rabbath. Model predictive control for the dynamic encirclement of a target. In *American Control Conference (ACC), 2012*, pages 2004–2009. IEEE, 2012.
- [37] Anthony J Marasco, Sidney N Givigi, Camille Alain Rabbath, and Alain Beaulieu. Dynamic encirclement of a moving target using decentralized nonlinear model predictive control. In *American Control Conference (ACC), 2013*, pages 3960–3966. IEEE, 2013.
- [38] V Mistler, A Benallegue, and NK M'sirdi. Exact linearization and noninteracting control of a 4 rotors helicopter via dynamic feedback. In *Robot and Human Interactive Communication, 2001. Proceedings. 10th IEEE International Workshop on*, pages 586–593. IEEE, 2001.
- [39] N. Miyata, J. Ota, T. Arai, and H. Asama. Cooperative transport by multiple mobile robots in unknown static environments associated with real-time task assignment. *IEEE Transactions on Robotics and Automation*, 18(5):769–780, 2002.
- [40] Abdellah Mokhtari, Abdelaziz Benallegue, and Boubaker Daachi. Robust feedback linearization and gh infinity controller for a quadrotor unmanned aerial vehicle. In *2005 IEEE/RSJ International Conference on Intelligent Robots and Systems (IROS 2005)*, pages 1198–1203. IEEE, 2005.
- [41] D.J. Pack, P. DeLima, G.J. Toussaint, and G. York. Cooperative control of uavs for localization of intermittently emitting mobile targets. *IEEE Transactions on Systems, Man, and Cybernetics, Part B: Cybernetics*, 39(4):959–970, 2009.
- [42] L.E. Parker and B.A. Emmons. Cooperative multi-robot observation of multiple moving targets. In *Proceedings of the 1997 IEEE International Conference on Robotics and Automation*, volume 3, pages 2082–2089. IEEE, 1997.
- [43] Quanser. Qball-x4 user manual. Technical Report 829.
- [44] AJM Raemaekers. Design of a model predictive controller to control uavs. *Technische Universiteit Eindhoven*, 2007.
- [45] W. Ren and R.W. Beard. A decentralized scheme for spacecraft formation flying via the virtual structure approach. In *Proceedings of the 2003 American Control Conference*, volume 2, pages 1746–1751. IEEE, 2003.
- [46] C.W. Reynolds. Flocks, herds, and schools: A distributed behavioral model. In *Proceedings of the Computer Graphics ACM SIGGRAPH '87 Conference*, volume 21, pages 25–34, July 1987.

- [47] A. Richards and J. How. Decentralized model predictive control of cooperating uavs. In *43rd IEEE Conference on Decision and Control CDC*, volume 4, pages 4286–4291. IEEE, 2004.
- [48] J.A. Sauter, R.S. Matthews, J.S. Robinson, J. Moody, and S.P. Riddle. Swarming unmanned air and ground systems for surveillance and base protection. In *Proceedings of AIAA Infotech@ Aerospace 2009 Conference*, 2009.
- [49] D.P. Scharf, F.Y. Hadaegh, and S.R. Ploen. A survey of spacecraft formation flying guidance and control. part ii: control. In *Proceedings of the 2004 American Control Conference*, volume 4, pages 2976–2985. IEEE, 2004.
- [50] R. Sharma, M. Kothari, C.N. Taylor, and I. Postlethwaite. Cooperative target-capturing with inaccurate target information. In *American Control Conference (ACC), 2010*, pages 5520–5525. IEEE, 2010.
- [51] Hyo-Sang Shin and Min-Jae Thak. Nonlinear model predictive control for multiple uavs formation using passive sensing. *International Journal of Aeronautical and Space Science*, 12(1):16–23, 2011.
- [52] T. Simeon, S. Leroy, and J.P. Laumond. Path coordination for multiple mobile robots: A resolution-complete algorithm. *IEEE Transactions on Robotics and Automation*, 18(1):42–49, 2002.
- [53] A. Sudsang and J. Ponce. On grasping and manipulating polygonal objects with disc-shaped robots in the plane. In *Proceedings of the 1998 IEEE International Conference on Robotics and Automation*, volume 3, pages 2740–2746. IEEE, 1998.
- [54] Gordon J. Sutton and Robert R. Bitmead. Performance and computational implementation of nonlinear model predictive control on a submarine. *Progress in Systems and Control Theory*, 26:461–472, 2000.
- [55] Holger Voos. Nonlinear control of a quadrotor micro-uav using feedback-linearization. In *IEEE International Conference on Mechatronics ICM 2009*, pages 1–6. IEEE, 2009.
- [56] H. Yamaguchi. A cooperative hunting behavior by mobile-robot troops. *The International Journal of Robotics Research*, 18(9):931–940, 1999.

## Curriculum Vitae

## Curriculum Vitae

Mohamad Iskandarani joined the Canadian Forces in 2008 as a Signals Officer (SIGS). After completing his B.Eng. in Electrical Engineering at the Royal Military College of Canada in 2012, he was posted to Kingston, Ontario, to complete his Master's of Applied Science on a scholarship from DRDC.